

DESIGN, SYNTHESIS AND CHARACTERIZATION OF FLUORESCENT HYPERBRANCHED
POLYGLYCEROLS AND ORGANIC NANOPARTICLES WITH COVALENTLY BOUND ANTI-
FADING AGENTS

BY

GRETCHEN ANN VINCIL

DISSERTATION

Submitted in partial fulfillment of the requirements
for the degree of Doctor of Philosophy in Chemistry
in the Graduate College of the
University of Illinois at Urbana-Champaign, 2014

Urbana, Illinois

Doctoral Committee:

Professor Steven C. Zimmerman, Chair
Assistant Professor Kami L. Hull
Assistant Professor Douglas A. Mitchell
Professor Catherine J. Murphy

Abstract

The photobleaching of fluorophores is a major limitation in fluorescence microscopy. We sought to create a brighter and more stable fluorophore by covalently attaching fluorescein and anti-fading agent (AFA) moieties to hyperbranched polyglycerols (HPG). The use of HPGs as a scaffold to link fluorescein and anti-fading agents proved intractable, so a norbornyl based ROMP polymer was used instead. Through the iterative use of ROMP and RCM, organic nanoparticles (ONPs) were synthesized incorporating multiple fluorescein and AFA units. The ONPs were brighter and more photostable than fluorescein. The photostability of the ONPs without AFAs was found to loosely correlate to its brightness. Incorporation of AFAs in the ONPs led to increased stability in some cases.

Acknowledgements

First and foremost, I would like to thank my advisor, Professor Steven Zimmerman, for guidance over the years. I would also like to thank my doctoral committee, Professor Kami Hull, Professor Doug Mitchell and Professor Catherine Murphy, for their feedback during the course of my graduate education. I would specifically like to thank two excellent lab partners I've enjoyed working with and learning from, Dr. Darrell Kuykendall and Justin Wright. Additionally, I would like to thank Yugang Bai and Dr. Andrew Zill for their insight and helpful discussions. Finally, I would like to thank my family for their support from afar during my time in Champaign-Urbana.

Table of Contents

| | |
|---|-----|
| I. Design, Synthesis and Characterization of Fluorescent Hyperbranched Polyglycerols with Covalently Bound Anti-Fading Agents | 1 |
| I.A. Introduction | 1 |
| I.B. Experimental Design | 3 |
| I.C. Results and Discussion | 11 |
| I.D. Conclusion and Future Directions | 29 |
| I.E. References | 31 |
| II. Synthesis and Characterization of Norbornyl Based Fluorescent Organic Nanoparticles with Improved Photostability | 37 |
| II.A. Introduction..... | 37 |
| II.B. Results and Discussion..... | 39 |
| II.C. Future Directions..... | 60 |
| II.D. References | 62 |
| III. Experimental | 63 |
| III.A. General Methods | 63 |
| III.B. Synthesis of Fluorescent HPGs and Precursors | 70 |
| III.C. Synthesis of Fluorescent ONP and Precursors | 91 |
| III.D. References | 120 |
| Appendices..... | 124 |
| Appendix A. Data Work-up Methods..... | 125 |
| Appendix B. Data Associated with Chapter I | 128 |
| Appendix C. Data Associated with Chapter II | 135 |

I. Design, Synthesis and Characterization of Fluorescent Hyperbranched Polyglycerols with Covalently Bound Anti-Fading Agents

I.A. Introduction

Background

Sir George Stokes first observed the phenomenon of fluorescence in the 16th century, although the term wasn't coined until 1853.¹ Over the intervening years, scientific inquiry has led to understanding of this process as well as the development of techniques to quantitatively measure the emission. Capitalizing on the ability of certain molecules to emit light (when excited), fluorophores are regularly used as probes to provide information about molecular level interactions.

The conjugation of dyes to biomolecules of interest (i.e., proteins, antibodies, nucleic acids) enables the labeling and subsequent tracking of molecules at the cellular, subcellular and molecular level via microscopy. In recent years, the commercial availability of functionalized fluorophores as well as the technological capabilities of processing large imaging data sets has led to a rapid expansion of the field of fluorescence microscopy. Newer techniques such as, confocal fluorescence microscopy, allow for collection of more detailed information but require intense laser excitation of fluorophores leading to photodegradation. An example of this is shown in Figure 1.1.² Currently, photobleaching is a major problem for the field, imposing limits on the information that can be gathered from a given study.

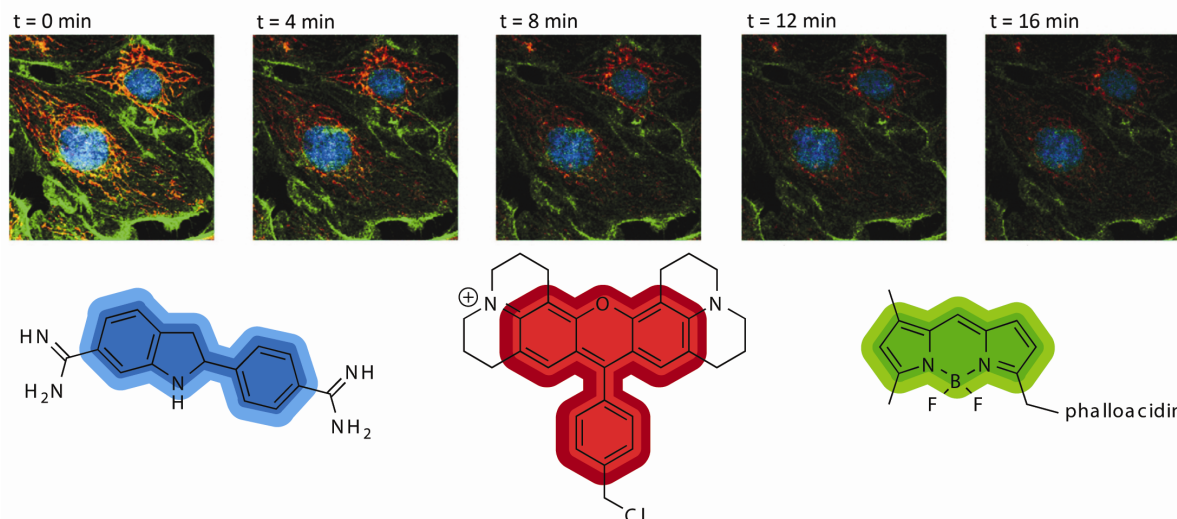


Figure 1.1. Photobleaching in confocal fluorescence microscopy. Loss of fluorescence intensity of three probes, bound to DNA (DAPI, blue), mitochondria (MitoTracker Red CMXRos, red), and actin filaments (BODIPY-FL phalloacidin, green) in fixed bovine pulmonary artery endothelial (BPAE) cells.²

Photobleaching

Photobleaching is a process by which a fluorophore, when exposed to light, degrades, becoming permanently non-fluorescent. In general, the reactions with molecular oxygen and reactions of the triplet state fluorophore are considered the two primary pathways in dye degradation. The specific pathways, and the extent to which each contributes to photobleaching, is fluorophore specific and highly sensitive to minor changes in conditions such as concentration, oxygen content, viscosity, etc. Regardless of the pathway, photobleaching of fluorophores is currently a major limitation in fluorescence microscopy.

In attempts to solve this problem, new designer dye series have been developed and are commercially available (e.g., Atto (*Atto-Tec* or *Sigma Aldrich*), Cy (*GE Healthcare*), Alexa Fluor (*Invitrogen*)). Many claims have been made regarding these being superior dyes in regard to their photostability, however, much of this is based on single examples that vary

greatly depending on which system the dye is incorporated, the fluorescence technique and the conditions. Although derivatives of the most commonly used fluorophores have led to the development of dyes with highly tunable properties, few withstand the intense laser irradiation necessary for fluorescence microscopy over time.

Another way to combat photobleaching is through the use of anti-fading agents (AFA). The term anti-fading agent (AFA) describes any compound additive that decreases the rate of photobleaching of a fluorophore. Traditional examples of AFAs include n-propyl gallate (nPG), mercaptoethylamine (MEA), and commercially available solutions like *SlowFade*[®] (with diazabicyclooctane (DABCO)), ProLong[®] Gold (undisclosed AFA) from *Invitrogen* and Vectashield (with p-phenylenediamine (PPD)) from *Vector Laboratories*.

There has been some success in increasing the photostability of fluorophores upon the addition of AFAs (see section below on AFAs). However, their use often causes other problems, particularly in live cell imaging due to the relatively high (mM) concentration required to be effective. AFAs can affect cellular activity and are generally toxic. The latter can limit their use to fixed cells. Furthermore, different dyes are stabilized by different AFAs, which can lead to potential complications in multi-fluorophore experiments.³

I.B. Experimental Design

Project Goals

The overall objective of this work was to create a fluorophores with superior fluorescent properties by covalently attaching dye moieties and AFAs to hyper-branched polyglycerols (HPG). This design concept is illustrated in Figure 1.2 features: 1) an HPG scaffold with a single alkyne linker, 2) multiple dye molecules, and 3) multiple AFA

moieties. The alkyne functionality serves as a single point of attachment allowing one fluorescent HPG to be linked to a single biomolecule. In principle, multiple copies of the fluorescent dye will increase the brightness of the molecule, compensating for the quenching expected upon conjugation. Furthermore, multiple fluorophores might produce a significantly brighter particle allowing for studies at lower concentrations as well as enhancing single molecule experiments. Covalent linkage of dye and AFA by the HPG will act to increase the effective concentration of AFA and alleviate the need for use of millimolar AFA concentrations. It was also anticipated that the covalent linkage to a polymeric scaffold would restrict the AFA's interaction with biomolecules potentially decreasing its toxicity.

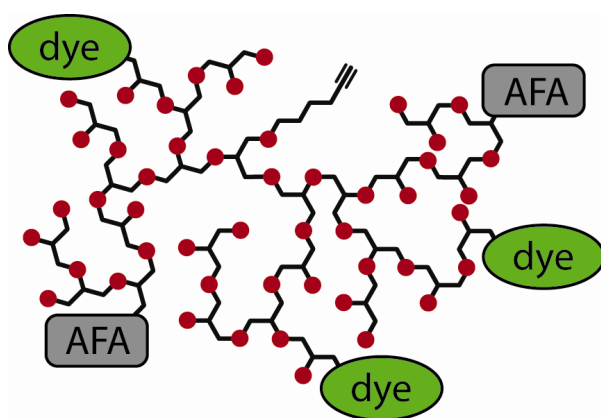


Figure 1.2. Conceptualization of HPG with multiple dye and multiple AFA moieties

Note: the dye: AFA: polymer size ratios have been arbitrarily chosen for this illustration

Hyperbranched Polyglycerols (HPGs)

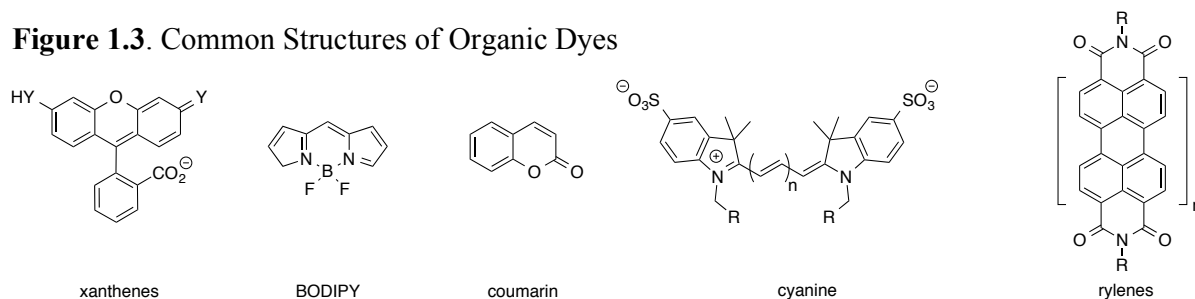
HPGs were regarded as ideal scaffolds for our purposes because they are water soluble, non-toxic, dendrimers-like macromolecules with high functionality.^{4,5} Furthermore, large quantities of polymer (kg scale) with relatively narrow polydispersity ($PDI \leq 1.8$) can be prepared in a single step via anionic ring-opening polymerization.⁶ Similar to their linear PEG counterparts, HPGs have been found to be non-toxic and well tolerated by living cells.

In addition, the HPG may act as a shield around each dye moiety to decrease the dye-dye quenching interactions typically observed when tethering multiple fluorophores together.

Fluorophores^{7,8,9}

Most organic dyes belong to a group of similarly structured molecules, the most common of which are shown in Figure 1.3. The most desirable dyes for this fluorescence application have large molar absorptivities ($\epsilon > 50,000 \text{ Abs}(\text{Mcm})^{-1}$), high quantum yields (QY, Φ), and a minimum Stoke's shift of greater than 10 nm. Further, they should be water-soluble, non-aggregating, and be easily derivatized if not commercially available.

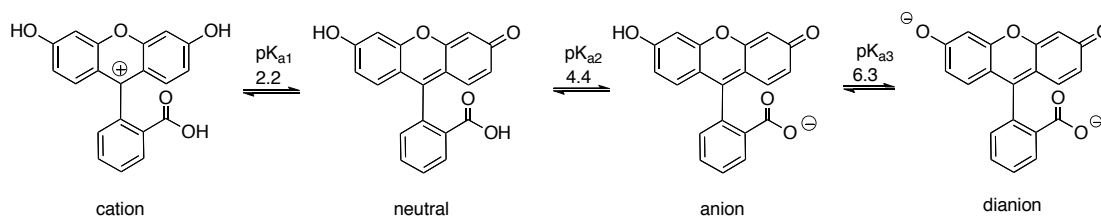
Figure 1.3. Common Structures of Organic Dyes



Fluorescein is a member of the xanthene family and one of the most commonly used fluorescent dyes. It was regarded as an ideal candidate for our studies because in aqueous solution at pH 8 or greater it has excellent fluorescent properties with a QY = 0.9, a molar absorptivity of $\epsilon_{490}=78,000 \text{ Abs}(\text{Mcm})^{-1}$, and therefore a brightness of 70,000 (brightness = $(\Phi)\epsilon_{\lambda_{\text{max}}}$). Moreover, fluorescein is known to photobleach quickly, a process that has been extensively studied.^{10,11,12} It is important to note that fluorescein can exist in the open or closed (lactone) form, as well as in multiple protonation states (Figure 4).¹³ These different species of fluorescein have unique spectral properties that result in a pH

dependent fluorescence.¹⁴ At physiological pH, dianionic fluorescein predominates, a factor that must be considered in experimental conditions.

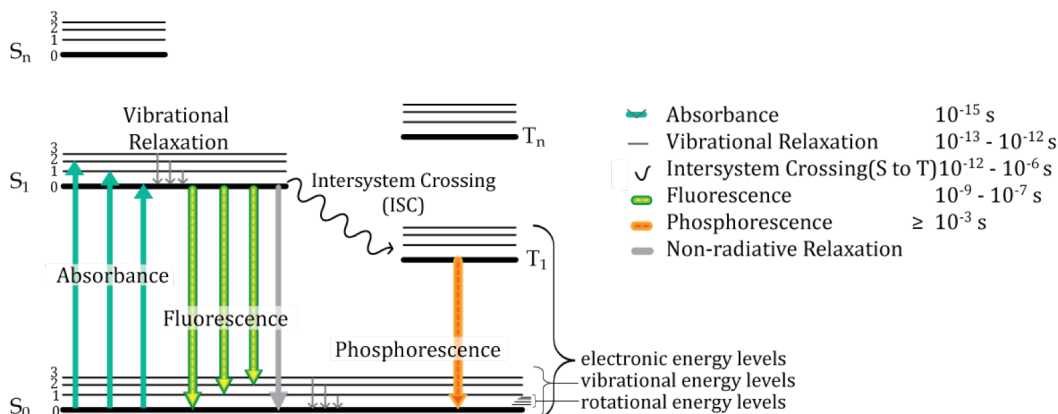
Figure 1.4. Protonation States of Fluorescein at pH 1-10¹⁵



Photobleaching of Fluorescein

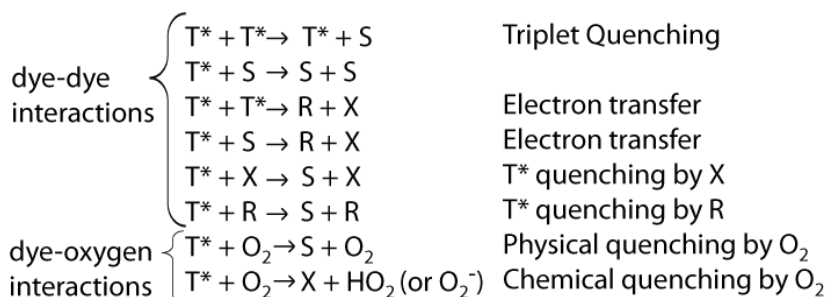
When designing a system to enhance the photostability of fluorescein, it would be prudent to understand how the dye photodegrades. The photobleaching processes of fluorescein are dependent on dye concentration, oxygen concentration and the presence of other species (e.g., quencher), among other variables. Of particular importance are the reactions of the triplet state, which is formed when an excited molecule, S^* , undergoes intersystem crossing (ISC), Figure 1.5. Despite the fact that the percentage of molecules that undergo ISC is small, a build-up of dye in the non-fluorescent triplet state (T^*) is observed due to its relatively long lifetime. Generally, at high dye concentration, dye-dye quenching of the triplet state is the primary cause of photobleaching, but when the concentration of dye is lowered, to $\sim 20\%$ that of dissolved oxygen, dye-oxygen reactions were found to predominate.¹⁶ There are, however, many reactions that contribute to the dye-dye and dye-oxygen photobleaching, a few of which are listed in Figure 1.6. A key mechanism to decrease photobleaching is to quench the triplet state. This is desirable because the ground state dye is regenerated allowing the fluorophore to be excited again,

Figure 1.5. Jablonski Diagram



but triplet state quenching can also form permanently non-fluorescent molecules or reactive oxygen species (ROS). The complexity of possible photodegradation pathways is further complicated by the fact that the mechanisms of photobleaching can be different depending whether the fluorophore is studied alone in free solution or whether it is linked to another species, e.g., a biomolecule.¹⁷

Figure 1.6. Reactions of Triplet State Fluorescein



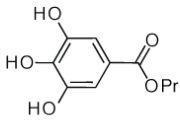
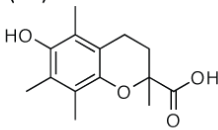
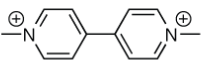
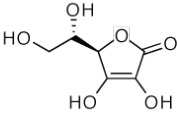

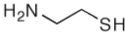


where S = ground state, T^* = triplet state, X = semi-oxidized dye, R = semi-reduced dye

Anti-Fading Agents

As indicated above, photobleaching can occur via several pathways and consequently, AFAs have been found to decrease photobleaching through several different mechanisms, namely triplet state quenching, radical quenching, and reacting with singlet oxygen. A

relatively new concept to fight photobleaching is a reducing and oxidizing system (ROXs), which employs both an oxidant and reductant to react with the triplet state sequentially, effectively returning the dye to the ground state.¹⁸ The most common AFAs and comments pertaining to their use are reported in Table 1.1.

Table 1.1. Common Anti-Fading Agents (AFA)s¹⁹

| AFA | structure | comments | AFA | structure | comments |
|---|---|---|-----------------------------------|--|--|
| <i>n</i> -propyl gallate (nPG) |  | necessary to modify the center phenol when conjugating to HPG, synthesis of derivatives has been achieved | trolox (TX) |  | can function as both oxidant and reductant through equilibrium with quinone form; derivitization effect the TX-quinone equilibrium |
| methyl viologen (MV) |  | toxic, is known to undergo redox cycling and generate ROS, easily derivitized, often used with AA | ascorbic acid (AA) |  | vitamin C, mild reductant |
| diazabicyclooctane (DABCO) |  | contained in Fluoro Gel, difficult to functionalize | mercaptoethylamine (MEA) |  | has been shown to quench decrease fluorescence, controlling reactivity of two nucleophiles may prove difficult |
| <i>p</i> -phenylenediamine (PPD) |  | toxic, contained in Vectashield, free amine can undergo undesirable reactions | cyclooctatetraene (COT) |  | not water soluble, not easily derivitized |

The published studies of anti-fading agents and fluorescein,^{20,21} indicate that propyl gallate is likely the best suited AFA to our system, thus preliminary work was carried out with gallate derivatives. Many of the reported studies are in solutions containing a high percentage of ethylene glycol^{22,23} which alters viscosity, known to be a key determinant in photostability, a factor that must be considered when evaluating the data.²⁴ Since the project began, several key reports about the use of ROXs have been published; suggesting that trolox and methyl viologen may also be well suited AFAs.²⁵ With these considerations

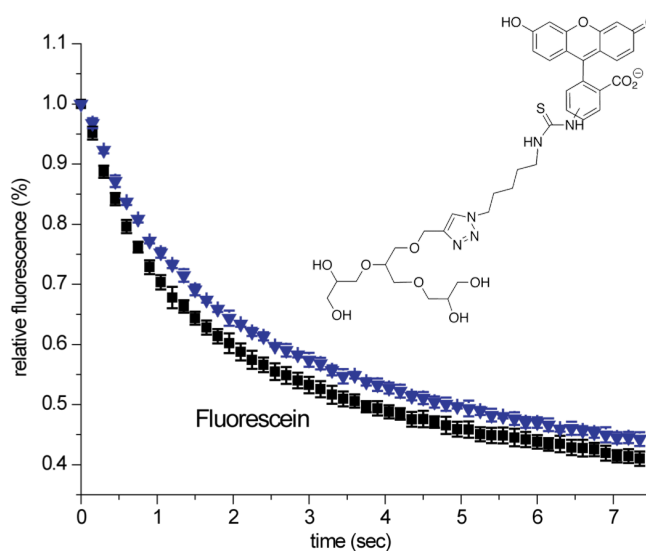
in mind, preliminary studies were conducted to determine the feasibility of synthesizing a brightly fluorescent HPG with superior photostability through the covalent conjugation of multiple fluorescein and AFA moieties.

Preliminary Work

The results of the initial work performed by Andrew Zill, are briefly discussed. The fluorescence and photobleaching rate of fluorescein, and fluorescein conjugated to an HPG were compared (Figure 1.7). Although there was initial quenching, no difference in the photostability was observed, indicating that conjugation to the HPG does not alter the photostability of fluorescein, at least not when a long (8 atom) tether was employed.

Propyl gallate has been shown to decrease the photobleaching of fluorescein,^{26,27} and was, therefore the initial AFA target. Several gallate derivatives were prepared and their ability to inhibit the photobleaching of fluorescein studied (Figure 1.8).²⁸

Figure 1.7. Photobleaching curves of fluorescein (black square) and a HPG-fluorescein derivative (blue triangle) at 1 μ M [dye].



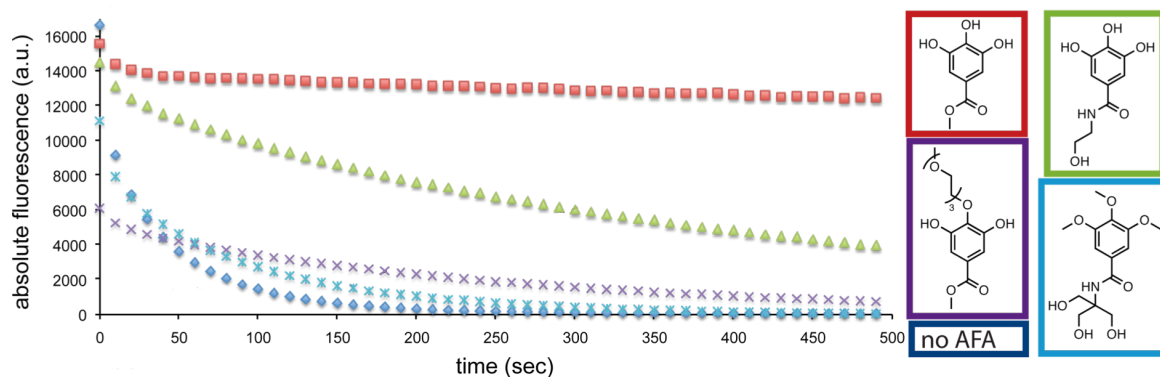
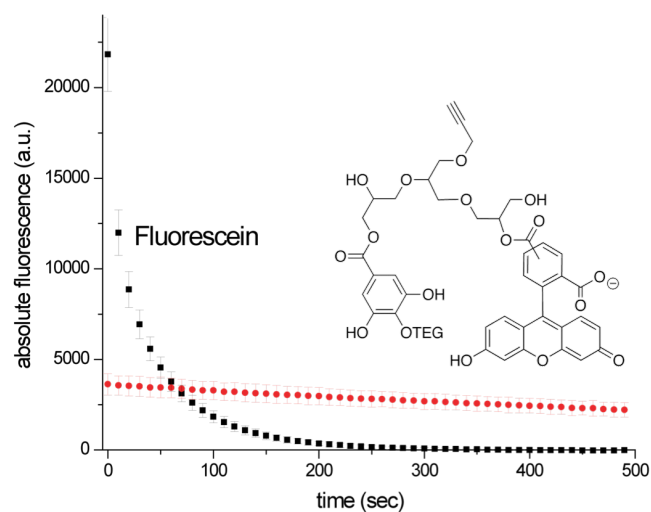


Figure 1.8. Photobleaching curves of fluorescein with various gallate derivatives

These data provide insight into possible modifications that can be made to gallate in order to conjugate the AFA to HPGs while maintaining the anti-fading properties. It was found that changing the ester to an amide or alkylating the phenoxy groups significantly decrease the anti-fading properties of methyl gallate. The methyl gallate derivative with triethyleneglycol (TEG) significantly quenches fluorescence but decreases photobleaching better than the other gallate derivatives tested.

The TEG-gallate derivative was successfully attached to HPG with a single copy of fluorescein. Photobleaching studies showed that despite initial quenching, the gallate moieties substantially increased the photostability of the conjugated fluorescein (Figure 1.9).

Figure 1.9. The photobleaching of fluorescein and a HPG with ~ 4 gallate moieties and a single fluorescein. TEG = triethylene glycol



Given these promising results, a more rigorous study was necessary to determine the optimal ratio between AFA and fluorescein to maximize photostability. To create a brighter fluorophore, and to counteract the quenching effect of dye conjugation to the HPG, multiple dye moieties were attached to the polymer. In addition, a control series was synthesized and studied to investigate the effects of the number of fluorescein and size of HPG has on brightness and photostability.

I.C. Results and Discussion

HPG Synthesis

HPGs were synthesized by deprotonation of 15-25% of the OH groups of 5-hexynol with base followed by slow addition of glycidol (Scheme 1.1).^{29,30} The molecular weight was controlled by the initiator to monomer stoichiometric ratio (core:glycidol) with a low polydispersity achieved ($PDI \leq 1.8$) by slow-addition of monomer. No difference was observed between product polymers obtained with potassium methoxide or sodium hydride as the base. Because of the high viscosity of the HPG as molecular weight increases, 1,4-dioxane was added to allow for stirring during polymerization of HPGs with target molecular weight over 20,000.²⁹

Large quantities of low molecular weight HPGs were prepared to ensure that all future studies were carried out with the same polymer sample. Isolating HPGs under 10 kDa proved most effective by precipitating from methanol with diethyl ether. By combining polymers of similar size from multiple reactions³¹ and reprecipitating multiple times, a series of 5 different sized polymers were isolated, Table 1.2.

Scheme 1.1. Synthesis of hyperbranched polyglycerol

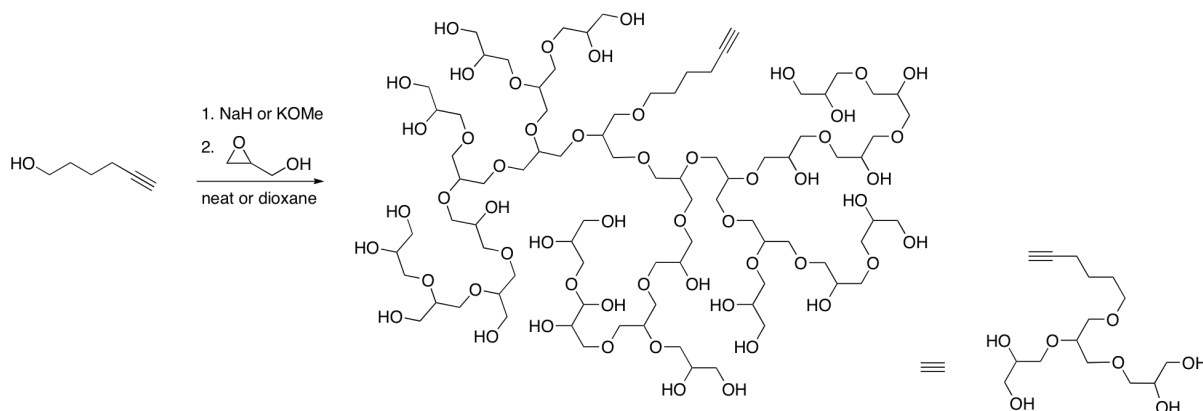


Table 1.2. Low Molecular Weight HPG Series (kDa)

| Name | Water SEC | | | ~ Mass | DMF SEC | | |
|------|-----------|-------|-----|--------|---------|-------|-----|
| | M_n | M_w | PDI | | M_n | M_w | PDI |
| A | 1.2 | 1.7 | 1.4 | 30 g | 1.5 | 1.8 | 1.3 |
| B | 1.8 | 2.9 | 1.6 | 40 g | 2.3 | 3.0 | 1.3 |
| C | 3.9 | 6.5 | 1.7 | 25 g | 4.3 | 5.4 | 1.3 |
| D | 4.6 | 8.0 | 1.8 | 100 g | 4.5 | 5.8 | 1.3 |
| E | 7.3 | 12.3 | 1.7 | 30 g | 7.8 | 9.7 | 1.3 |

MW determined based on calibration with linear PEG

Each value reported is an average of results of triplicate samples. A full table of results is in Chapter IV. Appendices.

Polymers with high molecular weight have also been prepared; however, it is difficult to predict the exact molecular weight of the product polymer (Table 1.3). This problem has been documented in the Zimmerman lab, as well as others.^{29,32} The poor predictability is thought to originate in small variations in the extent of deprotonation of the initiator, possibly a result of trace amounts of water, which results in large differences in product molecular weight. The relative pK_a s of the initiator and glycidol must also be considered. The larger HPGs form a white semi-solid when precipitated, which was filtered off, and

dialyzed (8000 kDa MWCO). Larger polymers were found to have narrower PDIs and required a less tedious work-up but were lower yielding.

Table 1.3. High Molecular Weight HPGs (kDa)

| Name | M _n | M _w | PDI | Target MW | Equivalents of base |
|------|----------------|----------------|-----|-----------|---------------------|
| F | 60.0 | 47.0 | 1.2 | 19,300 | 0.19 KOMe |
| G | 34.0 | 43.0 | 1.3 | 25,100 | 0.15 NaH |
| H | 42.0 | 52.6 | 1.2 | 20,900 | 0.24 KOMe |

Target MW is determined by the stoichiometric ratio of initiator: monomer

Equivalents base is equivalents relative to initiator

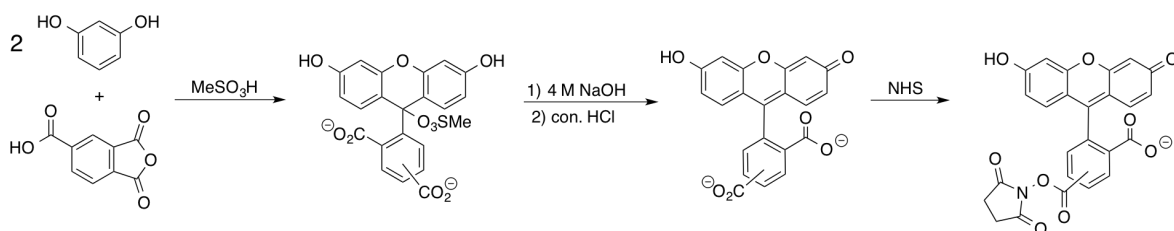
Values determined by comparison to linear PEG standards on water SEC

The HPGs were characterized by ¹H NMR, water SEC and DMF SEC in attempts to accurately determine their molecular weight but there were large discrepancies depending on the technique used.³³ Briefly, the values calculated from ¹H NMR integrations over-estimate the size of the polymers because it is assumed all polymers originate with 5-hexynol. The water SEC is thought to under-estimate the size of the polymers because of physical interactions with the matrix. The DMF SEC is believed to provide the most accurate MW values. The relationship between the determined MW values according to the three techniques has been quantified and discussed further in Chapter IV. Appendices. Comparison of the different values also allowed for the estimation of the percentage of HPGs that had initiator incorporated which was generally 30-50%.

Fluorescein Synthesis

Most applications of fluorescein require small (milligram) quantities of dye or the appropriate derivative, and are commercially available but for our studies larger quantities of dye were needed. Fluorescein is traditionally synthesized by Friedel-Crafts reaction as reported by Baeyer in 1871. Newer procedures have been published with higher yields

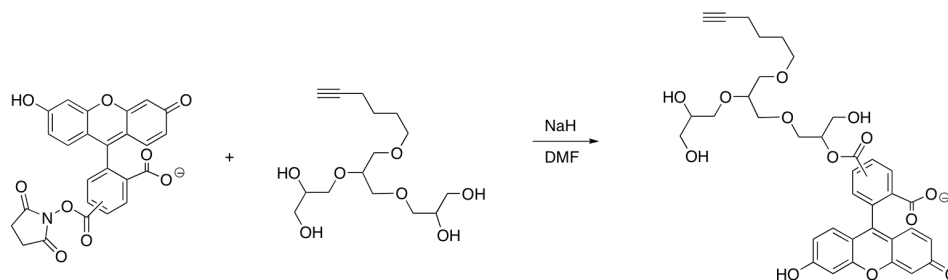
under milder conditions using methylsulfonic acid as a solvent (Scheme 1.2).³⁴ This synthetic pathway to carboxyfluorescein was scalable. The NHS ester was then generated.



Scheme 1.2. Synthesis of 5(6)-Carboxy Fluorescein and Fluorescein-NHS (F-NHS)

HPG-Fluorescein control series

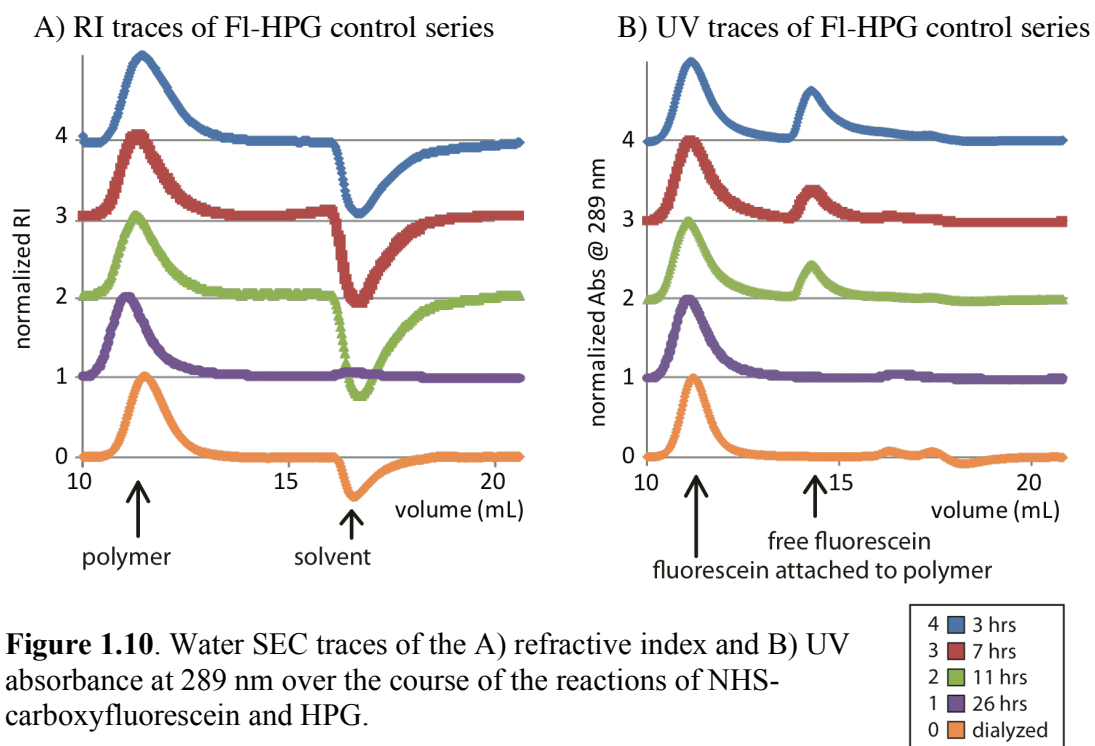
Once the HPGs and F-NHS were synthesized, a fluorescein control series was prepared to study the effects of the number of dye moieties as a function of polymer MW. Activated *N*-hydroxysuccinimide carboxyfluorescein was coupled to HPG, Scheme 1.3. Fluorescein



Scheme 1.3. Fluorescein conjugation to HPG

attachment to HPG was monitored by the UV absorbance trace of water SEC samples. Figure 1.10 shows the RI and UV traces at given time points during a representative reaction. The RI traces show the polymer peak at approximately 11 mL and residual solvent peak at 17 mL. The UV traces, again, show the polymer peak at 11 mL but also uncoupled fluorescein at 14-15 mL. HPGs have negligible UV absorbance. Therefore, the

peak observed was attributed to coupled fluorescein. Free fluorescein indicates that the reaction has not gone to completion and requires more time or base. On occasion the free fluorescein peak remained despite additional base and time, this was likely a result of degradation of the activated NHS ester to carboxyfluorescein which does not couple under the given conditions. After the reaction was complete, the polymer was dialyzed (2000 MWCO) to remove free fluorescein and other small molecule impurities.



The ^1H NMR of HPG-fluorescein polymers were collected but provided limited information, the ratio of peak integration was too large to be accurate. Some of the aromatic peaks of fluorescein appear broadened while others remain sharp. This difference was thought to result from the different environments of the conjugated fluorescein; i.e., the extent to which fluorescein is exposed to solvent or surrounded by

polymer. Once thoroughly dried to obtain an accurate mass, each polymer was characterized by UV-vis and fluorescence spectroscopy.

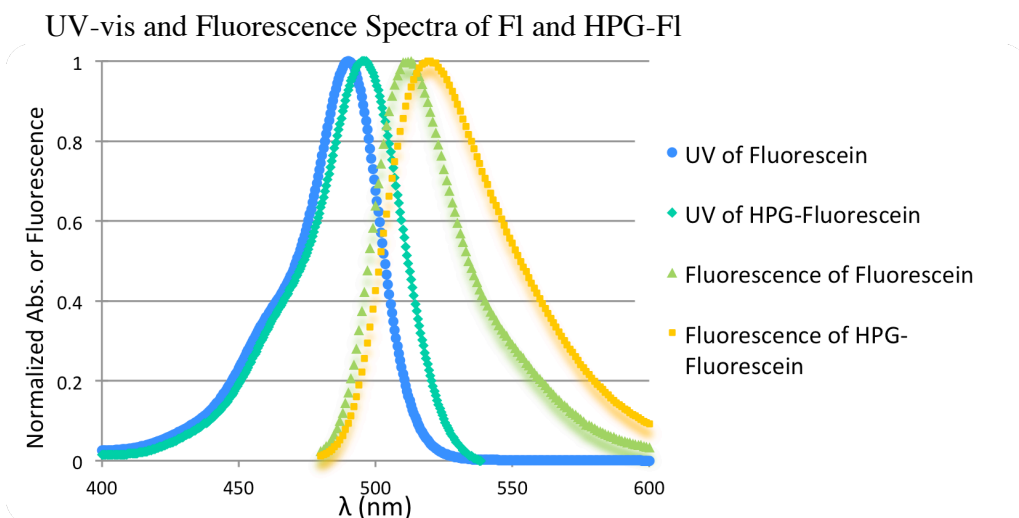


Figure 1.11. UV-vis and Fluorescence Spectra of free Fluorescein and HPG-fluorescein conjugate (excited at 475 nm).

The molar absorptivity, calculated from Beer's Law plots, was used to determine the number of fluorophores per polymer. The molar absorptivity of fluorescein was determined to be $\epsilon_{\lambda 490} = 78,000 \text{ Abs}(\text{Mcm})^{-1}$ in the given conditions, 10 mM sodium phosphate buffer at pH 8.0. Figure 1.11 shows representative spectra of the HPG-fluorescein control series. A slight bathochromic shift ($\leq 10 \text{ nm}$) was observed in both the UV and fluorescence spectra of fluorescein conjugated to HPG. To determine the quantum yield, Φ , and brightness, the fluorescence spectra of each sample was collected by exciting at $\lambda = 475 \text{ nm}$ and monitoring from 480–600 nm. The linear fit of absorbance vs. fluorescence plot provides a response factor (the slope) that when compared to fluorescence response factor of fluorescein, $\Phi = 0.9$, gives the quantum yield (Figure 1.12). The results of the spectroscopic studies are reported in Table 1.4. A lengthier explanation

of the work-up of fluorescence, as well as spectroscopic data for all polymers can be found in Chapter IV. Appendices.

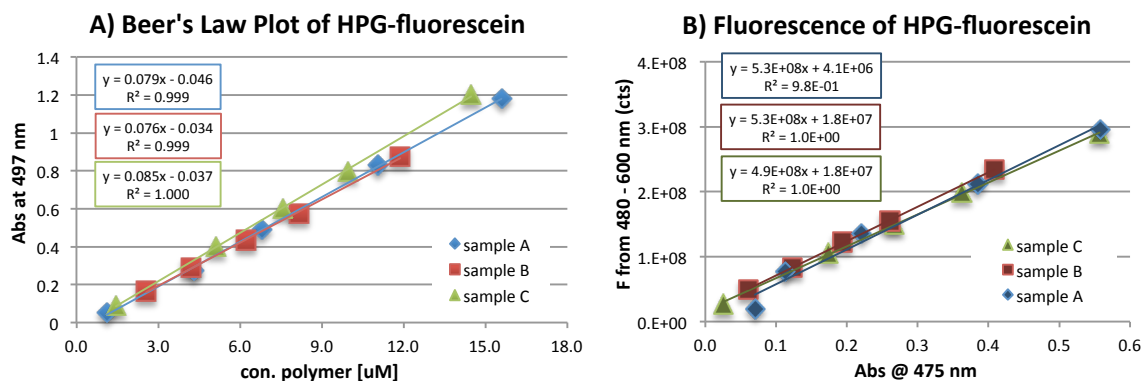


Figure 1.12. Plots of spectroscopic data of a representative polymer from the HPG-fluorescein control series. A) Beer's Law plot of three different samples of the same polymer B) Plot of integrated fluorescence value vs. absorbance at 475 nm.

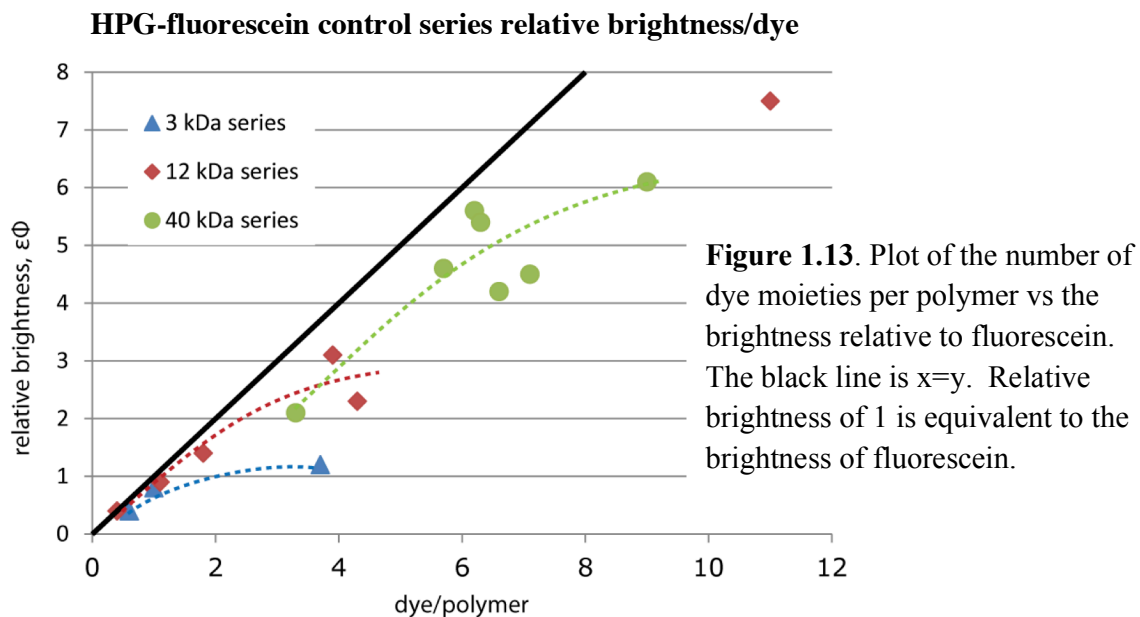
Table 1.4. Spectroscopic data of HPG-fluorescein control series

| Reference # | | 55 | 56 | 57 | 52 | 53 | 83 | 84 | 85 | 86 |
|--------------------------------------|-----|---------------|------|------|---------------|------|------|------|------|------|
| SM M_w (kDa) (SEC _{H2O}) | dye | 3 kDa series | | | 12 kDa series | | | | | |
| SM M_w (kDa) (SEC _{DMF}) | | 7 | 7 | 7 | 29 | 29 | 29 | 29 | 29 | 29 |
| dye / polymer | | 1.0 | 0.6 | 3.7 | 0.4 | 4.3 | 1 | 2 | 4 | 11 |
| $\epsilon_{\lambda_{max}}$ | 78 | 78 | 43 | 290 | 33 | 334 | 88 | 140 | 302 | 860 |
| ϕ | 0.9 | 0.71 | 0.61 | 0.28 | 0.77 | 0.49 | 0.71 | 0.69 | 0.71 | 0.61 |
| brightness (ϵ) ϕ | 70 | 55 | 26 | 81 | 25 | 164 | 62 | 97 | 214 | 525 |
| rel. brightness | 1.0 | 0.8 | 0.4 | 1.2 | 0.4 | 2.3 | 0.9 | 1.4 | 3.1 | 7.5 |
| reference # | | 69 | 70 | 72 | 78 | 79 | 80 | 81 | | |
| SM M_w (kDa) (SEC _{H2O}) | dye | 40 kDa series | | | | | | | | |
| SM M_w (kDa) (SEC _{DMF}) | | 82 | 82 | 82 | 82 | 82 | 82 | 82 | | |
| dye / polymer | | 9.0 | 6.2 | 5.7 | 3.3 | 6.6 | 7.1 | 6.3 | | |
| $\epsilon_{\lambda_{max}}$ | 78 | 700 | 480 | 445 | 261 | 519 | 557 | 488 | | |
| ϕ | 0.9 | 0.61 | 0.81 | 0.72 | 0.55 | 0.57 | 0.57 | 0.78 | | |
| brightness (ϵ) ϕ | 70 | 427 | 389 | 320 | 144 | 296 | 317 | 381 | | |
| rel. brightness | 1.0 | 6.1 | 5.5 | 4.6 | 2.0 | 4.2 | 4.5 | 5.4 | | |

$\epsilon_{\lambda_{max}}$ reported as Abs/Mcm⁻¹

dye = free fluorescein

Values reported are an average of triplicate samples measured



It was found that linking more fluorescein units to the polymer yields brighter polymer but with each additional fluorophore increase the brightness by a smaller increment (Figure 1.13). It is well documented that fluorescein is partially quenched when conjugated to biopolymers.³⁵ Furthermore, if the labeling density of dye is high, dye-dye interactions cause increased rates of photobleaching.^{36,37} Under a specific set of conditions, each fluorophore-biomolecule conjugate has an optimal number of dye moieties, after which additional dye decreases the total brightness, not just the additional brightness per dye. The above observations were consistent with reported studies where the maximum brightness hasn't clearly defined. The larger polymer was able to accommodate more dye moieties before reaching the perceived maximum brightness. The maximum brightness of the 40 kDa HPG-fluorescein series was achieved with ~ 9 dye per polymer resulting in a

molecule that is ~6 times as bright as free fluorescein. Although more polymers need to be synthesized and tested to draw firm conclusions about the smaller polymers, it does appear that the optimal number of dyes per polymer is considerably lower. This was what was expected; as the proximity of the dye molecules becomes closer the effective concentration is higher leading to dye-dye quenching.

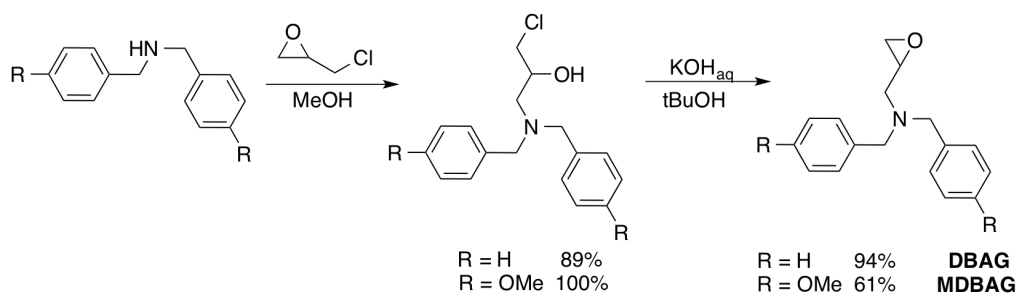
Amine-HPG Synthesis

An amine functionalized HPG was desired not only to circumvent the low loading of the fluorescein to hydroxyl-terminated polymer but also to form an amide linkage to the fluorophore and AFAs instead of the more labile ester. Although amine-HPGs have been reported via derivatization of HPG,³⁸ it was proposed that copolymerization of a protected epoxy amine with glycidol and subsequent deprotection would provide a more direct route. Furthermore, placement of the amines within the polymer (interior vs. exterior) would be controllable by the timing of monomer addition to the polymerization. This approach would also allow precise control over the number of amine groups per polymer.

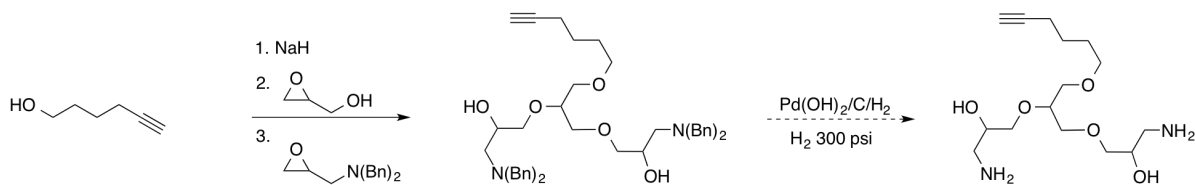
Glycidylphthalimide has been reported as an end-capping agent. It was prepared and successfully copolymerized with glycidol, but the phthalimide group could not be cleanly hydrolyzed. This was thought to be due to a Gabriel-Coleman rearrangement.

Frey and coworkers reported the preparation of a polymer incorporating dibenzylaminoglycidol (DBAG) and it was thought to be a viable alternative to the glycidylphthalimide.³⁹ DBAG was prepared in two steps from epichlorohydrin (Scheme 1.4). Dibenzylamine nucleophilic attack results in ring-opening of the epoxy to give 3-dibenzylamine-chloroisopropanol in high yield. Ring-closing displacement of the chloro in the presence of base produces the desired DBAG in ~90% crude yield.^{40, 41}

Copolymerizations of DBAG and glycidol were successful, achieving up to 8 groups per polymer (Scheme 1.5). However, attempts to remove the benzyl protecting groups to create the free amine failed. *Para*-methoxydibenzylaminoglycidol (MDBAG) was synthesized (Scheme 1.4), and copolymerized with glycidol. Again, it could not be deprotected.

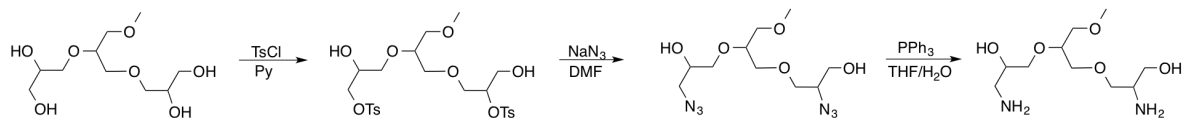


Scheme 1.4. Synthesis of dibenzylaminoglycidol (DBAG) and dip-*para*-methoxybenzylamino glycidol (MDBAG).



Scheme 1.5. Proposed synthesis of amine-HPG via copolymerization of glycidol and DBAG followed by hydrogenation.

Despite much effort to prepare an HPG with amine groups via copolymerization of glycidol and a protected amine monomer, this pathway failed to provide an efficient route to the desired product. Whereas the reported synthesis of amine containing HPG includes three steps after polymerization (Scheme 1.6) it has proved reproducible and less time consuming than the copolymerization pathway. First, HPG is mesylated or tosylated, followed by reaction with sodium azide and finally reduction to the desired amine.

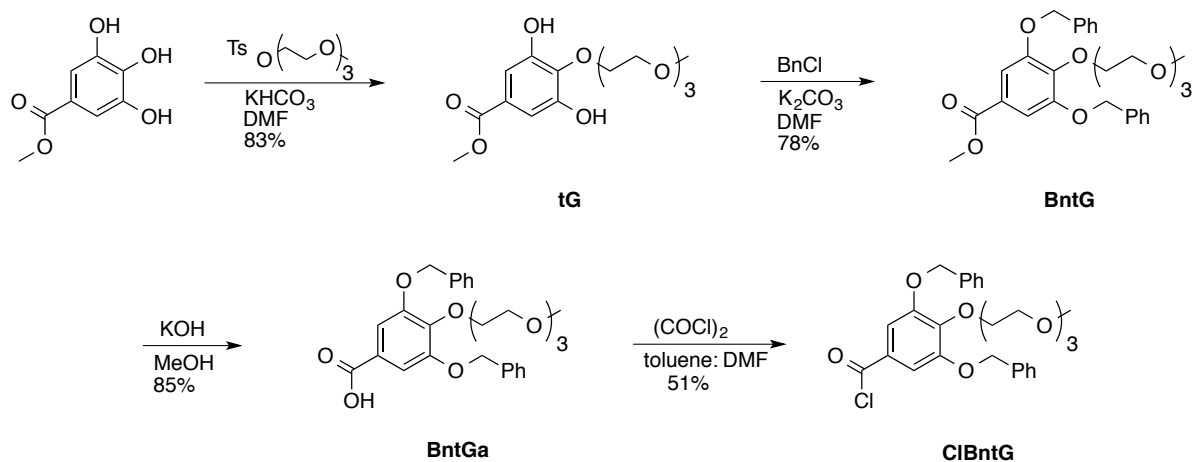


Scheme 1.6. Synthesis of HPG derivative containing amines

Anti-Fading Agent Derivatization

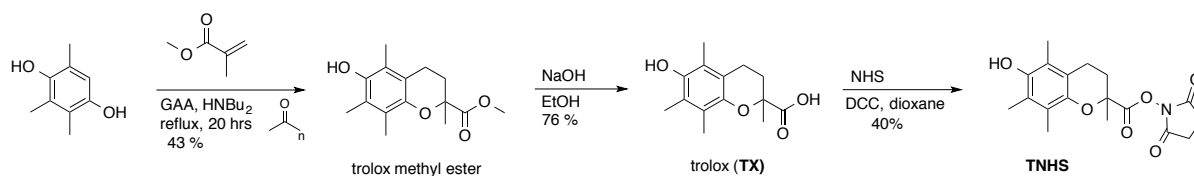
To directly attach AFAs to HPG, derivatives of the AFAs were synthesized. Gallate, and trolox, were both derivatized to include an acid chloride and activated ester group, respectively, functionality that allows ready coupling to HPG. The synthetic scheme to make dibenzylTEG gallic acid chloride (tG)⁴² is straight forward (Scheme 1.7). Thus, the *para*-phenol of methyl gallate was PEGylated with triethylene glycol tosylate and the 3,5 phenol groups were benzyl protected. It was found necessary to protect the phenol groups of gallate derivatives when coupling to HPG to avoid significant cross-linking.⁴³

Subsequent treatment of the methyl ester, BntG, with base gave the acid, BntGa, which was reacted with oxalyl chloride to yield the acid chloride, ClBntG.



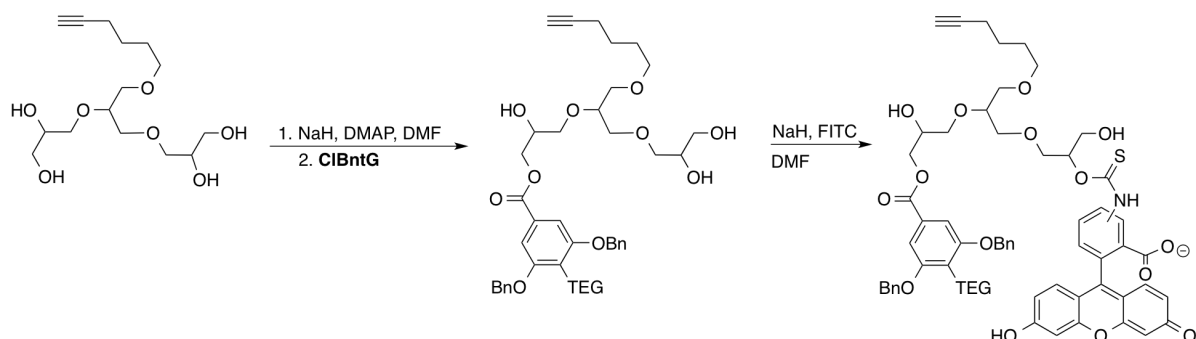
Scheme 1.7. Synthesis of gallate derivatives for attachment to HPGs

Trolox methyl ester has also been synthesized (Scheme 1.8).⁴⁴ Trolox (TX) was prepared by demethylation of the ester which was then reacted with NHS to yield *N*-hydroxy succinimide trolox (TNHS).



Scheme 1.8. Synthesis of Trolox Derivatives

To achieve direct attachment of gallate to HPG, ClBntG was reacted with HPG in large excess (Scheme 1.9). Successful conjugation of gallate to the HPG was sporadic and there was little control over the number of gallate moieties attached. Inconsistencies in the coupling were likely a result of trace amounts of water in the HPG despite significant efforts to dry the polymer (see Chapter III. Experimental for details). The SEC trace of the HPG-gallate polymer had slight shift to shorter retention times (than the starting HPG) indicated an increase in molecular weight (Figure 1.14). Incorporation of fluorescein into the polymer, increased the molecular weight slightly but was quite evident in the UV-vis spectrum by the peak around 500 nm. Attempts to deprotect the phenols groups of the gallate moieties via hydrogenation were unsuccessful. To circumvent this problem a gallate derivative was resynthesized with THP as the protecting groups.



Scheme 1.9. Synthesis of HPG-Gallate-Fluorescein conjugates (HPG-G-FI)

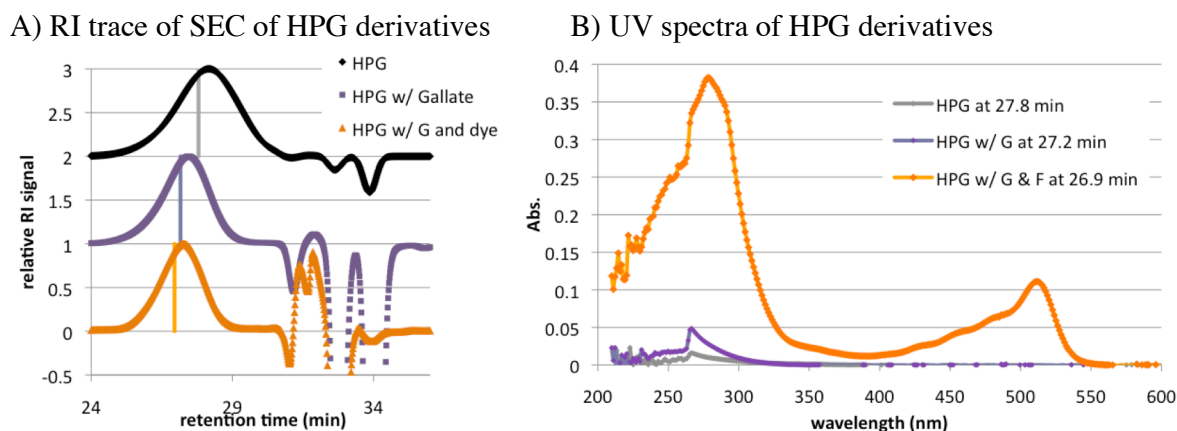


Figure 1.14. A) RI trace of SEC chromatograph of HPG, HPG with gallate and HPG with gallate and fluorescein. There's a slightly faster elution time of HPGs with appendages. B) UV spectra at the indicated time (line) during the SEC run. The HPG has negligible UV absorbance, the HPG with gallate has slight absorbance around 270 nm, and the HPG with gallate and fluorescein has significant absorbance around 500 nm and 270 nm.

New Direction

Blanchard and coworkers found that the stabilizing properties of trolox on Cy5 were largely dependent on their distance. This finding led to a new direction in the project. The new aim was to covalently attach the AFA and fluorescein prior to conjugating to the HPG, (Figure 1.15). This new design would guarantee the AFA and dye are in close proximity,

whereas before a random distribution was expected. It was also anticipated that connection of the dye and AFA might alleviate the difficult of direct conjugation to the HPG.

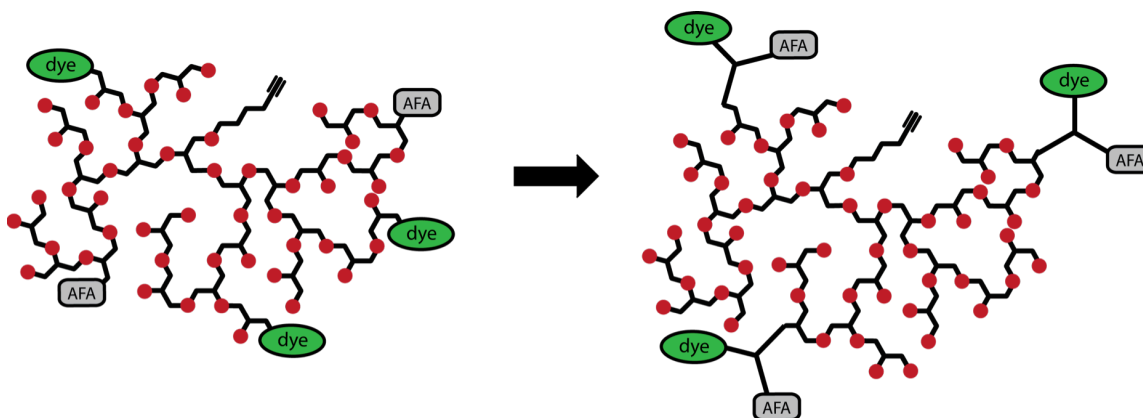


Figure 1.15. Previous conceptualization of HPG-AFA-FI design and the new conceptualization of dye and AFA linked and then linked to HPG.

Design and Synthesis

Lysine was chosen to link fluorescein and an AFA together prior to conjugation to the HPG because it was commercially

available as a free acid with two different protecting groups on the amines, allowing for reaction in controlled succession (Figure 1.16). However, this also requires that the HPG be derivatized to include functional groups capable of reacting with the lysine side-chain amine. Therefore, an HPG with carboxylic acid groups was pursued.

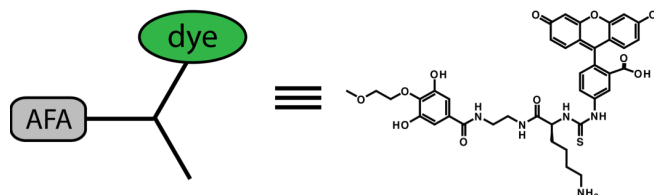
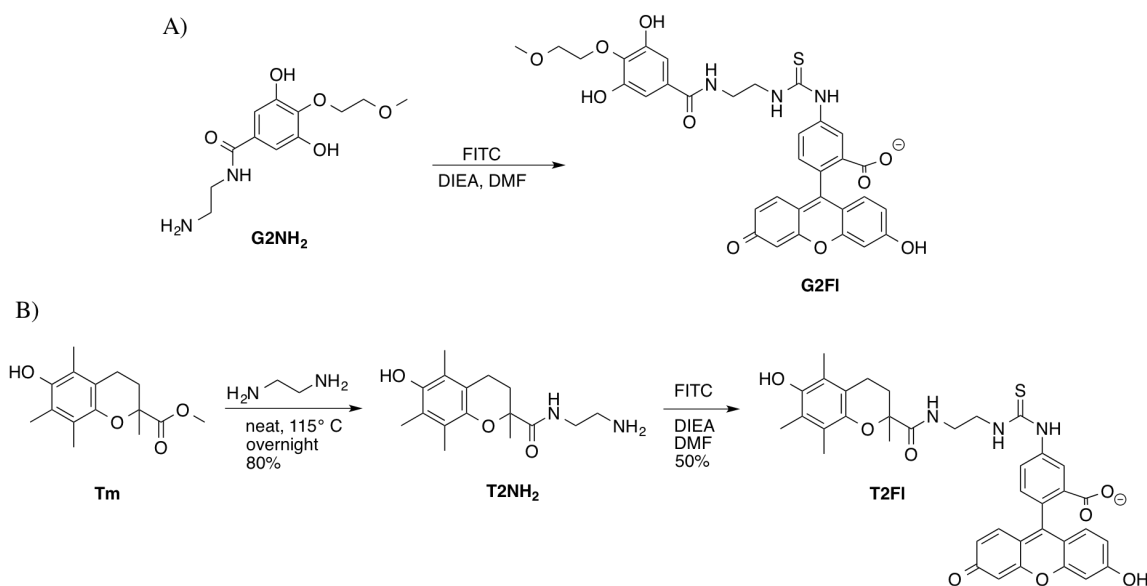


Figure 1.16: Conceptualization of AFA and dye linkage and molecular structure

Control Compounds

Control compounds to test the effects of covalently linking the AFAs of interest (gallate and trolox) to fluorescein were synthesized and studied. Ethylenediamine was chosen as the linker because of its reactivity and short length. Each AFA was reacted with excess ethylenediamine and then FITC to form the conjugates T2Fl and G2Fl (Scheme 1.10). It is



important to note that both conjugated AFAs contain amide groups where trolox is typically used as an acid and gallate as a methyl or propyl ester. These alterations to the AFAs structure were thought to effect the photostabilizing capabilities, however, amides were the proposed and pursued linkage to the lysine moiety, so the effect was relevant. The control compounds were studied as well as GLys(Boc)Fl (Table 1.5). A slight decrease in molar absorptivity and a slight bathochromic shift were observed in all three compounds. Both effects are common and anticipated. A significant decrease in the

Table 1.5. Spectroscopic Characterization of AFA-Fl Conjugates

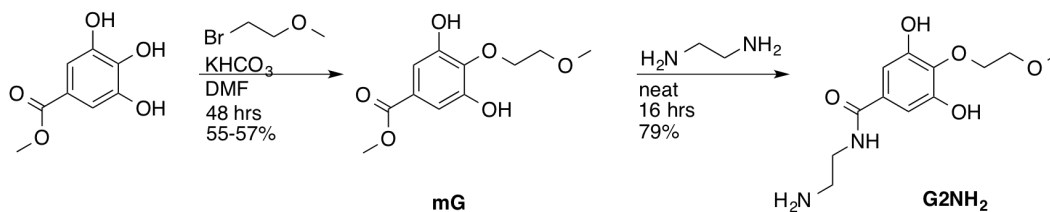
| | G2Fl | T2Fl | GLys(Boc)Fl | fluorescein |
|------------------------------|-------------|-------------|--------------------|-------------|
| $\epsilon_{\lambda_{\max}}$ | 75 | 70 | 72 | 78 |
| λ_{\max} (nm) | 494 | 494 | 493 | 488 |
| ϕ | 0.35 | 0.15 | | 0.9 |
| Brightness: $(\epsilon)\phi$ | 26.7 | 10.5 | | 70.2 |
| rel. brightness | 0.38 | 0.15 | | 1 |

quantum yield is often observed when dyes, particularly fluorescein, are conjugated, as observed in HPG-Fl compounds. The quantum yields of the control compounds were even lower, possibly due to the amide linkage or other functionalities introduced by the AFA.

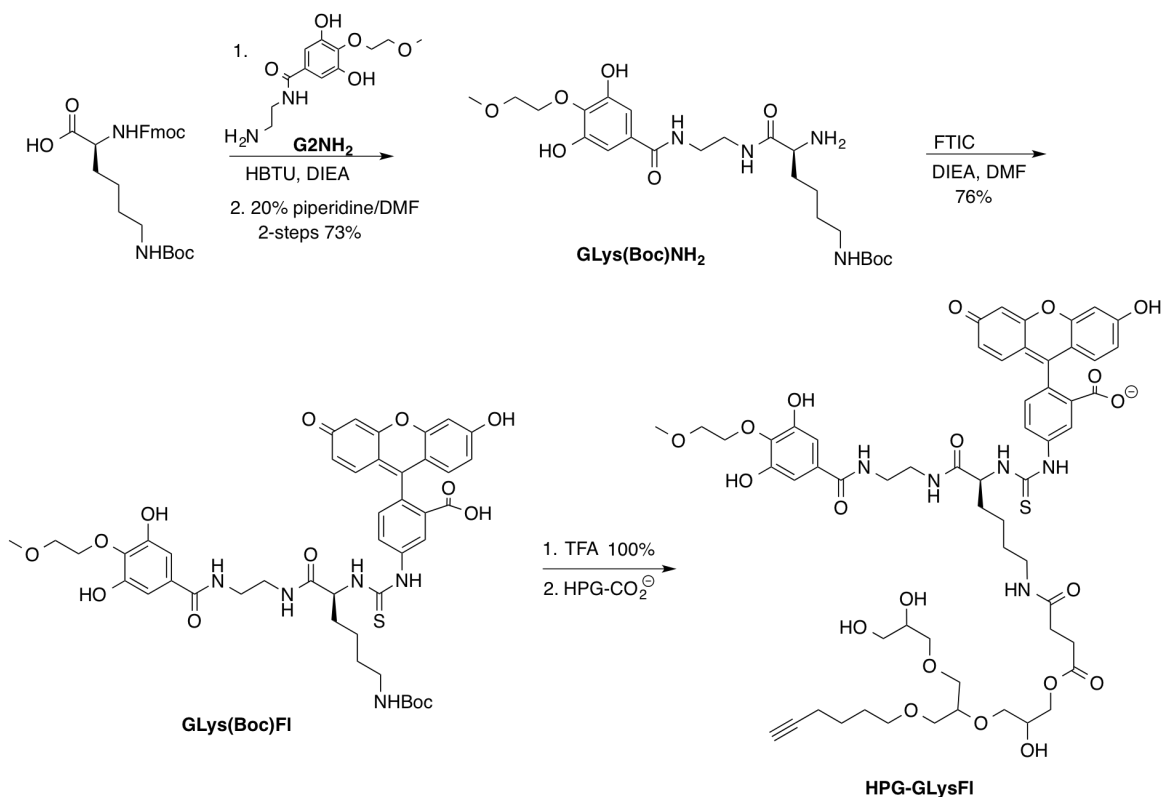
The decrease in brightness of the AFA-Fl conjugates was not a significant problem because it could be overcome by attaching multiple moieties to a HPG. The previously mentioned control HPG-Fl series indicated that the 12 and 40 kDa HPGs could accommodate many fluorescein residues before reaching maximum brightness.

Linker Synthesis

Once the effects of linking fluorescein and the AFAs were quantitatively evaluated, the synthesis of the gallate-lysine-fluorescein conjugate (GLys(Boc)Fl) was undertaken. The gallate-containing compound was pursued first because of the higher relative brightness of the control compound, G2Fl, compared to T2Fl. Like previously synthesized gallate compounds, the *para* phenol group was alkylated, to give mG (Scheme 1.11). The terminal amine group was coupled to the carboxylic acid group of Lys(boc)fmoc (Scheme 1.12). Selective deprotection of fmoc followed by coupling to FITC yielded GLys(boc)Fl.



Scheme 1.11. Synthesis of gallate amine derivative, G2NH₂. The para phenol group was reacted to help stabilize the gallate group, and then the methyl ester reacted with ethylenediamine for further conjugation with carboxylic acid groups.

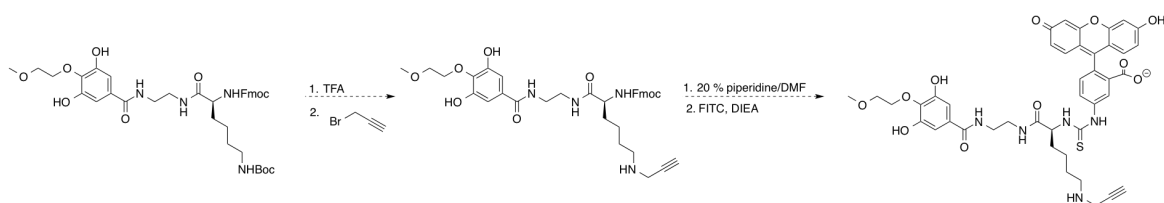


Scheme 1.12. Synthesis of HPG-GLysFl conjugate. The gallate derivative G2NH₂ was coupled to the acid of a diprotected lysine. Selective deprotection of one amine group allowed coupling to FITC to install a fluorescein moiety. Deprotection of the side-chain amine then allowed coupling to HPG-CO₂-C₃H₆-CO₂H.

methylester, mG, was then reacted with ethylenediamine to provide G2NH₂. The free
 Deprotection of the side-chain amine generated GLys(NH₂)Fl ready to be coupled to HPG.

changes in molecular weight were observed. This indicates that SEC is not a reliable way to determine the number of acid moieties incorporated. The relatively uniform increase in molecular weight could be due to alteration in how the polymer interacts with the SEC matrix or an increase in polymer size due to loss of the smallest polymers from repeated precipitation during work-up. ¹H NMR spectra were collected and integration of the acid peak relative to the polymer initiator peak indicates the number of acid moieties incorporated. Before GLys(NH₂)Fl could be conjugated it was decided to pursue a new polymer scaffold for our purposes.

If efforts on the project are resumed and the conjugation of the GLys(NH₂)Fl and HPG-CH₂-CO₂H fails, there are several other synthetic options available. One example is shown in Scheme 1.14, which involves incorporating an alkyne group that could then be clicked to the multi-azide HPG.



Scheme 1.14. Possible G-Lys-Fl derivative attach to HPG

I.D. Conclusions and Future Directions

A variety of HPGs were prepared and derivatized in using several different strategies. Efforts toward an AFA-Fl-HPG were protracted and stopped short of accomplishing their goal. Should HPG be considered for a scaffold in the future the following recommendations are made. The literature method of preparing HPG-amine via mesylation, substitution and reduction, although not ideal, works well enough. While developing an amine comonomer

would allow greater control, in theory, efforts were time intensive and did not work out. Avoid water sensitive reactions with HPG by developing a different synthetic pathway.

The work presented thus far suggests that a different scaffold might be worth pursuing to achieve our goal of covalently attaching multiple AFA and dye moieties in a single molecule. Yugang Bai, in the Zimmerman lab, obtained some promising results using a norbornyl backbone polymer and thus efforts were shifted to focus on this strategy.

I.E. References

1. Valeur, B.; Berberan-Santos, M. N. *J Chem. Ed.* **2011**, *88*, 731. A Brief History of Fluorescence and Phosphorescence before the Emergence of Quantum Theory
2. Image modified from Diaspro, A.; Chirico, G.; Usai, C.; Ramoino, P.; Dobrucki, J. *Handbook of Biological Confocal Microscopy: 39 Photobleaching*. 3rd Ed. ed Pawley, J. B.; Springer Science Business Media, LLC **2006**, 690.
3. Cordes, T.; Maiser, A.; Steinhauer, C.; Schermelleh, L.; Tinnefeld, P. *Phys. Chem. Chem. Phys.* **2011**, *13*, 6699. Mechanisms and advancement of antifading agents for fluorescence microscopy and single-molecule spectroscopy.
4. Calderón, M.; Quadir, M. A.; Sharma, S. K.; Haag, R. *Adv. Mater.* **2010**, *22*, 190. Dendritic Polyglycerols for Biomedical Applications
5. Wilms, D.; Stiriba, S.; Frey, H. *Acc. Chem. Res.* **2010**, *453*, 129. Hyperbranched Polyglycerols: From the Controlled Synthesis of Biocompatible Polyether Polyols to Multipurpose Applications.
6. Haag, R.; Sunder, A.; Stumbé, J. *J. Am. Chem. Soc.* **2000**, *122*, 2954. An Approach to Glycerol Dendrimers and Pseudo-Dendritic Polyglycerols
7. Resch-Genger, U.; Grabolle, M.; Cavaliere-Jaricot, S.; Nischke, R.; Nann, T. *Nat. Meth.* **2008**, *5*, 763. Quantum dots versus organic dyes as fluorescent labels
8. Lavis, L.; Raines, R. *ACS Chem. Bio.* **2008**, *3*, 142. Bright Ideas for Chemical Biology.
9. Giepmans, B. N. G.; Adams, S. R.; Ellisman, M. H.; Tsien, R. Y. *Science* **2006**, *312*, 217. The Fluorescent Toolbox for Assessing Protein Location and Function.

10. Krüger, J.; Memming, R. *Ber. Bunsenges. Phys.* **1974**, *78*, 670. Formation of Reactions of Long Lived Xanthene Dye Radicals. I. Photochemical Studies on Reactions of Semireduced Fluorescein
11. Krüger, J.; Memming, R. *Ber. Bunsenges. Phys.* **1973**, *78*, 879. Formation of Reactions of Long Lived Xanthene Dye Radicals. II. Photochemical Reduction of Rhodamine-B and Fluorescein Derivatives
12. Krüger, J.; Memming, R. *Ber. Bunsenges. Phys.* **1974**, *78*, 685. Formation of Reactions of Long Lived Xanthene Dye Radicals. III. Spectroelectrochemical Investigations on the Reduction of Xanthene Dyes
13. Yguerabide, J.; Talavera, E.; Alvarez, J. M.; Quintero, B. *Photochem. & Photobio.* **1994**, *60*, 435. Steady-State Fluorescence method for Evaluating Excited State Proton Reactions: Application to Fluorescein
14. Martin, M. M.; Lindqvist, L. J. *Luminescence* **1975**, *10*, 381. The pH Dependence of Fluorescein Fluorescence
15. Yguerabide, J.; Talavera, E.; Alvarez, J. M.; Quintero, B. *Photochem. & Photobio.* **1994**, *60*, 435. Steady-State Fluorescence Method for Evaluating Excited State Proton Reactions: Application to Fluorescein
16. Usui, Y.; Itoh, K.; Koizumi, M. *Bull. Chem. Soc. Japan* **1965**, *38*, 1015. Switch-over of the Mechanism of the Primary Processes in the Photo-oxidation of Xanthene Dyes as Revealed by the Oxygen Consumption Experiments
17. Song, L.; Hennink, E. J.; Young, I. T.; Tanke, H. J. *Biophysical J.* **1995**, *68*, 2588. Photobleaching Kinetics of Fluorescein in Quantitative Fluorescence Microscopy

18. Vogelsang, J.; Kasper, R.; Steinhauer, C.; Person, B.; Heilemann, M.; Sauer, M.; Tinnefeld, P. *Angew. Chem.. Int. Ed.* **2008**, *47*, 5465. A Reducing and Oxidizing System Minimizes Photobleaching and Blinking of Fluorescent Dyes
19. Table expanded and modified from Andrew Zill's Thesis
20. Song, L.; Varma, C. A. G. O.; Verhoeven, J. W.; Tanke, H. J.; *Biophysical J.* **1996**, *70*, 2959. Influence of the Triplet Excited State on Photobleaching Kinetics of Fluorescein in Microscopy
21. Kalinich, J. J.; Ramakrishnan, N.; McClain, D. E. *Free Rad. Res.* **1997**, *26*, 37. The Antioxidant Trolox Enhances the Oxidation of 2',7'-Dichlorofluorescein to 2',7'-Dichlorofluorescein
22. Ono, M.; Murakami, T.; Kudo, A.; Isshiki, M.; Sawadea, H.; Segawa, A. *J. Histochem. & Cytochem.* **2001**, *49*, 305. Quantitative Comparison of Ant-Fading Mounting Media for Confocal Laser Scanning Microscopy.
23. Florijn, R. J.; Slats, J.; Tanke, H. J.; Raap, A. K.; *Cytometry* **1995**, *19*, 177. Analysis of Antifading Reagents for Fluorescence Microscopy
24. The increased viscosity of ethylene glycol alters diffusion rates and oxygen concentration relative to water.
25. Campos, L. A. Liu, J.; Wang, Z.; Ramanathan, R.; English, D. S.; Muñoz, V. *Nat. Meth.* **2011**, *8*, 143. A photoprotection strategy for microsecond-resolution single-molecular fluorescence spectroscopy.
26. Giloh, H.; Sedat, J. W. *Science* **1982**, *217*, 1252. Fluorescence Microscopy: Reduced Photobleaching of Rhodamine and Fluorescein Protein Conjugates by *n*-Propyl Gallate

27. Gaigalas, A. K.; Wang, L.; Cole, K. D.; Humphries, E. J. *Phys. Chem. A* **2004**, *108*, 4378.
Photodegradation of Fluorescein in Solutions Containing *n*-Propyl Gallate
28. Visiting undergraduate Yin Nguyen contributed to this work
29. Kainthan, R. K.; Muliawan, E. B.; Hatzikiriakos, S. G.; Brooks, D. E. *Macromol.* **2006**, *39*, 7708. Synthesis, Characterization, and Viscoelastic Properties of High Molecular Weight Hyperbranched Polyglycerols
30. Haag, R. *Chem. Eur. J.* **2001**, *7*, 327. Dendrimers and Hyperbranched Polymers as High-Loading Supports for Organic Synthesis
31. The work was done in conjunction with two undergraduate students, Jinny Shin and Aaron Gore, who were being taught the art of making and isolating HPGs. The product polymers were combined from five different reactions. Multiple reactions were necessary to allow students the opportunity to carry out the reaction themselves.
32. Zill, A.; Rutz, A. L.; Kohman, R. E.; Alkilany, A. M.; Murphy, C. J.; Kong, H.; Zimmerman, S. C. *Chem. Commun.* **2011**, *47*, 1279. Clickable polyglycerol hyperbranched polymers and their application to gold nanoparticles and acid-labile nanocarriers.
33. Only small HPG with molecular weight of a couple thousand have been observed via MALDI MS and only if a HABA (2-(4'-hydroxybenzeneazo)benzoic acid) matrix was used.
34. Ueno, Y.; Jiao, G.; Burgess, K. *Synthesis* **2004**, *15*, 2591.
35. a. Der-Balian, G. P.; Kameda, N.; Rowley, G. L. *Anal. Biochem.* **1988**, *173*, 59. Fluorescein Labeling of Fab' while preserving single thiol b. Zuk, R. F.; Rowley, G. L.; Ullman, E. F. *Clin. Chem.* **1979**, *25*, 1554. Fluorescence Protection Immunoassay: a new homogenous assay technique.

36. Song, L.; van Gijlswijk, R. P. M.; Yound, I. T.; Tanke, H. J. *Cytometry* **1997**, *27*, 213.
Influence of Fluorochrome Labeling Density on the Photobleaching Kinetics of Fluorescein in Microscopy.
37. Chen, R. F.; Knutson, J. R. *Anal. Biochem.* **1988**, *172*, 61. Mechanism of Fluorescence Concentration Quenching of Carboxyfluorescein in Liposomes: Energy Transfer to Nonfluorescent Dimers.
38. Shen, Y.; Kuang, M.; Shen, Z.; Nieberle, J.; Duan, H.; Frey, H. *Angew. Chem. Int. Ed.* **2008**, *47*, 2227. Gold Nanoparticles Coated with Thermosensitive Hyperbranched Polyelectrolyte: Towards Smart Temperature and pH Nanosensors
39. Tonhauser, C.; Obermeier, B.; Mangold, C.; Löwe, H.; Frey, H. *Chem. Commun.* **2011**, *47*, 8965. Introducing an amine functionality at the block junction of amphiphilic block copolymers by anionic polymerization strategies
40. Obermeier, B.; Wurm, F.; Frey, H. *Macromolecules* **2010**, *43*, 2244. Amino Functional Poly(ethylene glycol) Copolymers via Protected Amino Glycidol.
41. Bakalarz-Jeziorna, A.; Heliński, J.; Krawiecka, B. *J. Chem. Soc., Perkin Trans. 1*, **2001**, 1086. Synthesis of multifunctionalized phosphonic acid esters *via* opening of oxiranes and azetidinium salts with phosphoryl-substituted carbanions.
42. Synthesis worked out by Andrew Zill synthesis derived from
a) first synthesis by undergraduate Yin Nguyen
b) Boger, D. L.; Borzilleri, R. M.; Nukui, S. *J. Org. Chem.* **1996**, *61*, 3561. Synthesis of *R*-(4-Methoxy-3,5-dihydroxyphenyl)glycine Derivatives: The Central Amino Acid of Vancomycin and Related Agents.

c) procedure from Andrew Zill's thesis with modified work-up.

d) Dodo, K.; Minato, T.; Noguchi-Yachide, T.; Suganuma, M.; Hashimoto, Y. *Bio. Med. Chem.* **2008**, *16*, 7975. Antiproliferative and apoptosis-inducing activities of alkyl gallate and gallamide derivatives related to (-)-epigallocatechin gallate

43. Doctoral Thesis of Andrew Zill

44. Hyatt, J. A. *Synth. Commun.* **2008**, *38*, 8. Convenient Preparation of 2,7,8-Trimethyl-6-hydroxychroman-2-carboxylic Acid (gamma-Trolox)

II. Synthesis and Characterization of Norbornyl Based Fluorescent Organic Nanoparticles with Improved Photostability

Portions of this chapter have been published by Yugang Bai, Hang Xing, Gretchen A. Vincil, Jennifer Lee, Essence J. Henderson, Yi Lu, N. Gabriel Lemcoff and Steven C. Zimmerman, “Practical synthesis of water-soluble organic nanoparticles with a single reactive group and a functional carrier scaffold” *Chem. Sci.* **2014**, 5, 2862-2868.

II.A. Introduction

A new approach toward the development of bright photostable fluorescent macromolecules was pursued. In a strategy very different than that presented in Chapter I, here the fluorophore was incorporated into the macromolecule during synthesis rather than post-polymer synthesis. The macromolecule still needed to fulfill the same properties as discussed before: 1) water-soluble and biocompatible, 2) mono-functional for conjugation, 3) able to incorporate multiple fluorophore and AFA moieties.

Described herein is a polynorborene polymer prepared via ring opening metathesis polymerization (ROMP) followed by further derivation to form water-soluble organic nanoparticles with fluorescein and AFAs. For the ROMP process ruthenium catalyst, $\text{RuCl}_2(\text{pyridine})_2(\text{H}_2\text{IMes})(\text{CHPh})$ was chosen because of its high functional group tolerance including protected fluorescein and AFA moieties.¹ Additionally, monotelechelic ROMP polymers have been prepared via end capping.² Once the linear ROMP polymer was prepared it was modified to include allyl groups that then underwent ring-closing metathesis (RCM) to form an organic nanoparticle (ONP). Dihydroxylation of the alkene back-bone and cross-linking units created a hydrophilic ONP. Figure 2.1 illustrates the desired final structure of the ONP as well as the monomers required to prepare it. The diol monomer (blue) introduced some water solubility and acted as a spacer unit. The activated

ester monomer (pink) was a point of attachment for the cross-linking allyl groups. The fluorophore, fluorescein, (green) and AFA, gallate, (red) monomers were modified to attach a norbornyl component. The end cap (purple) served as a point of further derivatization.

Design

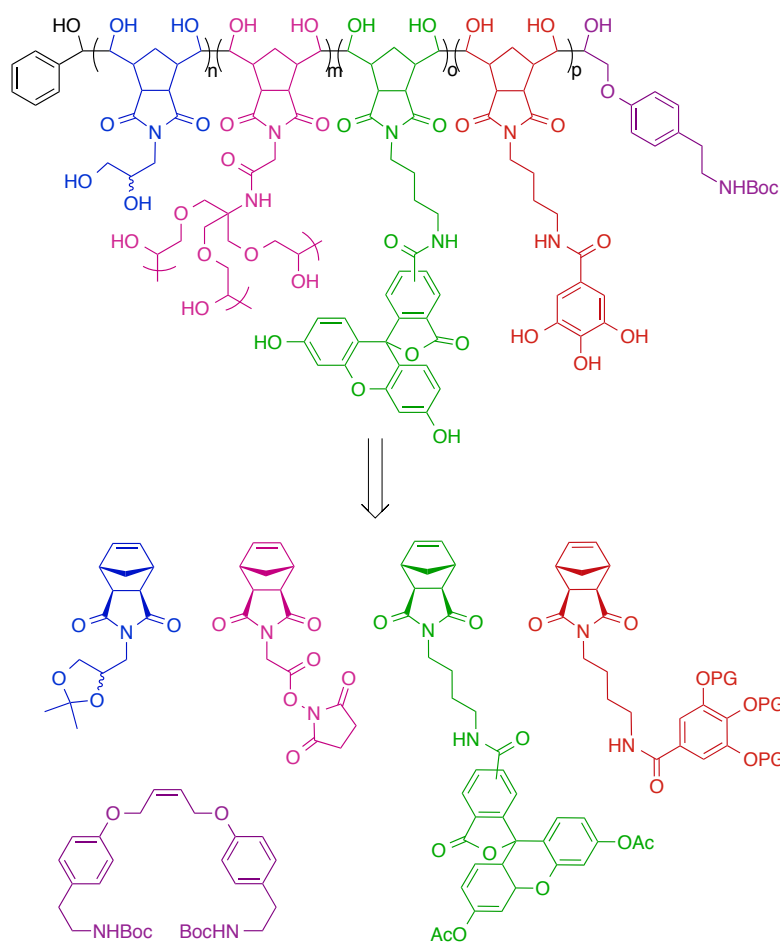


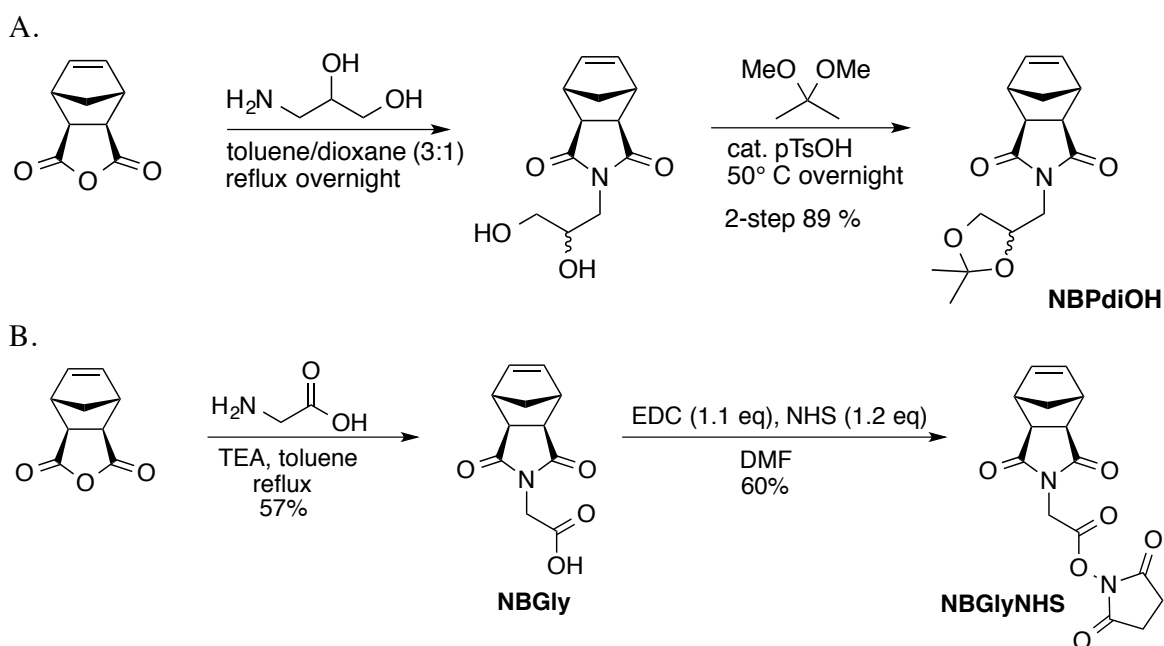
Figure 2.1. Structure of the desired ONP and monomers. Water soluble/ spacer, blue, Activated ester, pink, Fluorophore, green, AFA, red Mono-functionality, purple

The iterative ROMP-RCM process allowed for the preparation of ONPs with the desired composition and properties. The ONPs were then studied and found to have higher photostability than free fluorescein. ONPs of different molecular weights and containing different ratios of monomers were prepared and studied to determine the source of the increased stability, the results of which are discussed herein.

II.B. Results and Discussion

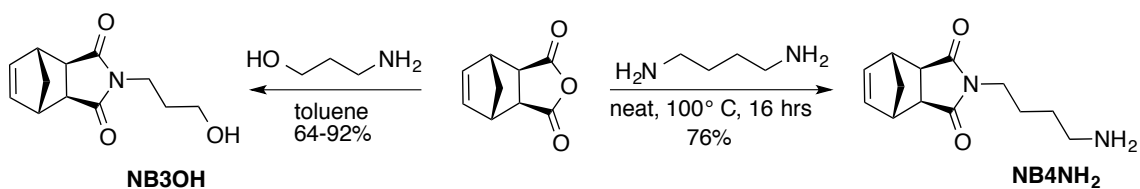
Synthesis

The required monomers were prepared in a straightforward manner as outlined in Schemes 2.1-2.4. The water solubilizing spacer monomer, NBPdiOH, was prepared in a two-step, one pot, reaction of carbic anhydride with 3-amino-1,2-propanediol to generate a diol. The diol was then protected with an acetonide group by reacting with 2,2-



dimethoxypropane (Scheme 2.1). The activated ester monomer, NBGlyNHS, was synthesized by reacting carbic anhydride with glycine and subsequently, coupling it with *N*-hydroxysuccinimide.

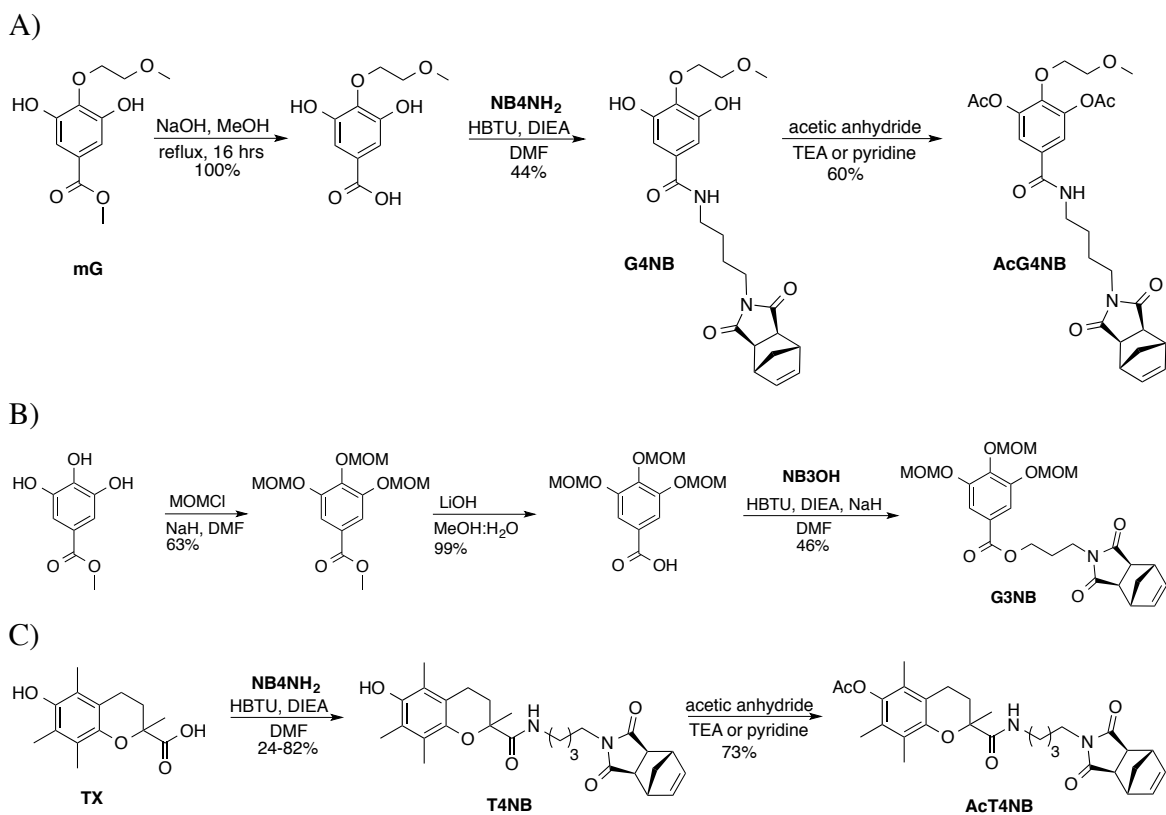
Two carbic anhydride derivatives were prepared (Scheme 2.2) to couple a norbornyl unit to the AFAs and dyes. NB4NH₂, was prepared by reacting carbic anhydride with putrescine. This reaction gave much better yields when done using neat conditions than in solvent(s). NB3OH was prepared by reacting carbic anhydride with 1-aminopropanol.



Scheme 2.2. Synthesis of NB3OH and NB4NH₂

The anti-fading agents, gallate and trolox, were derivatized and conjugated to the aforementioned carbic anhydride derivatives (Scheme 2.3). A previously synthesized gallate derivative, mG, was demethylated and coupled to NB4NH₂. The phenol groups of G4NB were protected with acetate groups to give AcG4NB.

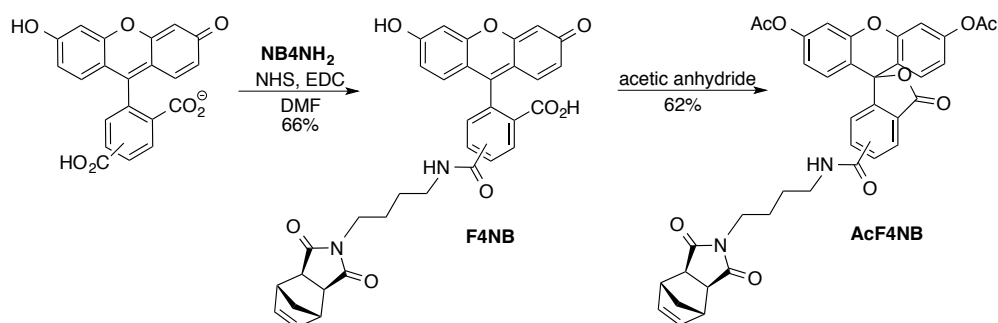
Previous group members found that when center phenol group on gallate was unprotected cross-linking occurred when conjugated to HPG. Thus the center phenol



Scheme 2.3. Synthesis of AFA monomers A) mG was demethylated, coupled to NB4NH₂ and then protected by reacting with acetic anhydride B) methyl gallate was triMOM protected, demethylated and coupled to NB4NH₂ C) Trolox was coupled to NB4NH₂ and protected by reacting with acetic anhydride.

group was alkylated on one of the gallate monomers, AcG4NB. However, it was possible to protect all the phenol groups during the synthesis of the ONP and deprotect all of them at the end. Three deprotected phenol groups was desirable because preliminary studies found that there was significantly less initial quenching of fluorescein than when the phenols were protected (Figure 1.8). Additionally, an ester linkage instead of an amine

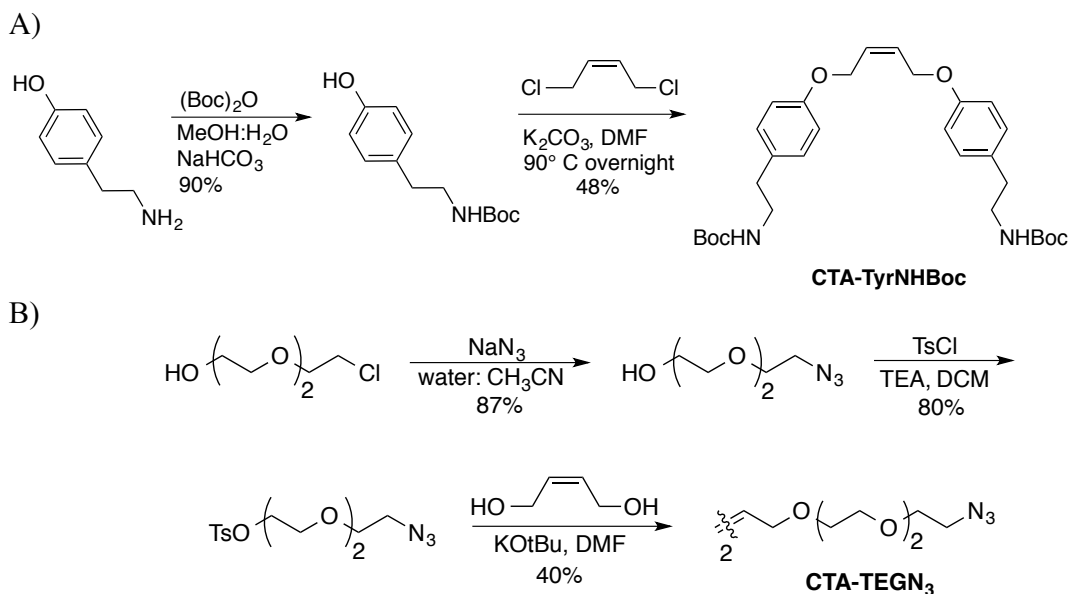
linkage was found to have better photostabilizing abilities. For these reasons, G3NB was synthesized, by triMOM protecting methyl gallate followed by demethylation and coupling to NB3OH. This synthetic strategy worked better than demethylation followed by MOM protection. A trolox monomer, AcT4NB, was prepared by coupling trolox to NB4NH₂ and protecting the phenol groups (Scheme 2.3).



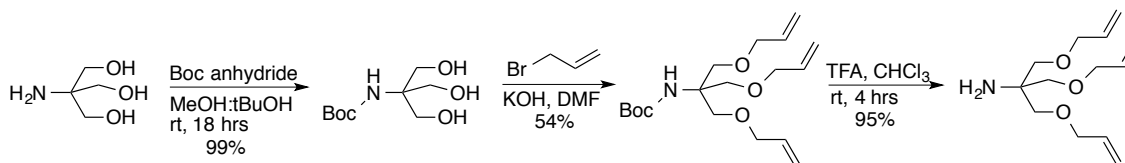
Scheme 2.4. Synthesis of fluorescein monomer, AcF4NB, by coupling NB4NH₂ and 5,6-carboxyfluorescein and then protecting the phenols.

The fluorescein monomer, AcF4NB, was synthesized by coupling carboxyfluorescein to NB4NH₂, and subsequently protecting the phenols (Scheme 2.4). Chain-transfer agents used to end cap the polymer were synthesized according to Scheme 2.5. CTA-TyrNH₂Boc was synthesized by *N*-Boc protecting tyramine then reacting it with Z-1,4-dichlorobutene. CTA-TEGN₃ was synthesized to introduce an azide functionality into the ONPs. A PEG linker was chosen to enhance water solubility and to form a long linker to the ONP to ensure the azide group would be accessible. Triethylene glycol monochloride was reacted with sodium azide to afford triethylene glycol monoazide in high yield. Triethylene glycol monoazide was then reacted with Z-1,4-dichlorobutene but, unfortunately, the major product formed was the result of a substitution on one side and an elimination to yield a 1,3 diene. The synthetic strategy was modified to first form a tosylate and then react it

with *Z*-1,4-butenediol to afford the desired product. Triallyltris was also prepared according to Scheme 2.6.



Scheme 2.5. Synthesis of CTAs A) The amine of tyramine was boc protected and then the phenol reacted with *Z*-dichlorobutene to yield CTA-TyrNHBoc. B) Triethylene glycol monochloride undergoes a substitution reaction with sodium azide and then a tosylate was formed and reacted with *Z*-butenediol to give CTA-TEGN₃.



Scheme 2.6. Tris was sequentially *N*-boc protected, allylated, and deprotected to yield triallyltris.

Once all the monomers were synthesized, the ONPs were prepared according to Scheme 2.7. Monomers were mixed in the desired ratio and RuCl₂(pyridine)₂(H₂IMes)(CHPh) added. The polymerization was allowed to proceed for 20 min and the chain-transfer agent was added. To incorporate terminal alkene groups, the activated *N*-hydroxysuccinimide

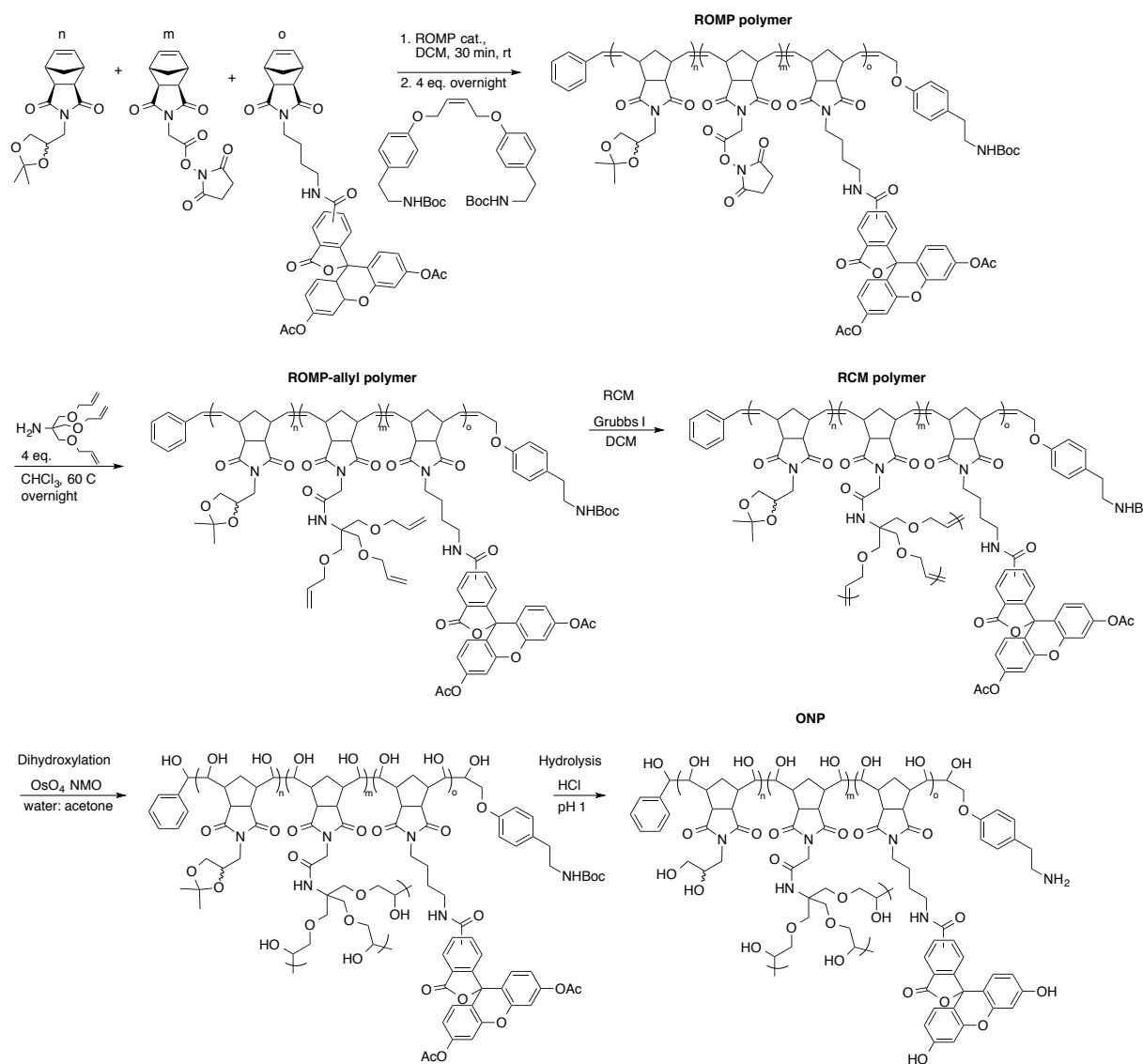
esters of the linear ROMP polymer were reacted with triallyltris. The ROMP-allyl polymer was then reacted with Grubbs I catalyst at high dilution to undergo ring-closing metathesis. The alkene groups on the polymer backbone and those resulting from the RCM reaction were dihydroxylated with OsO₄ and NMO to afford an aqueous soluble ONP. Treatment with acid removed the protecting groups. Preparation of the ONPs was scalable. Figure 2.2 shows the large-scale synthesis of over 1.5 g of ONP150-4F-LS.

All ONPs that were prepared, with the exception of two, were composed of NBPdiOH and NBGlyNHS in a 2:1

mol ratio whereas the mol % of fluorescein and the AFAs were varied to study their effect. Naming of the ONP was as follows: ONP-base number-equivalents of fluorescein monomer-equivalents of AFA monomer-other information; where the base number was the equivalents of NBPdiOH and NBGlyNHS added together. For example ONP150-10F-10T-a is the ONP synthesized by polymerizing 100 eq. NBPdiOH, 50 eq. NBGlyNHS, 10 eq. AcF4NB, and 10 eq. AcT4NB. Additionally, lower case letter following the name indicated the polymer was prepared multiple times and was differentiated sequentially by these letters. A table of all the ONPs synthesized can be found in Chapter IV. Appendices.



Figure 2.2. Picture of the large scale ONP synthesis: ONP150-4F-LS. Approximately 1.5 g of product is in the RBF above.



Scheme 2.7. Synthesis of ONPs. First the monomers are polymerized via ROMP. The activated esters of the linear polymer are reacted with triallyltris. Next, the polymer then underwent RCM with Grubbs I catalyst. The alkene groups on the backbone and those resulting from the RCM process were dihydroxylated. Finally, the protecting groups were removed with acid to give the desired ONP.

ONP synthesis was monitored by DMF SEC and ^1H NMR. Figure 2.3 shows the refractive index traces of SEC runs during the preparation of ONP150-4F-LS. The data were typical of that observed. A small increase in retention time between the ROMP polymer and ROMP allyl polymer was observed. A much larger increase in retention time, 0.5-1 min, was generally observed between the ROMP allyl polymer and RCM product. The significant change in retention time after the RCM process was a result of the smaller hydrodynamic radius of the polymer not the relatively small change in molecular weight. It is important to note that the molecular weights were determined using polystyrene standards so are not absolute values.

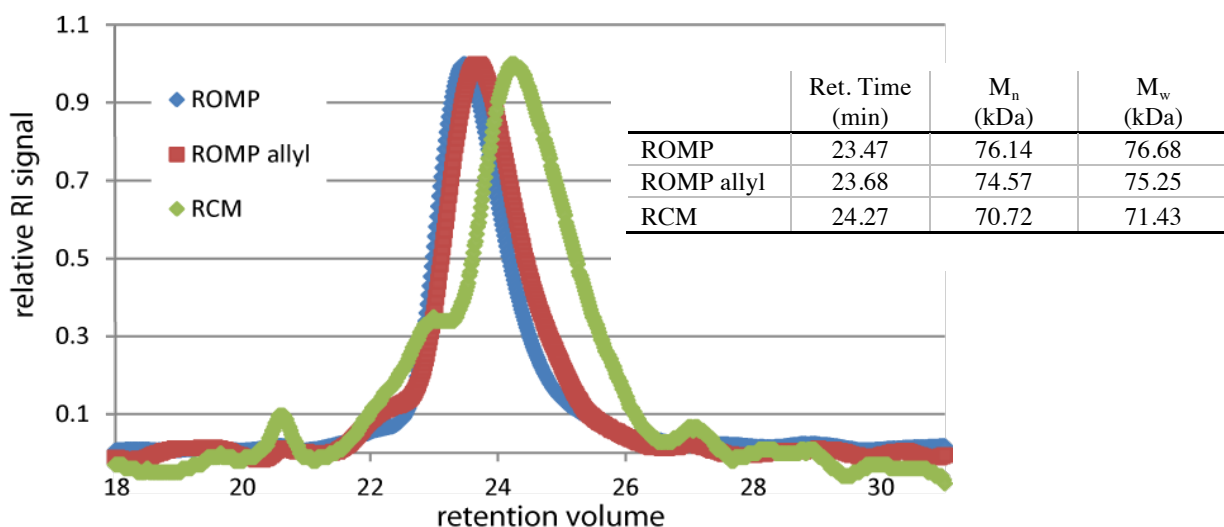


Figure 2.3. Refractive index trace of SEC runs during the preparation of ONP150-4F-LS. The table (inset) reports the retention volume as well as the M_n and M_w relative to the PS standards.

Figure 2.4 shows the ^1H NMR spectra of four ROMP polymers each with a different monomer composition. The spectrum of the ROMP polymer was used to confirm that the stoichiometry of the monomers added was consistent with the integration of the associated

peaks. Spectrum A is of a polymer composed of only NBPdiOH monomer units and was used for comparison purposes only. Spectrum B is of the polymer with NBPdiOH and NBGlyNHS monomer units. Spectrum C is of a ROMP polymer that has fluorescein incorporated. The aromatic peaks of fluorescein could not be used to assess reliably the AcF4NB stoichiometry in the polymer due to excessive broadening. Spectrum D is of the typical ROMP polymer with fluorescein and gallate monomers. The peaks associated with the MOM protecting groups on the gallate monomer, G3NB, were used to confirm the incorporation of the AFA into the polymer in the desired stoichiometry. Figure 2.5 shows the ^1H NMR spectra of the A) ROMP polymer, B) ROMP allyl polymer and C) RCM product during the preparation of ONP150-10F. The spectrum of the ROMP allyl polymer indicated that the activated esters of the NBGlyNHS successfully reacted with triallyltris. The spectrum of the RCM product then showed the disappearance of allyl peaks indicating that the RCM process was complete. The final ONP product was not soluble in chloroform so spectra were collected in D_2O . However, few features were discernable because of significant broadening of peaks and no information could be obtained.

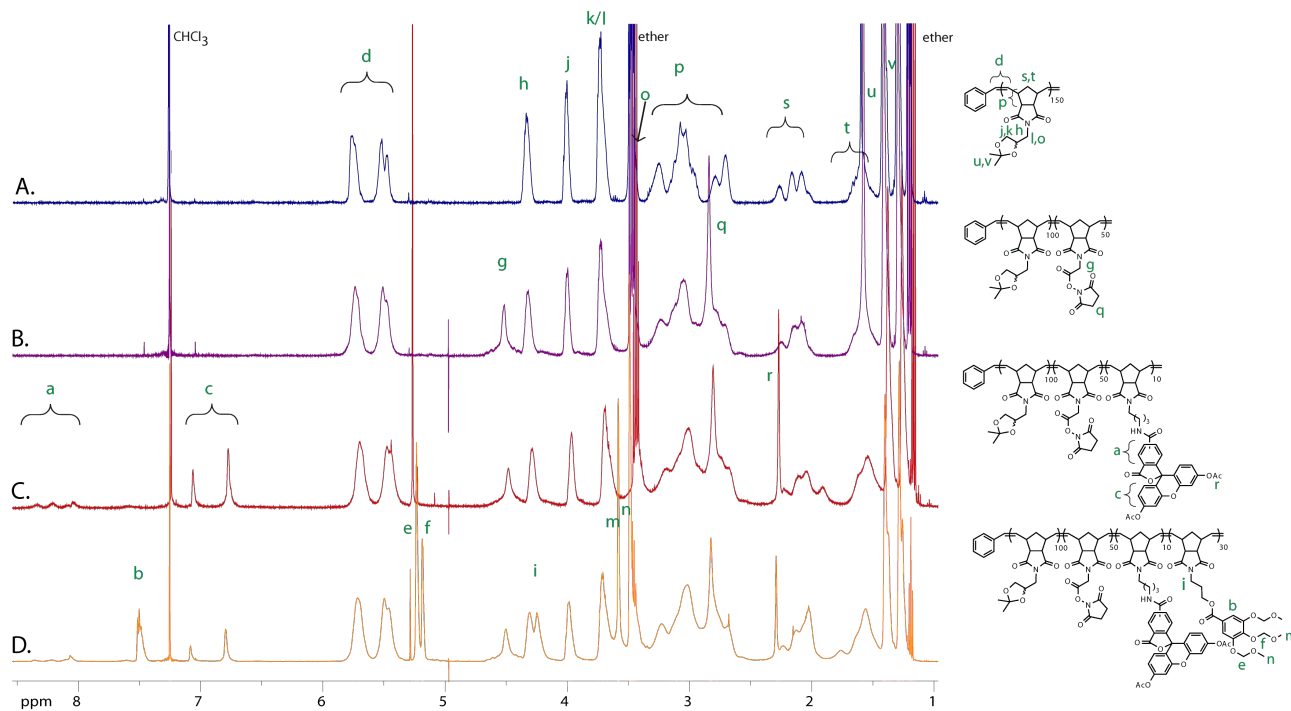


Figure 2.4. ^1H NMR of different ROMP polymers in chloroform. A) The top spectrum, blue, is a polymer with only NBPdiOH units. B) The second spectrum, purple, contains NBPdiOH and NBGlyNHS monomers. C) The third spectrum, red, has AcF4NB incorporated into it. D) The bottom spectrum, orange, has the G3NB monomer incorporated. By comparing the spectra peaks can be identified as well as confirmation of stoichiometries by integration.

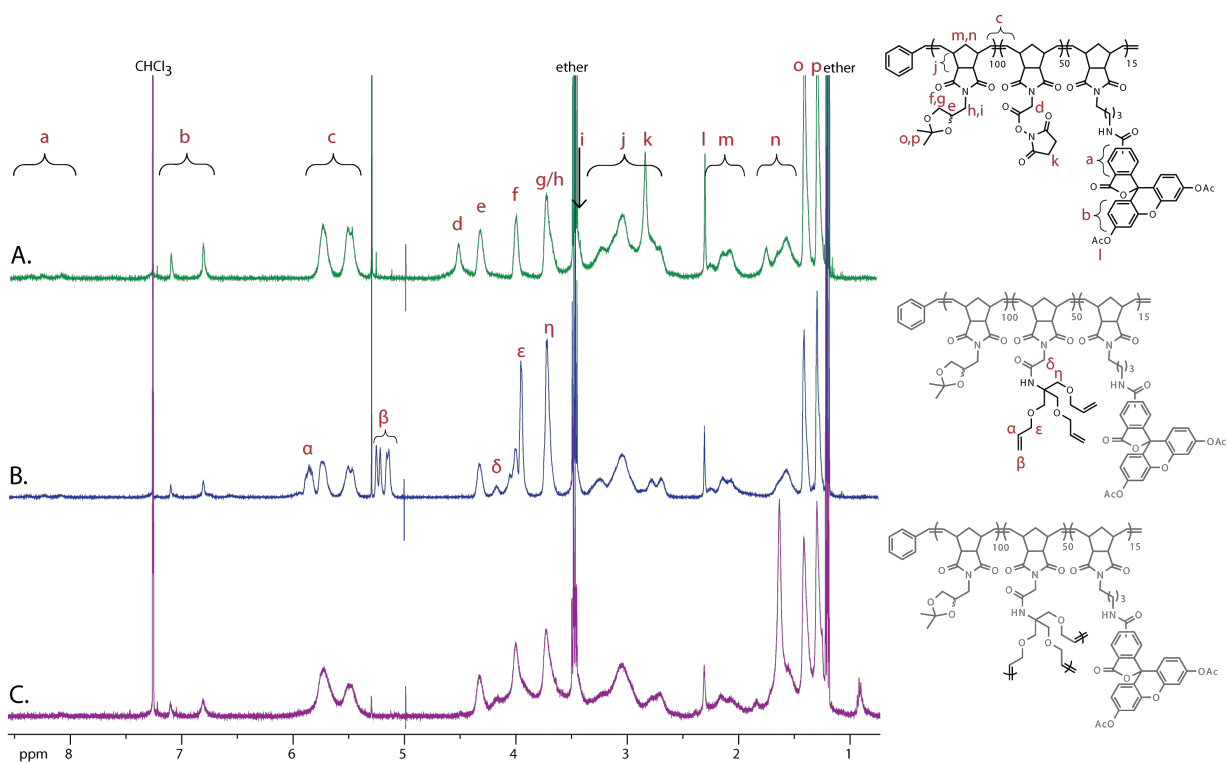


Figure 2.5. ^1H NMR of ONP150-10F synthesis. A) Spectrum of the linear ROMP polymer and peaks corresponding to the incorporated monomers. B) Spectrum of ROMP allyl polymer showing the successful incorporation of triallyltris units as indicated by Greek letters and disappearance of the NHS peak k. C) Spectrum of the RCM product lacks the alpha and beta peaks indicating the complete cross-linking.

Spectroscopic Studies

All ONPs prepared were studied by UV and fluorescence spectroscopy. The spectroscopic properties of the ONPs are summarized in Table 2.1. The data for each ONP can be found in Chapter IV. Appendices. A

bathochromic shift was observed in both the absorbance and emission spectra. No trend in the size of the shift was found. Figure 2.6 depicts the absorbance and emission spectra of fluorescein compared to ONP150-10F.

The molar absorptivity of the ONP varied with the number of fluorescein monomers incorporated. However, a significant decrease in the absorptivity per fluorescein ($\sim 30 \text{ Abs}(\text{Mcm})^{-1}$) was observed regardless of the equivalents of fluorescein incorporated. In many reports of fluorescein conjugation to

macromolecules it is assumed that the molar absorptivity doesn't change, but this was not valid for the ONPs in this study. One possible explanation for the decrease in absorptivity was a lack of incorporation into the polymer. However, integration of the ^1H NMR peaks confirmed the stoichiometry of the fluorescein moieties was consistent with number of equivalents added during the polymerization. The quantum yields of the ONPs were found

Table 2.1. Spectroscopic Properties of ONPs

| | fluorescein | ONPs |
|--|-------------|-----------|
| Abs. λ_{max} (nm) | 490 | 496-507 |
| $\epsilon_{\lambda_{\text{max}}}$ ($\text{kAbs}(\text{Mcm})^{-1}$) | 78 | 38-697 |
| Em. λ_{max} (nm) | 514 | 521-528 |
| QY (Φ) | 0.9 | 0.17-0.72 |
| brightness | 70 | 12-277 |

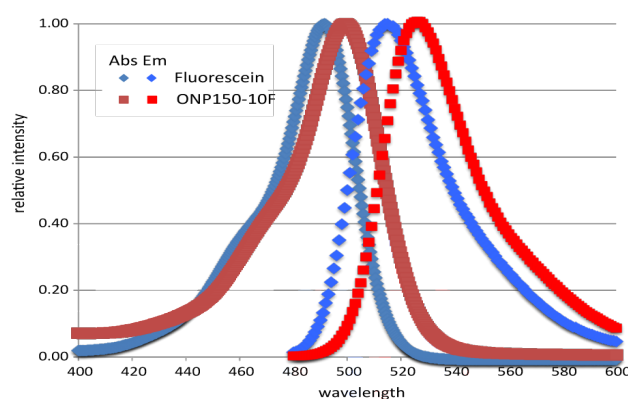


Figure 2.6. Example of UV and fluorescence spectra of fluorescein compared to ONPs. This specific example is ONP150-10F, similar shifts are observed for all ONPs with slight variation.

to vary significantly from $\Phi=0.17$ to 0.72 with an average of $\Phi=0.48 \pm 0.12$. ONP75-20F was the only ONP prepared with 20 fluorescein moieties and a notable outlier with a $\Phi=0.17$ (next lowest was $\Phi=0.31$). This was thought to be the result of dye-dye quenching.

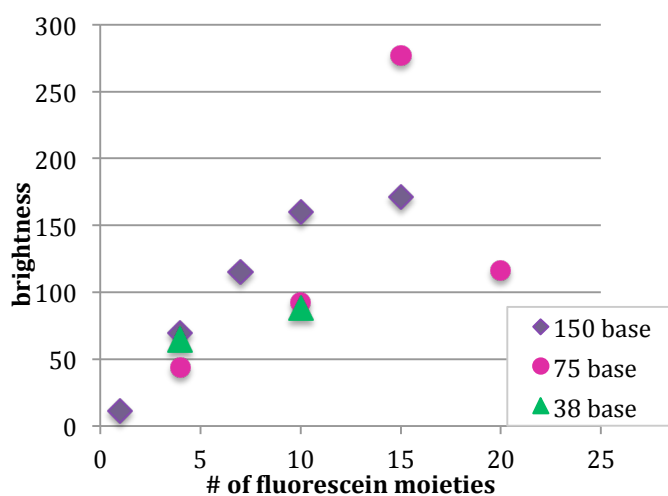


Figure 2.7: Plot of the number of fluorescein moieties per ONP verse the brightness of the ONP.

Photobleaching

Photobleaching

experiments were conducted on the ONPs to determine the photostability of fluorescein incorporated into the ONP as well as the influence of the AFAs. ONP samples were tested in aqueous solution at 1 μM and compared to a fluorescein standard. Figure 2.8 depicts a plot of the bleaching curve derived from a typical photobleaching experiment. The plot and Figure 2.9 shows that fluorescein and ONP150-4F had similar initial brightness while ONP150-10F was much brighter. At the end of 8 h fluorescein has no detectable fluorescence whereas both ONPs retain some fluorescence. The fluorescent ONPs were found to have increased photostability over free fluorescein. Table 2.2 reports the half-times of ONPs of two different sizes with different equivalents of fluorescein monomer incorporated. Half-time is defined as the time to a 50% reduction in the initial fluorescence intensity. The derivation of the value is explained in Chapter IV. Appendices. The general trend observed, was the more fluorescein, the more stable the ONP was when

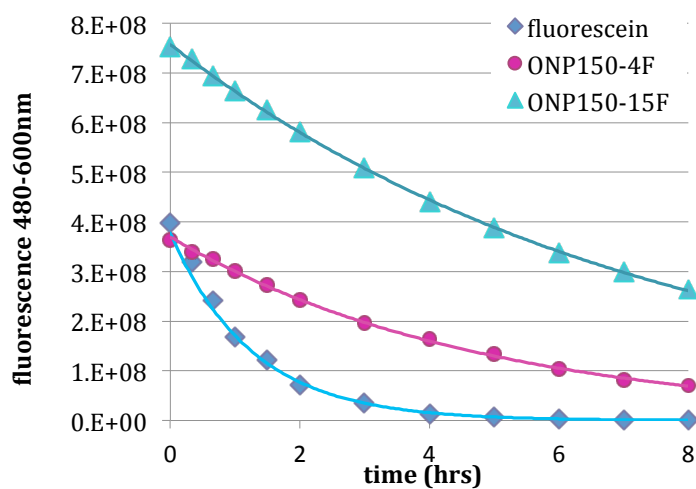


Figure 2.8: Photobleaching curves of fluorescein, ONP150-4F and ONP150-15F.

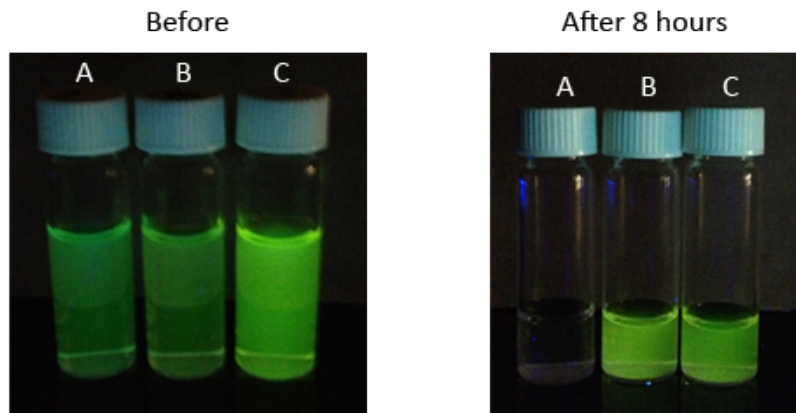


Figure 2.9. Before and after pictures of a photobleaching experiment. Vial A contains fluorescein, vial B contains ONP150-4F and vial C contains ONP150-15F.

Table 2.2. Photobleaching study reported as halftimes

| Number of Fluorescein on ONP 150 base | | | | Number of Fluorescein on ONP 75 base | | | | |
|---------------------------------------|-------|-------|---------|--------------------------------------|-------|-------|-------|---------|
| | Run A | Run B | Average | | Run A | Run B | Run C | Average |
| fluorescein | 0.81 | 0.935 | 0.87 | fluorescein | 0.84 | 0.798 | 0.763 | 0.80 |
| ONP150-4F | 3.41 | 3.38 | 3.40 | ONP75-4F | 1.86 | 1.79 | 1.79 | 1.81 |
| ONP150-7F | 4.07 | 4.32 | 4.20 | ONP75-10F | 5.39 | 5.73 | 4.59 | 5.24 |
| ONP150-10F | 4.75 | 4.94 | 4.85 | ONP75-15F | 10.05 | 10.01 | 8.9 | 9.65 |
| ONP150-15F | 5.26 | 5.62 | 5.44 | ONP75-20F | 7.32 | 5.73 | 5.73 | 6.26 |

photobleached (Figure 2.10). ONP75-20F was the only ONP that did not follow the trend. It is likely that with 20 fluorescein moieties on the ONP dye-dye interactions occurred and led to quicker bleaching. It is important to note, however, that the ONP still had a half-time of 7-8 times longer than free fluorescein.

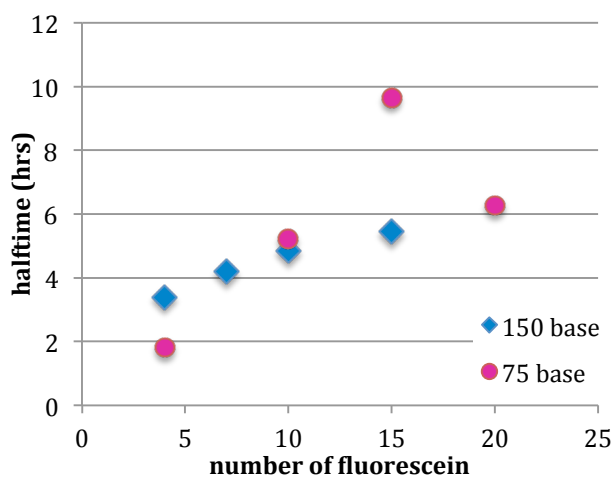


Figure 2.10: Plot of photobleaching study of the effects of number of fluorescein on the half-times (data above). In general, the more fluorescein moieties on the ONP, the longer the half-time.

Table 2.3: Photobleaching Study of the ONP Size

| 4 fluorescein on different size ONP | | | | 10 fluorescein on different size ONP | | | | |
|-------------------------------------|-------|-------|---------|--------------------------------------|-------------|-------|-------|---------|
| | Run A | Run B | Average | Size* | | Run C | Run D | Average |
| fluorescein | 0.82 | 0.78 | 0.80 | | fluorescein | 0.79 | 0.80 | 0.80 |
| ONP150-4F | 3.04 | 3.14 | 3.09 | 49 | ONP150-10F | 5.53 | 5.59 | 5.56 |
| ONP75-4F | 1.86 | 2.01 | 1.94 | 26 | ONP75-10F | 6.05 | 6.19 | 6.12 |
| ONP38-4F | 3.91 | 4.01 | 3.96 | 14 | ONP38-10F | 4.71 | 4.68 | 4.70 |

*theoretical MW kDa

Next, the effect of the size of the ONP on the photostability was studied. Three different sized ONPs were studied (150, 75 and 38 base) with two different levels of fluorescein incorporation (4 and 10 equivalents of AcF4NB). All the ONPs with 10 fluorescein moieties had longer half-times than the same sized ONP with 4 fluorescein moieties (Table 2.3). It was clear from the plot, however, that no trend was present. Smaller ONP were just as stable as larger ONPs.

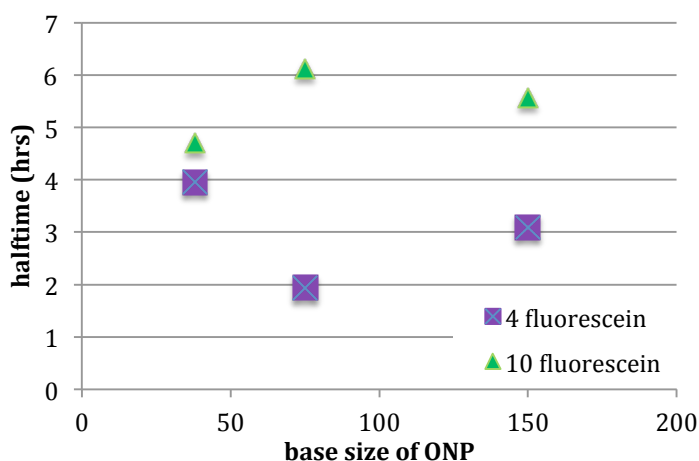


Figure 2.11. Plot of photobleaching study of the effects of the size of the ONP on the half-times. There appears to be no trend.

A set of three ONPs were prepared with no AFA, with gallate, and with trolox. The results of the photobleaching experiments on these ONPs are reported in Table 2.4. The half-time of the ONP with gallate had the longest half-time of 10.81 h which was 160% longer than ONP without the gallate. The ONP with trolox also showed an increase in stability with a half-time of 8.85 h. Interestingly, when photobleaching experiments were conducted by entrapping the ONPs in agarose gel, the ONP with trolox out-performed the ONP with gallate (Figure 2.12).³ The difference in the stability of the ONPs between the two studies is likely a result of the differences in the mechanism of photobleaching in solution verses a gel. Regardless, both results suggest that addition of AFAs to the ONP further improves the photostability of fluorescein.

Table 2.4: Photobleaching Study of Different Anti-Fading Agents

| | Run A | Run B | Run C | Average | AFA |
|------------------|-------|-------|-------|---------|------|
| fluorescein | 0.78 | 0.76 | 0.717 | 0.77 | |
| ONP150-10F-B | 6.80 | 6.56 | 6.47 | 6.68 | none |
| ONP150-10F-10G-B | 9.80 | 11.82 | 10.8 | 10.81 | 10G |
| ONP150-10F-10T-B | 9.00 | 8.69 | 9.14 | 8.85 | 10T |

note: samples prepared to accommodate biotin, but it was not conjugated to the photobleached samples

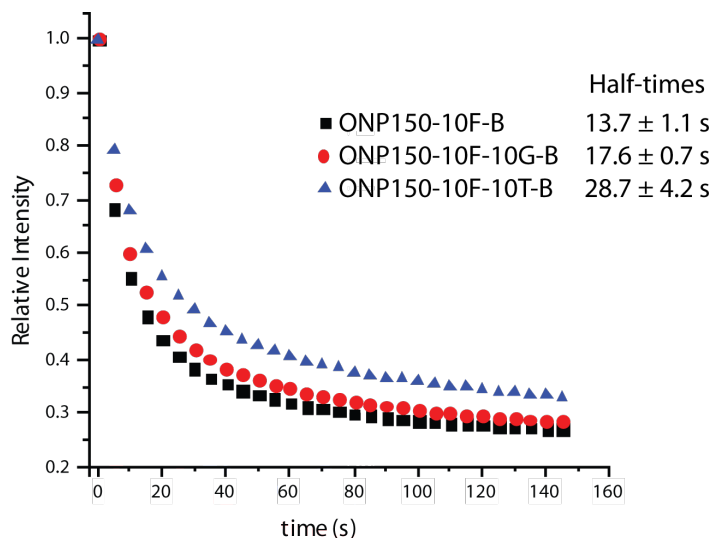


Figure 2.12. Photobleaching experiment with ONPs trapped in agarose gel. Performed by Dan Riley in the Schroeder lab.

A series of ONPs with fluorescein and gallate incorporated were studied to determine if an optimal ratio of fluorescein to gallate could be found. Table 2.5 reports the results of the photobleaching experiments on ONPs with gallate and the fluorescein to gallate ratio. No optimal ratio was determined

Table 2.5: Photobleaching of Gallate Containing ONPs

| ONP | F/G | half-time (h) |
|------------------|------|---------------|
| ONP150-10F-10G-B | 1.00 | 10.81 |
| ONP150-4F-4G | 1.00 | 3.69 |
| ONP150-4F-10G | 0.40 | 1.84 |
| ONP150-4F-20G | 0.20 | 2.09 |
| ONP150-10F-20G | 0.50 | 4.30 |
| ONP150-10F-30G | 0.33 | 4.12 |
| ONP75-3F-3G | 1.00 | 4.82 |
| ONP75-3F-6G | 0.50 | 5.30 |
| ONP75-3F-9G | 0.33 | 5.72 |
| ONP75-6F-12G | 0.50 | 6.18 |
| ONP75-6F-18G | 0.33 | 5.44 |

F/G is the fluorescein:gallate ratio

nor was a trend found. Some of the gallate containing ONPs were less stable than their counterpart with no gallate and some were more stable. At this point, it was unclear what factors dictate the photostability of the ONPs. The factor that correlated most closely with photostability was the ONP's brightness, but this only applied to ONPs without AFAs. Table 2.6 reports the some spectroscopic data and the half-times of ONPs without AFAs. Figure

2.13 is a plot of brightness verse half-time showing a general trend, but not a direct relationship.

Table 2.6: Data for fluorescent ONPs without AFAs

| | $\epsilon_{\lambda_{\max}}$ (kAbs(Mcm) ⁻¹) | QY (Φ) | Brightness | Half-time (h) |
|-------------|---|---------------|------------|------------------|
| ONP150-4F-a | 131.7 | 0.53 | 70 | 3.24 |
| ONP150-7F | 231.6 | 0.49 | 115 | 4.20 |
| ONP150-10F | 335.5 | 0.48 | 160 | 5.20 |
| ONP150-15F | 359.7 | 0.48 | 171 | 5.44 |
| ONP75-10F | 295.5 | 0.31 | 92 | 5.66 |
| ONP75-15F | 473.1 | 0.58 | 277 | 9.65 |
| ONP75-4F | 90.0 | 0.49 | 44 | 1.90 |
| ONP75-20F | 697.4 | 0.17 | 116 | 6.90 |
| ONP38-4F | 138.0 | 0.47 | 65 | 3.96 |
| ONP38-10F | 265.8 | 0.33 | 89 | 4.70 |

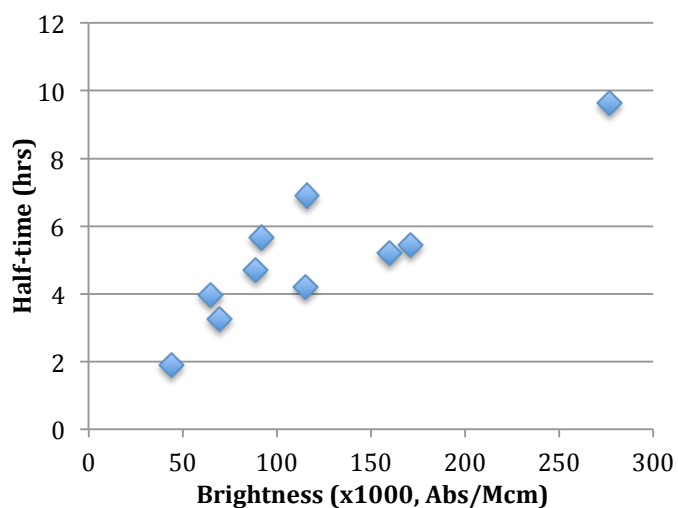


Figure 2.13. Plot of brightness vs. halftimes of ONPs containing no AFA moieties.

More data is needed to be able to pin point the causal factors in the photostability of ONPs. Possible factors contributing to photostability to be investigated include: residual metal content, degree of cross-linking (ONP density), placement of fluorescein moieties within the polymer, among other factors.

Metal removal

The toxic effect of heavy metals found in materials with biological application is a common concern. Because both ruthenium and osmium were used in the synthesis of the ONPs, it was necessary to attempt to remove the metals. Many of the ONPs prepared were studied by UV and fluorescence spectroscopy and then treated with a polymer designed to remove metals, Smopex 105 by Alfa Aesar, a vinyl pyridine grafted polyolefin fiber. ICP analysis of the residual ruthenium and osmium in the ONPs indicated widely variable levels (Table 2.6). Of the seven ONPs analyzed, the concentration of osmium ranged from 280-72,800 ppm and the ruthenium ranged from 3,400-11,300 ppm. Samples of the ONPs were treated with Smopex-105 and reanalyzed by ICP. The metal concentrations were successfully lowered, often by several orders of magnitude, to where osmium ranged from 15-1,510 ppm and ruthenium ranged from 7-5,532 ppm. It was found that the initial concentration of metals had little effect on the final concentration of metals indicating that the efficiency of metal removal varied significantly. The spectroscopic properties of the treated ONP samples were studied and found to have altered, in some cases dramatically. The detailed results of the studies can be found in Chapter IV. Appendices. Due to the effect of the metals, a more systematic effort was made to optimize their removal. The synthesis of ONP150-4F-LS generated enough material to study the effect of multiple conditions on the same sample. Table 2.7 reports the findings of the study. ONP150-4F-LS was treated with different weight equivalents of metal removing polymer, Smopex-105, and the metal concentration was reanalyzed. In some cases, the ONP was treated with multiple iterations of Smopex-105. The amount of ONP recovered after treatment was calculated because

significant lost of the ONP was observed in the initial studies. Repeated treatment of the ONP with the Smopex-105 did not reduce the metal level better than a single treatment.

Table 2.7. Results of Treatment of ONPs with Smopex-105 to Remove Metals

| | Initial Values | | Treated Samples | |
|------------------|----------------|----------|-----------------|----------|
| | Os (ppm) | Ru (ppm) | Os (ppm) | Ru (ppm) |
| ONP150-7F | 7000 | 3600 | 1510 | 1732 |
| ONP75-10F | 280 | 7500 | 15 | 7 |
| ONP75-15F | 40400 | 9400 | 37 | 5532 |
| ONP72-20F | 72800 | 11300 | 922 | 2633 |
| ONP150-4F-20T-a | 14600 | 6800 | 208 | 3646 |
| ONP150-4F-20T-a* | 6800 | 3400 | 398 | 160 |
| ONP150-4F-20T-b | 23000 | 9700 | 37 | 3799 |

Note: When ONP75-10F was retested the levels were Os: 17 ppm and Ru: 3842 ppm
 Samples were stirred in a water with ~1 eq. Smopex 105

Table 2.8. Studies to Determine the Optimal Metal Removal

| Equivalents | 0 | 0.5 | 0.5 x 2 | 0.5 x 3 | 0.67 | 1 | 1 x 2 | 1 x 3 | 1.5 | 2 | 3 |
|-------------|------|------|------------|------------|------|------|----------|----------|------|-----|-----|
| Os | 1751 | 1500 | 831 | 1050 | 2192 | 810 | 438 | 255 | 379 | 310 | 274 |
| Ru | 4407 | 3829 | 2086 | 2554 | 3592 | 1884 | 1058 | 482 | 821 | 479 | 308 |
| total | 6158 | 5329 | 2917 | 3604 | 5784 | 2694 | 1496 | 737 | 1200 | 789 | 582 |
| % recovered | | 97 | 86 | 80 | 98 | 88 | 70 | 49 | 61 | 48 | 31 |

0 equivalents indicates the initial metal level without treatment and was the average of two different samples
 The value below the equivalents indicates how many times the sample was treated with the specified equivalents (with filtering in between). Total residual metal concentration was tallied because some regulation agencies monitor the total concentration of like metals, not the individual concentrations (Ru and Os are considered together).

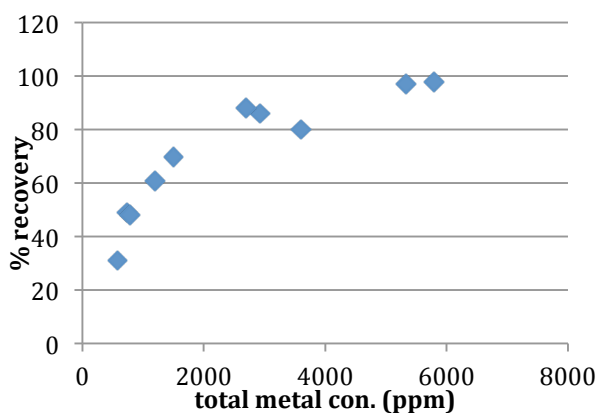


Figure 2.14. Plot of the total residual metal concentration vs. the percent recovered ONP. A clear trend is observed, the more the metal removed the less material recovered.

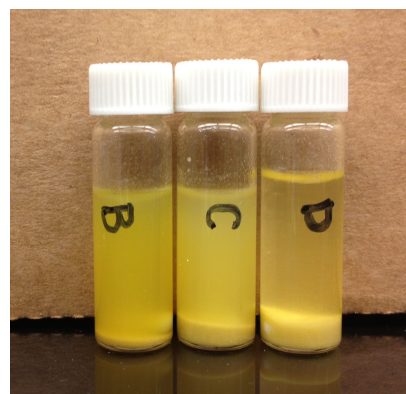


Figure 2.15. ONP treated with different amounts of Smopex 105. B. 1 eq. C. 2 eq. D. 3 eq.

For example, two treatments of 1 equivalent of polymer reduced the metal levels to 438 ppm Os and 1058 Ru but a single treatment of 2 equivalents of polymer reduced the metal levels to 310 ppm Os and 479 ppm Ru. A close correlation was found between the amount of ONP recovered and the amount of metal removed, shown graphically in Figure 2.14. The Smopex-105 was thought to be binding the ONP as well as the metals. Figure 2.15 shows qualitatively the removal of ONP from solution. It was thought that a different metal removal polymer may work better with the ONPs. SiliaMetS DMT, a dimercaptotriazin, was used to treat ONP150-4F-LS and was found to remove slightly more ruthenium if only one equivalent was used but the level of osmium unexpectedly jumped to ~8000 ppm, four times the initial concentration. The cause of the increase in osmium concentration is unknown.⁴ It was decided that for the current purposes of the ONPs the metal levels were acceptable.

II.C. Future Directions

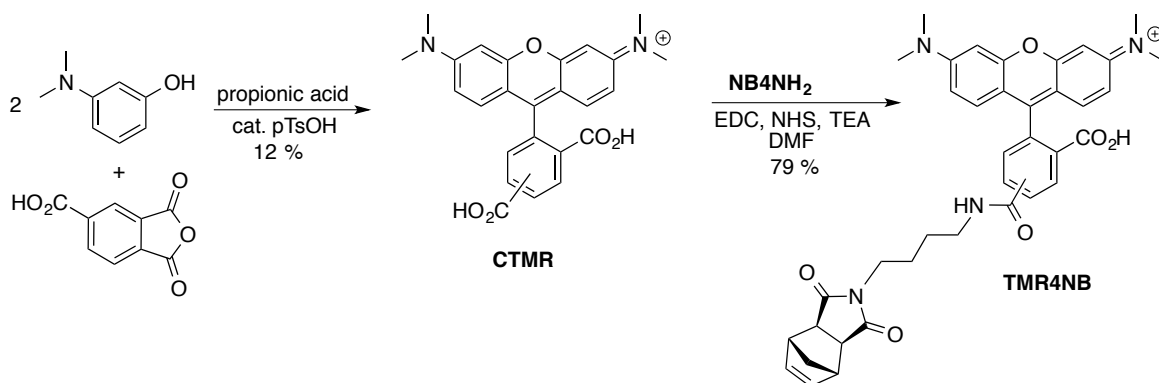
Studies need to be performed to probe the source of the increased photostability of fluorescein when incorporated into the ONPs. The effect needs to be further explored by preparing several ONP of a given size with different ratios of NBPdiOH:NBGlyNHS. Studies of the series should elucidate the cross-linking densities affect on the photostability.

Almost all the ONPs studied thus far have had a NBPdiOH:NBGlyNHS ratio of 2:1. Two ONPs were prepared with a 1:1 ratio: ONP40-4F and ONP40-10F, both contained 20 equivalents of NBPdiOH and NBGlyNHS. The spectroscopic data was found to be comparable to ONP38-4 and ONP38-10F: two ONPs with the 2:1 ratio of NBPdiOH:NBGlyNHS. The photostability remains to be tested and compared. It is recommended that ONP with fewer equivalents of NBGlyNHS also be synthesized and studied to try to discern a trend.

Photobleaching studies need to be conducted on the trolox containing ONPs to determine if trolox increases the photostability of the ONPs. Thus far, only one ONP150-10F-10T-B, has been tested and was found to be more stable than similar ONPs without trolox. Other ONPs with trolox have been prepared and require testing.

Single molecule studies are also recommended to provide insight into the possible photobleaching mechanism. To do this, biotin needs to be conjugated to the ONP. Three ONPs were synthesized with the CTA-TEGN₃ and propargyl biotin clicked on to ONP150-10F-B, ONP150-10F-10G-B and ONP150-10F-10T-B. However, these ONP were not bright enough to conduct single molecule studies. Another set of ONPs with more fluorescein moieties should be synthesized to determine if single molecule studies are possible.

Another possible direction of the project is to incorporate other dyes into the ONP. It would be interesting to see if an increase in photostability is observed for other dyes that are structurally similar to fluorescein, such as rhodamine. Tetramethylrhodamine was chosen because its absorbance is at ~555 nm and emission is at ~580 nm.⁵ These spectra properties would allow for an ONP with both fluorescein and rhodamine incorporated to be excited at 475 nm and emit at 580 nm (Figure 2.16). Carboxy tetramethyl rhodamine was synthesized and coupled with NB4NH₂ to prepare a rhodamine monomer, TMR4NB (Scheme 2.8) and awaits incorporation into an ONP.



Scheme 2.8. Synthesis of rhodamine monomer, **TMR4NB**.

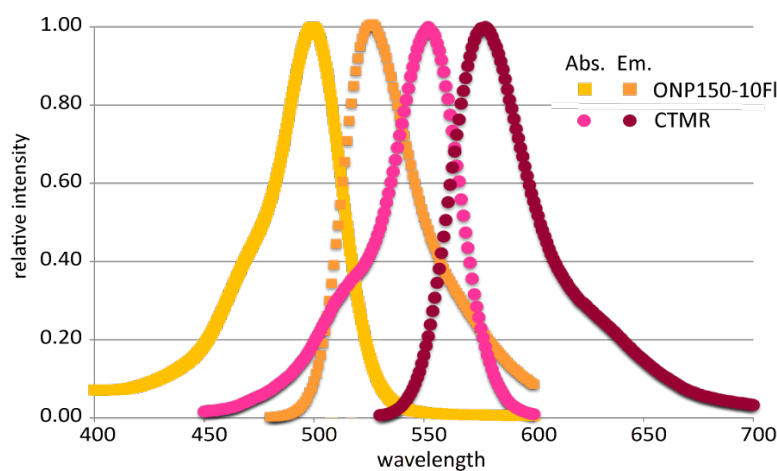


Figure 2.16. Overlay of the absorbance and emission of ONP150-10F and carboxytetramethylrhodamine. The overlap of the emission of the ONP and absorbance of CTMR suggest the two would work well as a FRET pair.

II.D. References

1. Matson, J. B.; Grubbs, R. H. *J. Am. Chem. Soc.* **2008**, *131*, 6731. Synthesis of fluorine-18 functionalized nanoparticles for use as in vivo molecular imaging agents
2. Matson, J. B.; Grubbs, R. H. *Macromol.* **2010**, *43*, 213. Monotelechelic Poly(oxa)norbornenes by Ring-Opening Metathesis Polymerization Using Direct End-Capping and Cross-Metathesis.
3. Experiments performed by Dan Riely in the Schroder Group
4. Contamination of samples at microanalysis is one possibility
5. Life technologies website: <https://www.lifetechnologies.com/us/en/home/life-science/cell-analysis/fluorophores/tritc-dye.html>

III. Experimental

The following chapter includes information regarding the standard practices used to prepare and study the compounds in this work. Many of these compounds have been reported in literature and are cited. However, the specific details herein are the author's work and methods described are not necessarily the same as the literature. Portions of Chapter III.C. Synthesis of Organic Nano Particles and Related Compounds have been published by Yugang Bai, Hang Xing, Gretchen A. Vincil, Jennifer Lee, Essence J. Henderson, Yi Lu, N. Gabriel Lemcoff and Steven C. Zimmerman, "Practical synthesis of water-soluble organic nanoparticles with a single reactive group and a functional carrier scaffold" *Chem. Sci.* **2014**, 5, 2862. The details of the large-scale ONP synthesis were adapted from this publication.

III.A. General Methods

Reagents

All reagents were used without purification unless specified and most were purchased from Sigma Aldrich or Acros. Key reagents purchased from other companies include: EDC, NHS and HBTU (Chem Impex International), Fmoc-Lys(Boc)-OH (Advanced Chem Tech), chloromethylmethylether (Waterstonetech LLC) and HOBt (Nova Biochem).

The following reagents were distilled prior to use: 5-hexynol, 66-69 °C at 24-25 torr, ethylene diamine 56-57 °C at 88 torr, 3-aminopropanol 56-57 °C at 985 microns, epichlorohydrin 40-50 °C at 60-70 torr, glycidol 68 °C at 36 torr (doubly distilled), p-anisaldehyde 61 °C at 153 microns, 4-methoxybenzylamine 57 °C at 145 microns, dibenzylamine 97 °C at 0.4 mm Hg.

Abbreviations of chemical names used throughout include: DCC: *N,N'*-Dicyclohexylcarbodiimide, HOBT: *N*-Hydroxybenzotriazole, TEA: trimethylamine, HBTU: *O*-(Benzotriazol-1-yl)-*N,N,N',N'*-tetramethyluronium hexafluorophosphate, DIEA: diisopropylethylamine, EDC-HCl: *N*-(3-Dimethylaminopropyl)-*N'*-ethylcarbodiimide hydrochloride, PE: petroleum ether, NHS: *N*-hydroxysuccinimide, DMAP: 4-(dimethylamino)pyridine, H₂IMes = *N,N*-dimesityl-4,5-dihydroimidazol-2-ylidene), NMO: *N*-Methylmorpholine *N*-oxide.

A Mettler Toledo XA105 was used to weigh masses under 20 g. Masses greater than 20 g up were measured on a Mettler Toledo ML802E. A series of VWR micropipettes were used for all measurements of 2 mL to 2 μ L of aqueous solvent. Hamilton Co. gastight syringes were used for all measurements of 5 mL to 10 μ L of organic solvent/solutions.

Reactions

Unless specified otherwise, all reactions were carried out in a round bottom flask and stirred with a magnetic stir bar. All reactions with fluorescein, fluorescein derivatives, rhodamine or rhodamine derivatives were covered with foil. If the reaction was performed multiple times with a different yield, a range is indicated as well as an explanation for the discrepancy. Reactions dried with MgSO₄ had the drying reagent removed via gravity filtration. Many reactions required the removal of DMF. This was accomplished using a rotary evaporation equipped with a high vacuum, ~800 microns.

Reactions to prepare small molecules were monitored by thin-layer chromatography. Plates from EMD Chemicals Inc. with 0.2 mm silica 60 coated on glass with F₂₅₄ indicator were used. Silicycle SilicaFlash® P60 40-63 μ m SiO₂ was used for chromatography. "Dry" silica indicates that the silica was heated to 120 °C for 48 h under -762 mm Hg.

Tetramethylrhodamine and its derivatives were purified using flash chromatography on a Teledyne Combiflash Rf.

Dry Solvents

The indication of anhydrous or dry solvent (specifically DMF, DMSO, pyridine) indicates the solvent was dried with a mixture of 3 and 4 Å activated molecular sieves for at least 48 h prior to use. Methanol was dried using 3 Å sieves. Sieves were washed, air dried, dried in a 200 °C oven for 60 h followed by flame drying under high vacuum four times until the vacuum pressure no longer rose when heat was applied. (Note: Coupling reactions in DMF from the SPS were unsuccessful.) Anhydrous 1,4-Dioxane and acetonitrile used were obtained from a SPS system.

Dialysis

HPGs were purified with one of two different dialysis membranes. For MWCO 2,000, benzoylated dialysis membranes from Sigma Aldrich were used and were stored in a 0.1 M aqueous solution of NaN₃. The dialysis tubing for MWCO 12,000 was regenerated cellulose *SPECTRA/POR*[®] 1 which was stored dry, was soaked in 1:1 MeOH-H₂O for at least 48 h prior to use.

To purify ONPs Thermo Scientific slide-A-Lyzer dialysis cassettes G2 (3,500 or 10,000 MWCO) made of regenerated cellulose (synthesized by the Viscose method) were used. All samples were dialyzed in 1-4 L covered beakers in which solvent was changed at least four times allowing for equilibration for 6-12 h. The water was kept slightly basic with sodium bicarbonate and ~ 5% brine by volume was added.

Nuclear Magnetic Resonance (NMR)

All NMR spectra were acquired at the VOICE laboratory on a Varian instrument in chloroform-*d*, unless otherwise specified. Residual protio solvent peaks, CD₃OD, D₂O, DMSO-*d*₆, CDCl₃, were used as internal standards for all spectra unless specified otherwise. Coupling constants are reported in hertz (Hz). Spectra of HPGs with dye were acquired in D₂O adjusted to pH 9.0 with NaOD. Spectra were worked-up and analyzed using iNMR reader 3.4 © Mestrelab Research. Occasionally two different ¹H NMR are reported. This was necessary to compare the spectrum to other compounds in the same solvent when differences in solubility were an issue.

Mass Spectrometry (MS)

Matrix assisted laser desorption ionization (MALDI) mass spectra were collected on a Quattro system and electrospray ionization mass spectra were collected with an automated ZMD system. Mass spectral results are reported as well as the mode (positive or negative) followed by the exact mass, abbreviated EM.

Size Exclusion Chromatography (SEC)

The analytical water SEC system used was an Ultrahydrogel™ 250 column (7.8 x 300 mm) in series with an Ultrahydrogel™ 120 column. The water eluent contain 10 mM NaN₃ to keep microbial growth to a minimum. Eluent was monitored by UV at 289 nm followed by refractive index. Note: this accounts for the slight difference in peak signals. Elution times were calibrated using a series of linear PEG standards.

The analytical DMF SEC system was series of 3 ViscoGEL™ columns monitored by RI and calibrated with PS standards. This instrument became inoperable shortly after the

synthesis of the first HPG and has since been decommissioned. These two systems were calibrated against one another; see Chapter IV. Appendices.

The analytical DMF SEC for later HPG and ONP work was conducted on a Waters SEC with a refractive index detector and photodiode array and later a miniDAWN Treos (MALS detector) from Wyatt Technology. The system contained three columns in series Styragel HR 3, 4 and 5 and were kept at 50 °C with a flow rate of 1 mL min⁻¹. Breeze 2 software was used to work up the data from the RI and PDA. Astra 6.1 was used to work up the MALLS data. The eluent, DMF, contained 0.1 M LiBr, which was added to improve peak shape. Linear PEG was used as the standard for HPGs and polystyrene for the ONP polymers. It is important to note values derived from the PS curve are not considered accurate but used as a means to compare successive reactions.

The above Waters system was changed to a water system to use the systems detectors to study water soluble ONPs (ONPs were not DMF soluble). Waters Ultrahydrogel 250 and 1000 columns were used at 35 °C with a flow rate of 0.75 mL/min. PEG was again used as a standard. The eluent contained 10 mM NaN₃ and 20 mM sodium phosphate buffer pH 8.0. All analytes were filtered through a 0.45 µm PTFE filter prior to running.

Preparatory size exclusion chromatography was used to separate fluorescent HPGs from free fluorescein and fluorescein derivatives. BioRad polyacrylamide resin P2,



Figure 3.1. Example of purification of HPG-Fl (orange) and the unconjugated fluorescein (yellow)

P6, P10 and P100 (medium mesh, 90-180 μm) was used with 20% (v/v) methanol in an aqueous 20 mM phosphate buffer solution at pH 8 eluent. The separation was distinguishable visually by the two different colored bands, Figure 3.1.

Inductively Coupled Plasma

Analysis of the residual metal in the ONP was carried out on a PerkinElmer 2000DV ICP-OES by the Microanalysis Lab of SCS at UIUC. Samples were submitted as flaky solids and the residual Os and Ru levels reported.

UV-visible Spectroscopy

The absorbance spectra and molar absorptivity of each polymer was studied with a UV-2501PC instrument using UV Probe software. Spectra were collected from 200-750 nm with 0.5 or 1 nm sampling interval. To study the polymers, three separate samples were massed and a stock solution prepared (5-500 μM). Each stock solution was diluted to 4-6 different concentrations to attain an absorbance from 1 to 0.1. Molar absorbance was determined from the average of the slope of linear fit of the aforementioned data.

Example data and work-up can be found in Chapter IV. Appendices.

Fluorescence Spectroscopy

Fluorescence spectra were collected on a Horiba Scientific FluoroMax4 Spectrofluorometer and used in conjunction with FluorEssence V3.5 software. For quantum yield determination, the aforementioned UV-vis samples were diluted 10-fold for fluorescent spectroscopy. Spectra were collected by exciting at 475 nm (2 nm slit) and collecting from 480-600 nm (2 nm slit) using 3 mm 6Q quartz cuvettes. Fluorescence values are reported as the sum of fluorescence intensity from 480-600 nm.

Fluorescein was used as a standard for fluorescence as well as determining the number of dye moieties per polymer molecule. Fluorescein was experimentally determined to have $\epsilon_{490}=78,000 \text{ Abs/Mcm}^{-1}$, and assumed to have $QY = 0.9$ therefore a brightness of 70,200. Further information can be found in the Chapter IV. Appendices.

Photobleaching Studies

A ThorLabs 470 nm LED (M470L3) regulated with T-cube LED Driver (LEDD1B) set to 1000 mA (reported to produce 710 mW) was used to bleach samples. Polymers solutions were prepared in vials, 5 mL at 1 μM by diluting the stock solutions from the UV-vis and fluorescence studies, 20 mM pH 8.0 phosphate buffer was used. Samples were placed 3 inches from the LED and rotated positions at each time point (Figure 3.2). Three to five samples could be bleached at once, but artifacts were observed, in bleaching curves, with more than 5 samples. Aliquots (200 μL) were removed at given timed intervals, generally, 0, 0.5, 1, 1.5, 2, 3, 4, 5, 6, 7, 8 h. The fluorescence spectra of these samples were then collected. Each study (set of samples) included fluorescein as a standard.

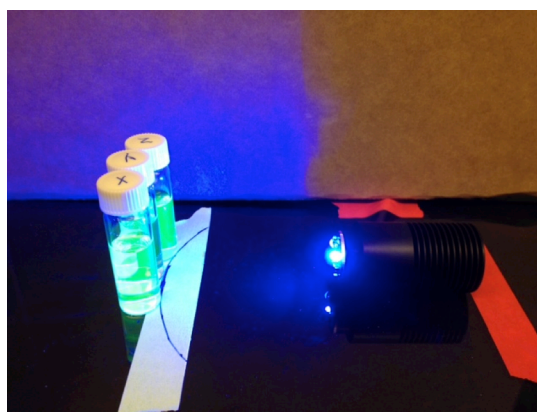


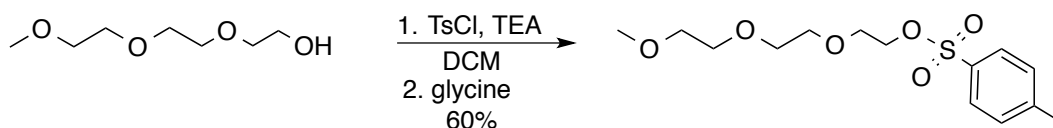
Figure 3.2: Photobleaching Set-up

III.B. Synthesis of Fluorescent HPGs and Precursors

This section covers the synthesized of compounds from I. Design, Synthesis and Characterization of Fluorescent Hyperbranched Polyglycerols with Covalently Bound Anti-Fading Agent.

Synthesis of Gallate, Trolox and Fluorescein Derivatives

2-(2-(2-methoxyethoxy)ethoxy)ethyl 4-tosylate.¹



To a flame dried flask was added 35 mL (0.20 mol) of 2-(2-(2-methoxyethoxy)ethoxy)-ethan-1-ol, 42 mL (0.301 mol) of TEA, and 300 mL of DCM (from SPS) and cooled in an ice-bath to 0° C. To the cooled solution was added via syringe pump (0.57 mL/min), 46.5 g (0.244 mol) of tosyl chloride, dissolved in 150 mL of DCM (from SPS). The reaction was allowed to stir at room temperature overnight and 3.1 g (41 mmol) of glycine was added to react with excess tosyl chloride and the mixture stirred for 5 h at room temperature. The reaction was washed twice with 150 mL of water. The organic layer was dried with MgSO₄ and the solvent was removed via rotary evaporation to afford 38.2 g (60%) of the desired product as a clear viscous liquid.

¹H NMR (500 MHz; CDCl₃) δ 7.80 (d, *J* = 8.5, 2H), 7.34 (d, *J* = 8.5, 2H), 4.17-4.15 (m, 2H), 3.69-3.68 (m, 2H), 3.62-3.60 (m, 2H), 3.54-3.52 (m, 2H), 3.37 (s, 3H), 2.44 (s, 3H).

with 50 mL brine and again with water. The oil was dried with MgSO₄, filtered, the solvent removed under reduced pressure. The ~3 mL of brown oil remained and was put on high vacuum for 90 minutes, and then it was washed with 25 mL of ether and thrice with 10 mL of water. The solvent was removed to afford 860 mg (78%) of a golden yellow oil.

Rf: 0.45 in 50% EtOAc/PE

¹H NMR (500 MHz; CDCl₃): δ 7.50-7.46 (m, 4H), 7.43-7.37 (m, 6H), 7.37-7.32 (m, 2H), 5.14 (s, 4H), 4.25 (t, 5.0 2H), 3.89 (s, 3H), 3.78 (t, 5.0 2H), 3.62 (d, 4.4 2H), 3.61 (d, 3.3 2H), 3.57 (d, 4.4 2H), 3.56 (d, 3.3 2H), 3.54-3.48 (m, 4H), 3.35 (s, 3H).

3,5-bis(benzyloxy)-4-(2-triethyleneglycol)benzoic acid (BntGa).

To a solution of 0.770 g (1.51 mmol) of **BntG** in methanol was added 138 mg (2.45 mmol, 1.6 eq.) of KOH. The mixture was refluxed for 12 h. To the brown residue was added 10 mL water and 2 mL of 2M HCl. When removing the solvent a white precipitate formed which was isolated by filtration and dried under vacuum to afford 640 mg (85%).

¹H NMR (500 MHz; CDCl₃): δ 7.46 (d, 7.1 4H), 7.42 (s, 2H), 7.38 (dd, 7.4 4H), 7.32 (dd, 7.3 2H), 5.15 (s, 4H), 4.27 (d, 5.0 2H), 3.79 (d, 5.0 2H), 3.62 (dd, 5.9, 3.8 2H), 3.57 (dd, 5.8, 3.6 2H), 3.53 (d, 5.7, 4.0 2H), 3.50 (dd, 5.7, 3.6 2H), 3.35 (s, 3H). ¹³C NMR (126 MHz; CDCl₃): δ 169.8, 152.2, 136.8, 128.7, 128.2, 127.6, 107.0, 72.8, 72.1, 71.4, 70.73, 70.70, 70.67, 70.6, 59.2.

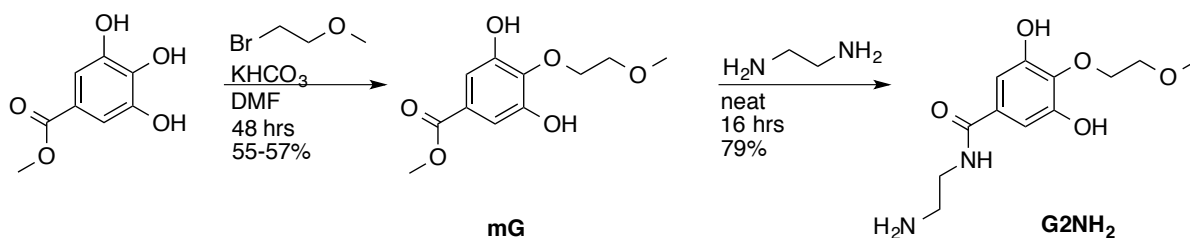
3,5-bis(benzyloxy)-4-(2-triethyleneglycol)benzoyl chloride (ClBntG).⁴

A solution of 629 mg (1.27 mmol) of dibenzyl PEG-gallic acid in 0.2 mL dry DMF and 10 mL toluene, was purged with Ar. To the solution was added 150 μL (1.75 mmol, 1.4 eq.) of

oxalyl chloride (make sure it has a vent, preferably through a basic solution), Figure 3.3. Bubbles observed as gas evolved. A second aliquot of 70 μL (0.82 mmol, 0.6 eq.) of oxalyl chloride was added. The reaction was stirred 5 h and the solvent was removed via rotary evaporation. The remaining residue was dried overnight on high vacuum to afford 334 mg (51%) of cream solid and used directly in further reactions. MS ESI⁺ corresponded to the mass of the methyl ester ¹H NMR (500 MHz; CDCl₃): δ 7.46 (d, 7.1 4H), 7.43 (s, 2H), 7.39 (dd, 7.3 4H), 7.34 (dd, 7.3 2H), 5.15 (s, 4H), 4.31 (m, 2H), 3.78 (m, 2H), 3.61 (m, 2H), 3.56 (m, 2H), 3.52 (m, 2H), 3.49 (m, 2H), 3.35 (s, 3H). ¹³C NMR (126 MHz; CDCl₃): δ 167.6, 163.9, 152.4, 145.3, 136.3, 128.8, 128.3, 127.7, 111.4, 72.9, 72.0, 71.6, 70.71, 70.69, 70.64, 70.58, 59.1.



Figure 3.3: Set-up for synthesis of ClBntG



Methyl 3,5-dihydroxy-4-(2-methoxyethoxy)benzoate (mG).

To a solution of 31.54 g (171 mmol) of methyl gallate in 500 mL of DMF was added 17.13 g (171 mmol, 1 eq.) of potassium bicarbonate. The solution was stirred 30 min at 60 °C then 21.0 g (151 mmol, 0.88 eq) of 1-bromo-2-methoxyethane was added. The reaction was stirred for 48 h at 60° C. All but ~75 mL of DMF was removed by rotary evaporation. The

reaction was diluted with 200 mL of 10% MeOH/CHCl₃ and washed thrice with 100 mL brine. The combine brine washes were back extracted with 50 mL of 10% MeOH/CHCl₃ and combine with the organic layer. Solvent was removed from the organic layer by rotary evaporation followed by drying overnight in the vacuum oven (-762 mm Hg, 80° C). The solid was dissolved in ~200 mL boiling DCM covered and allowed to cool. Three crystals were isolated and the remaining solution was gravity filtered to remove the insoluble powder, which was washed with twice 50 mL of warm DCM. The solvent was removed from the filtrate and the solid crystallized from DCM twice, Figure 4, to afford 20.30 g (55-57%) of light brown crystals.

Rf: 0.51 in 10% MeOH/(DCM:CHCl₃)

MS ESI⁻ Calc'd: 242.08. Found: 241.0.

¹H NMR (400 MHz; CDCl₃): δ 7.19 (s, 2H), 6.94 (br, 2H), 4.19 (t, 4.3 2H), 3.87 (s, 3H), 3.72 (t, 4.3 2H), 3.55 (s, 3H).



Figure 3.4: Crystals of mG massed to over 20 g.

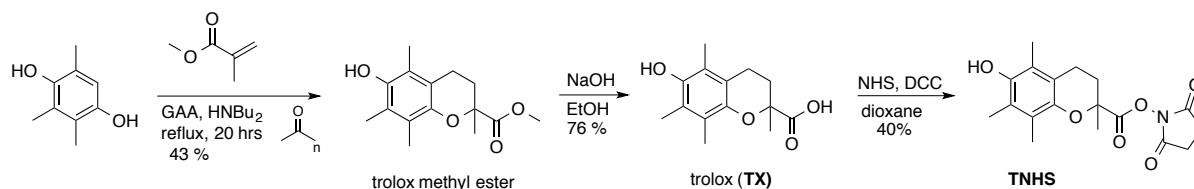
***N*-(2-aminoethyl)-3,5-dihydroxy-4-(2-methoxyethoxy)benzamide (G2NH₂).**

A solution of 13.61 g (56.2 mmol) of methyl 3,5-dihydroxy-4-(2-methoxyethoxy)benzoate in ~200 mL (~3 mol) of freshly distilled ethylenediamine was stirred at 85 °C for 18 h.

Unreacted ethylenediamine was removed by rotary evaporation and the remaining product dried on high vacuum at 50 °C for 36 h. The solid was titrated with 200 mL warm water and vacuum filtered. The product was dried in vacuum oven at 60 °C at -635 mm Hg for 3 h to afford 11.98 g (79%) of a cream colored solid.

MS ESI⁺ Calc'd: 270.12. Found: 271.3.

^1H NMR (500 MHz; $\text{DMSO-}d_6$): δ 8.10 (t, 5.5 1H), 6.81 (s, 2H), 4.04 (dd, 5.9, 4.0 2H), 3.60 (dd, 5.9, 4.1 2H), 3.40 (s, 2H), 3.31 (s, 3H), 3.18 (q, 6.3 2H), 2.63 (t, 6.3 2H).



Trolox methylester.⁵

To a solution of 27.97 g (184 mmol, 1eq.) of 3-methyl hydroxyl quinone in 31 mL glacial acetic acid was added 102 mL (964 mmol, 5.2 eq.) of methylmethacrylate, 4.2 mL (24.9 mmol, 0.13 eq.) of dibutylamine, and 7.26 g (242 mmol, 1.3 eq.) of paraformaldehyde. The reaction was reflux for 20 h then cooled to 0 °C. The precipitate that formed was filtered and washed with methanol to afford 21 g (43%) pale tan solid.

^1H NMR (500 MHz; CDCl_3): δ 4.23 (bs, 1H), 3.67 (s, 3H), 2.65 (ddd, 16.9, 6.2, 3.2 1H), 2.51 (ddd, 16.9, 11.0, 6.2 1H), 2.43 (ddd, 13.3, 6.3, 3.2 1H), 2.19 (s, 3H), 2.16 (s, 3H), 2.06 (s, 3H), 1.87 (ddd, 13.3, 11.0, 6.3 1H), 1.60 (s, 3H). ^{13}C NMR (126 MHz; CDCl_3): δ 174.6, 145.7, 145.4, 122.7, 121.3, 118.5, 117.0, 77.4, 52.5, 30.8, 25.6, 21.1, 12.3, 12.0, 11.4. calc 264.14

(±)-6-Hydroxy-2,5,7,8-tetramethylchromane-2-carboxylic acid (Trolox (TX)).⁶

To a solution of 0.809 g (3.1 mmol) of methyl ester trolox in 20 mL of methanol was added 2 mL of 10.0 M (20 mmol, 6.5 eq.) NaOH. The resulting green solution and was refluxed for 2 h. Once cool, the reaction was acidified with 2M HCl and cooled to -20 °C. The resultant precipitate was isolated by vacuum filtration and washed with ice water to afford 589 mg (76%) of off-white powder. Yield: 56-76%.

MS ESI- Calc'd: 250.12. Found: 249.1.

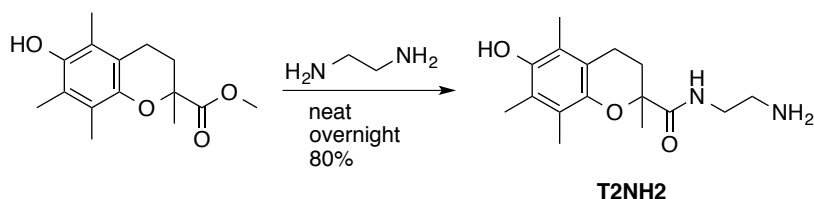
^1H NMR (500 MHz; CDCl_3): δ 2.68 (dt, 17.1, 6.2 1H), 2.65 (ddd, 17.1, 8.8, 6.2 1H), 2.36, (dt, 13.6, 6.1 1H), 2.18 (bs, 6H), 2.10 (s, 3H), 1.97 (ddd, 13.6, 8.7, 6.4 1 H), 1.61 (s, 3H), 1.26 (s, 3H). The phenol H was not observed. ^1H NMR (500 MHz; $\text{DMSO-}d_6$): δ 7.43 (s, 1H), 2.56 (ddd, 16.9, 6.1, 2.8 1H), 2.40 (ddd, 16.9, 11.4, 6.5 1H), 2.28 (ddd, 13.3, 6.5, 2.8 1H), 2.05 (s, 3H), 2.02 (s, 3H), 1.97 (s, 3H), 1.73 (ddd, 13.3, 11.4, 6.1 1H). ^{13}C NMR (126 MHz; CDCl_3): δ 177.3, 145.9, 144.7, 122.6, 121.6, 188.8, 117.2, 77.4, 30.1, 24.6, 20.7, 12.4, 12.0, 11.4.

***N*-hydroxysuccinimide trolox (TNHS).**

To a solution of 5.38 g (21.5 mmol) of trolox in 80mL dioxane was added 2.71 g (23.5 mmol, 1.1 eq) of *N*-hydroxy succinimide. The reaction was then cooled via an ice bath to 0° C, and 4.30 g (20.8 mmol, 1.0 eq.) of DCC was added in ~ 1 g aliquots every 5 min. The reaction was allowed to stir overnight gradually warming to ambient temperature. The solvent was removed and crude product purified by column chromatography in 5 to 10% EtOAc/PE to afford 2.99 g (40%) pale tan powder.

MS ESI- Calc'd: 347.14. Found: 346.1.

^1H NMR (500 MHz; CDCl_3): δ 2.87 (ddd, 17.3, 11.8, 6.2 1H), 2.80 (s, 3H), 2.75 (ddd, 17.1, 6.2, 2.8 1H), 2.59, (ddd, 13.7, 6.3, 2.9 1H), 2.19 (s, 3H), 2.18 (s, 3H), 2.12 (s, 3H), 2.06 (ddd, 13.6, 11.8, 6.2 1 H), 1.55 (s, 3H).



***N*-(2-aminoethyl)-6-hydroxy-2,5,7,8-tetramethylchroman-2-carboxamide (T2NH₂).**⁷

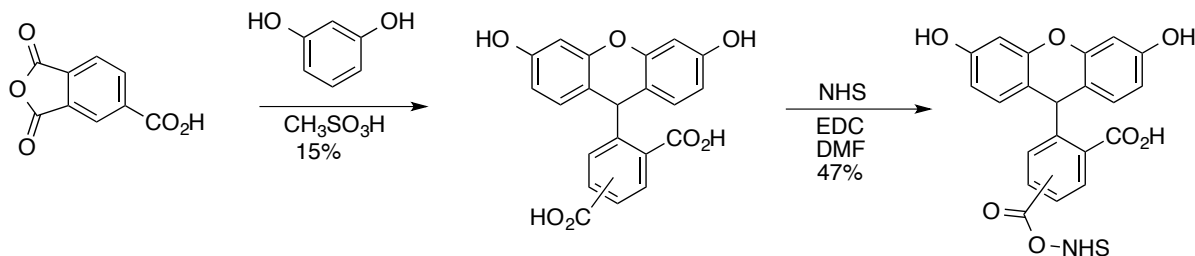
A solution of 3.8 g (14 mmol) of trolox methylester in 200 mL (3 mol) of ethylenediamine was heated to 115 °C overnight. The reaction volume was reduced to 20 mL by rotary evaporation then diluted with ~ 200 mL CHCl₃. The solution was washed twice with 100 mL sat. NaHCO₃ and dried with MgSO₄ and filtered. The remaining chloroform was removed affording an oil which was titrated with ether and vacuum filtered to yield 3.4 g (80%) of the desired product as a cream colored solid.

Rf: 0.13 in 10% MeOH/(DCM:CHCl₃)

MS ESI⁺ Calc'd: 292.18. Found: 293.2.

¹H NMR (500 MHz; CDCl₃): δ 6.80 (t, 5.5 1H), 3.30 (dq, 13.5, 6.0 1H), 3.21 (dq, 13.5, 5.9 1H), 2.70 (t, 5.9 2H), 2.63 (dt, 16.7, 6.1 1H), 2.56 (ddd, 16.7, 8.8, 6.9 1H), 2.37 (dt, 13.4, 6.1 1H), 2.19 (s, 3H), 2.17 (s, 3H), 2.09 (s, 3H), 1.89 (ddd, 13.4, 8.8, 6.2 1H), 1.53 (s, 3H).

¹H NMR (500 MHz; DMSO-*d*₆): δ 7.50 (s, 1H), 7.32 (t, 5.7 1H), 3.32 (s, 1H), 3.04 (dd, 6.2, 2.1 1H), 3.02 (dd, 6.2, 2.1 1H), 2.53 (dt, 10.8, 5.9 1H), 2.48 (t, 6.4 2H), 2.42 (ddd, 16.6, 7.8, 6.9 1H), 2.16 (dt, 13.2, 6.2 1H), 2.10 (s, 3H), 2.07 (s, 3H), 1.99 (s, 3H), 1.73 (ddd, 13.4, 8.4, 6.1 1H), 1.37 (s, 3H), 1.24 (s, 2H). Peak at ~2.53 ppm occulted by DMSO peak.



5,6-carboxyfluorescein.⁸

A mixture of 26.4 g (138 mmol) of dried trimellitic anhydride and 30.2 g (274 mmol) of resorcinol were ground together and suspended in 300 mL methane sulfonic acid. The color immediately turned cerulean blue and was heated to 80° C. As the reaction progressed, the color changed to dark red and then to orange. After 5 h, all solids were dissolved. The solution was poured into 2.1 L of ice water and vacuum filtered. The filter cake was dried and the ~20 g of solid were dissolved in 500 mL 4 M NaOH, to which concentrated HCl was added drop-wise until precipitation ceased (pH ≤ 1). The solution was vacuum filtered and washed twice with 100 mL 1M HCl to afford 7.8 g (15%) of the desired orange product as a mixture of 5 and 6 isomer.

MS ESI⁻ Calc'd for C₂₁H₁₁O₇: 375.3. Found: 375.0.

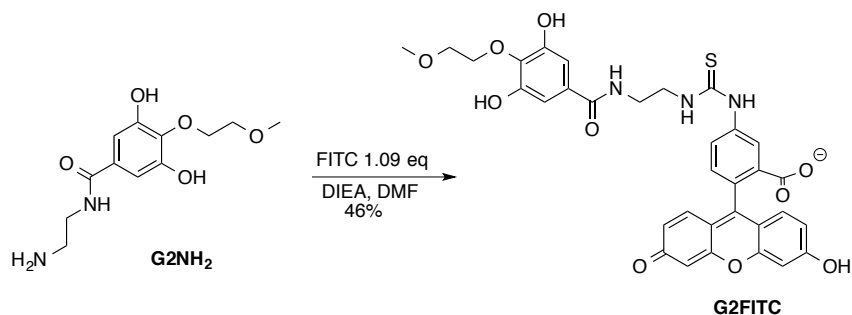
¹H NMR (500 MHz; CD₃OD): δ 8.69 (d, 0.8 1H), 8.40 (dd, 8.0, 1.6 1H), 8.36 (dd, 8.1, 1.4 1H), 8.21 (d, 8.1 1H), 7.84 (d, 0.7 1H), 7.38 (d, 8.0 1H), 6.90 (d, 2.0 2H), 6.87 (d, 9.6 2H), 6.85 (d, 2.1 2H), 6.83 (d, .9.3 2H), 6.74 (dd, 9.1, 2.0 2H), 6.71 (dd, 8.8, 2.0 2H).

5,6-carboxyNHS fluorescein.⁹

To a 100 mL RBF was added 3.01 g (8.0 mmol) of 5,6-carboxy fluorescein, 3.04 g (15.2 mmol, 1.9 eq.) of EDC and 2.22 g (19.3 mmol, 2.4 eq.) of N- hydroxy succinimide and dissolved in 2 mL of DMF. The reaction was allowed to stir at room temperature for an hour and then the solvent was removed under reduced pressure. The product was purified by column chromatography in 1 to 3 % MeOH/CHCl₃ to afford 1.75 g (47%) of an orange solid.

MS ESI⁺ Calc'd: 473.01. Found: 474.0.

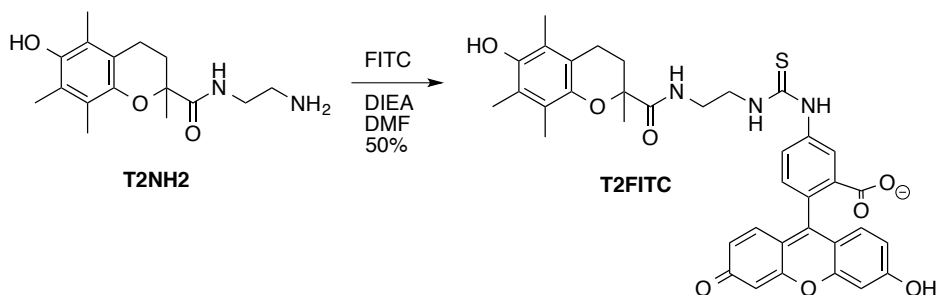
^1H NMR (500 MHz; CD_3OD): δ 8.72 (dd, 1.5, 0.7 1H), 8.46 (dd, 8.1, 1.6 1H), 8.42 (dd, 8.1, 1.4 1H), 8.21 (dd, 8.1, 0.7 1H), 7.91 (dd, 1.4, 0.7 1H), 7.45 (dd, 8.1, 0.7 1H), 6.71 (d, 2.4 2H), 6.70 (d, 2.4 2H), 6.66 (d, 1.6 2H), 6.64 (d, 1.6 3H), 6.58 (dd, 4.5, 2.4 3H), 6.56 (dd, 4.5, 2.4 3H), 2.94 (s, 4H), 2.87 (s, 4H).



G2FITC.

To a solution of 134 mg (0.496 mmol) of G2NH_2 in 6 mL DMF was added 350 μL (2.0 mmol, 4 eq.) of DIEA and 210 mg (0.539 mmol, 1.09 eq.) of FITC. The mixture and stirred for 45 h at ambient temperature. The solvent was removed and the product purified by column chromatography in 5 \rightarrow 18 % MeOH/ CHCl_3 to afford 150 mg (46%) of an orange solid.

^1H NMR (500 MHz; $\text{DMSO-}d_6$): δ 10.12 (br, 1H), 10.08 (br, 1H), 9.09 (br, 1H), 8.35 (br, 1H), 8.24 (d, 1.9 1H), 8.17 (s, 1H), 7.74 (d, 5.2 1H), 7.17 (d, 8.3 1H), 6.86 (s, 2H), 6.67 (d, 2.3 2H), 6.61 (d, 8.7 2H), 6.56 (dd, 8.7, 2.3 2H), 4.10 (q, 5.0 2H), 4.04 (dd, 5.9, 4.0 2H), 3.61 (dd, 5.9, 4.0 2H), 3.45 (q, 5.8 2H), 3.31 (s, 3H).



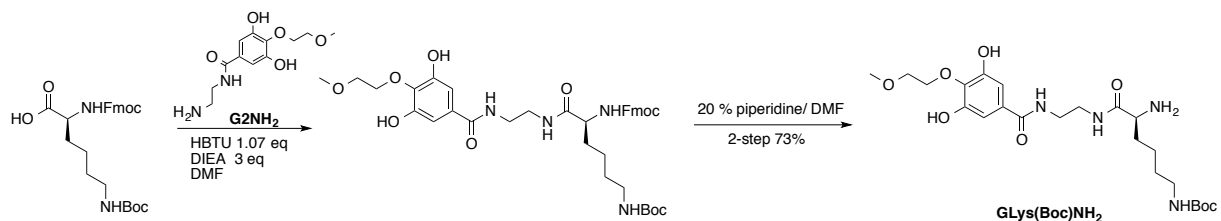
T2FITC.

A solution of 50 mg (0.17 mmol) of T2NH₂, 150 μ L (0.86 mmol, 5 eq) of DIEA and 65 mg (0.17 mmol) of FITC was stirred overnight in 3 mL dry DMF at ambient temperature. The solvent was removed and product purified by column chromatography in 5 \rightarrow 15 % MeOH/DCM to afford 57 mg (50%) of the product as a dark orange solid.

R_f: 0.42 in 10 % MeOH/DCM

¹H NMR (500 MHz; DMSO-*d*₆): δ 11.70 (br, 1H), 10.14 (br, 1H), 8.15 (d, 1.3 1H), 7.71 (d, 6.2 1H), 7.58 (t, 5.4 1H), 7.17 (d, 8.3 1H), 6.67 (d, 2.3 2H), 6.61 (d, 8.7 2H), 6.56 (dd, 8.7, 2.3 2H), 3.61 (br, 2H), 3.40 (td, 12.9, 6.4 2H), 3.33 (br, 2H), 3.26 (td, 12.5, 6.4 2H), 2.41 (dt, 16.3, 7.6 1H), 2.13 (dt, 13.3, 6.6 1H), 2.09 (s, 3H), 2.05 (s, 3H), 1.98 (s, 3H), 1.73 (dt, 14.0, 6.8 1H), 1.36 (s, 3H). peak at \sim 2.53 ppm occluded by DMSO peak.

Synthesis of AFA-Lysine-Fluorescein Conjugate



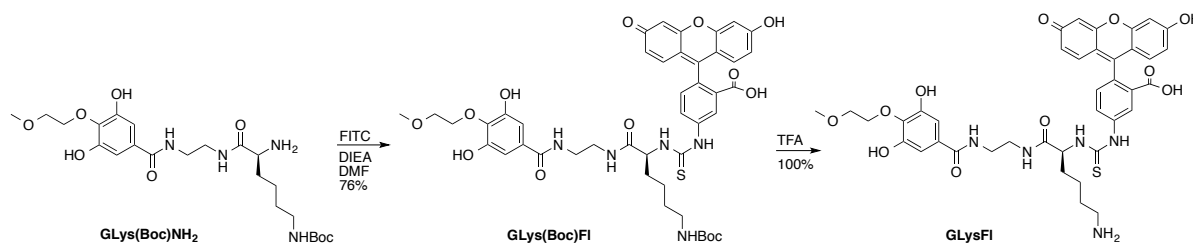
GLys(Boc)NH₂.

To a solution of 3.43 g (7.32 mmol, 1.07 eq.) of FmocLys(Boc)OH in 125 mL of DMF was added 1.92 mL (11.0 mmol, 1.5 eq.) of DIEA and 2.98 g (7.86 mmol, 1.07 eq.) of HBTU. After 30 min. 2.38 g (8.81 mmol) of G2NH₂ and 2.05 mL (11.8 mmol, 1.6 eq.) of DIEA were added and stirred at room temperature overnight. The DMF was removed by rotary

evaporation and the product isolated by column chromatography in 3 →8% MeOH 1% GAA/DCM. The solvent was removed from fractions containing product and stirred in 30 mL 20 % piperidine in DMF for 2 h. The solvent was removed the product isolated by column chromatography in 9% MeOH 1% GAA/DCM until the residual HOBT eluted. The running solvent was then switched to 10% MeOH/DCM and then 9% MeOH 1% TEA/DCM to afford 1.54 g of a cream colored solid. Two-step yield: 1.54 g, 73%. Note: HBTU works better than DCC.

MS ESI⁺ Cal'd for: 498.27. Found: 500.0

¹H NMR (500 MHz; DMSO-*d*₆): δ 8.23 (t, 5.2 1H), 8.18 (t, 5.4 1H), 6.84 (s, 2H), 6.72 (t, 5.5 1H), 5.70 (s br, 2H), 4.05 (dd, 5.9, 4.0 2H), 3.60 (dd, 5.9, 4.0 2H), 3.31 (s, 3H), 3.26 (t, 5.3 2H), 3.22 (q, 6.4 2H), 2.86 (q, 6.4 2H), 1.56 (m, 1H), 1.41 (m, 1H), 1.36 (s, 9H), 1.32 (m, 2H), 1.24 (m, 2H).



GLys(Boc)FI.

To a solution of 555 mg (1.11 mmol) of GLys(Boc)NH₂ in 10 mL dry DMF was added 0.78 mL (4.47 mmol, 4eq.) of DIEA and 490 mg (1.26 mmol, 1.1 eq) of FITC. The mixture was stirred at ambient temperature for 4 days. The solvent was removed via rotary evaporation and the product purified by column chromatography in 5 →10% MeOH 1% GAA/DCM to afford 750 mg (76%) of an orange solid.

Rf: 0.26 in 10% MeOH 1% GAA/DCM

MS ESI- Calc'd: 887.3. Found: 886.1.

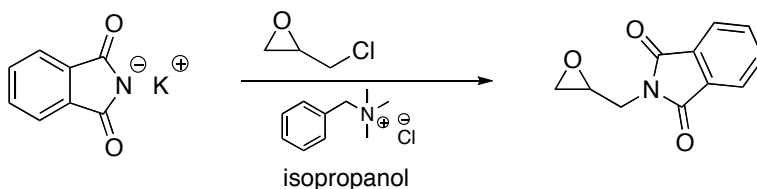
^1H NMR (; DMSO- d_6): δ 11.30 (br, 1H), 10.31 (s, 1H), 9.13 (br, 2H), 8.46 (s, 1H), 8.31 (s, 1H), 8.24 (d, 7.5 1H), 8.21 (t, 4.4 1H), 7.78 (dd, 8.4, 1.2 1H), 7.17 (d, 8.4 1H), 6.83 (s, 2H), 6.74 (t, 5.4 1H), 6.67 (d, 2.1 2H), 6.60 (dd, 8.7, 3.1 2H), 6.56 (dd, 8.7, 2.0 2H), 4.85 (q, 6.2 1H), 4.04 (dd, 5.7, 4.0 2H), 3.60 (dd, 5.7, 4.2 2H), 3.31 (s, 3H), 3.27 (m, 4H), 2.88 (q, 6.4 2H), 1.77 (m, 1H), 1.69 (m, 1H), 1.37 (occluded, 2H), 1.35 (s, 9H), 1.25 (m, 2H).

GLysFl.

A solution of 183 mg (0.21 mmol) of **GLys(Boc)Fl** in 3 mL CHCl_3 and 6 mL TFA was stirred for 4 h. The solvent was removed to afford 160 mg (quant.) of the desired product as an orange solid.

^1H NMR (500 MHz; DMSO- d_6): δ 10.32 (s, 1H), 10.16 (br, 1H), 9.12 (br, 1H), 8.56 (s, 1H), 8.34 (d, 9.9 1H), 8.31 (t, 5.6 1H), 7.76 (dd, 8.3, 2.0 1H), 7.70 (d, 13.1 1H), 7.21 (d, 8.3 1H), 6.86 (s, 2H), 6.68 (d, 2.2 2H), 6.60 (d, 8.7 2H), 6.56 (dd, 8.7, 2.2 2H), 4.91 (dd, 12.9, 6.6 1H), 4.05 (dd, 6.0, 3.9 2H), 3.61 (dd, 6.0, 3.9 2H), 3.43 (q, 5.7 2H), 3.31 (s, 3H), 2.94 (s, 2H), 2.88 (d, 68.9 5H), 2.80 (s, 2H), 1.82 (dtt, $J=20.7, 13.8, 6.9$ 2H), 1.58 (tq, 14.0, 7.0 2H), 1.42 (quintet, 7.7 Hz)

Synthesis of Amine Comonomers



Potassium phthalimide.¹⁰

A solution of 40 g (272 mmol) of phthalimide in 800 mL of 200 proof EtOH was refluxed for 30 min. The solution was decanted into a solution of 15.4 g (274 mmol) of KOH in 12 mL water and 45 mL ethanol and allowed to cool to ambient temperature. The resulting precipitate was vacuum filtered and washed with acetone to afford 40.3 g (80%) of shiny white solid.

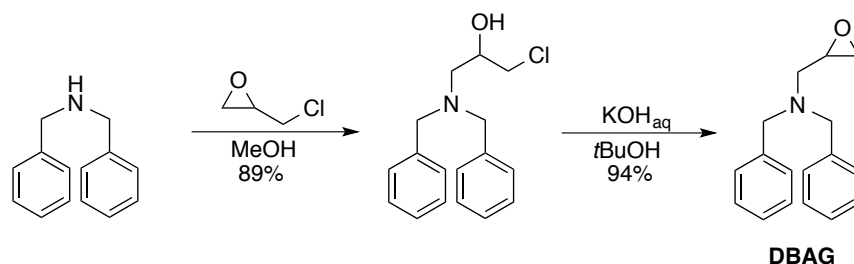
Glycidylphthalimide.¹¹

In a flame-dried flask, 36.05 g (194 mmol) of potassium phthalimide and 3.78 g (20 mmol) of benzyltrimethylammonium chloride were dissolved in 600 mL dry isopropanol under nitrogen. Approximately 45 mL, 53 g (575 mmol, 3 eq.) of epichlorohydrin was added in 11 mL aliquots in 15 min intervals. The reaction was heated to 50 °C for 29 h then allowed to cool to room temperature. The solvent was removed via rotary evaporation and the residue dissolved in 300 mL EtOAc. The organic layer was washed thrice with 100 mL water and the solvent removed via rotary evaporation to afford 34.6 g (88%) of white solid.

Note: The following reaction was only successful with freshly prepared potassium phthalimide (thoroughly dried). Literature procedure cooled the flask when adding the epichlorohydrin, but when this attempted previously significant precipitation was observed.

MS ESI⁺ Calc'd: 203.06 Found: 242.02 (+K⁺)

¹H NMR (500 MHz; CDCl₃): δ 7.87 (dd, 5.4, 3.1 2H), 7.74 (dd, 5.4, 3.1 2H), 3.96 (dd, 14.4, 5.0 1H), 3.81 (dd, 14.4, 5.0 1H), 3.14 (ddt, 5.0, 4.0, 2.5 1H), 2.81 (dd, 4.8, 4.0 1H), 2.69 (dd, 4.8, 2.5 1H).



1-chloro-3-(dibenzylamino)propan-2-ol.¹²

To a solution of 200 mL (1.04 mol) of dibenzylamine in 100 mL dry methanol was added a solution of 735 mL (9.08 mol) of epichlorohydrin in 100 mL of methanol. The reaction was allowed to stir at room temperature for 16 h under nitrogen. The solvent and excess epichlorohydrin was removed under reduced pressure to afford 266.8 g (89%) of the desired product as a slightly yellow oil. Yield: (86-94%).

Note: When a single equivalent of epichlorohydrin was used, as in literature, only 20 % conversion was seen, as determined by ¹H NMR.

¹H NMR (500 MHz; CDCl₃): δ 7.37-7.27 (m, 10H), 2.89 (ddt, 8.6, 5.6, 4.9 2H), 3.78 (d, 13.5 2H), 3.53 (d, 13.5 1H), 3.49 (dd, 10.7, 4.6 1H), 3.46 (dd, 10.7, 5.2 1H), 2.66 (dd, 12.9, 4.8 1H), 2.60 (dd, 12.9, 8.6 1H). ¹³C NMR (126 MHz; CDCl₃): δ 138.4, 129.1, 128.6, 127.5, 67.8, 58.9, 56.8, 47.5.

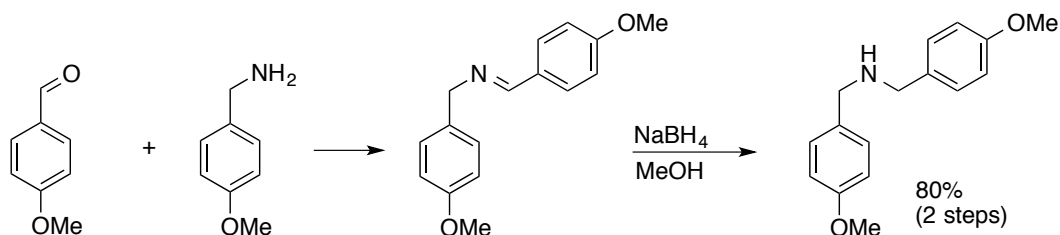
***N,N*-dibenzyl-1-(oxiran-2-yl)methanamine (DBAG).**

To a solution of 266.8 g (921 mmol) of 1-chloro-3-(dibenzylamino)propan-2-ol in 1.2 L *t*BuOH was added a solution of 87 g (1.55 mol) of KOH in 120 mL water. The mixture was stirred at 50 °C for 16 h under nitrogen. The reaction was vacuum filtered to remove the KCl and aqueous layer separated. The solvent was removed from the organic layer to give

very thick oil. Vacuum distillation under high vacuum (120 °C at 190 microns) afforded 233 g (93.5%) of a very viscous clear liquid that was stored over sieves.

MS ESI⁺ Calc'd: 253.25. Found: 254.2.

¹H NMR (500 MHz; CDCl₃): δ 7.41 (d, 7.3 4H), 7.36 (m, 4H), 7.26 (d, 7.3 2H), 3.82 (d 13.7 2H), 3.59 (d, 13.7 2H), 3.10 (ddt, 6.4, 3.8, 2.7 1H), 2.79 (dd, 13.8, 3.6 1H), 2.69 (dd, 4.9, 4.2 1H), 2.47 (dd, 13.8, 6.3 1H), 2.45 (dd, 4.9, 2.9 1H). ¹³C NMR (126 MHz; CDCl₃): δ 139.5, 128.9, 128.4, 127.1, 59.1, 56.0, 51.3, 45.2.



***N,N*-di(4-methoxybenzyl)amine.**

To a flame dried 1 L RBF equipped with a dean-stark trap was added 190 mL (1.46 moles) of methoxybenzylamine and 177 mL (1.46 moles) of *p*-anisaldehyde while stirring vigorously under nitrogen and gradually heating to 150° C. (Note: quite exothermic on this scale) Overnight, 20 mL water was isolated in the dean-stark trap and removed. The reaction was cooled to 0 °C and ~550 mL anhydrous methanol added. To this was added 74 g (1.96 moles, 1.3 eq.) of NaBH₄ over 100 min and the reaction was allowed to warm to room temperature and stirred overnight. The solvent was removed via rotary evaporation until ~ 150 mL methanol remained. To the viscous solution was added ~750 mL water and the product was extracted by washing thrice with 300 mL CHCl₃ and dried with MgSO₄. The

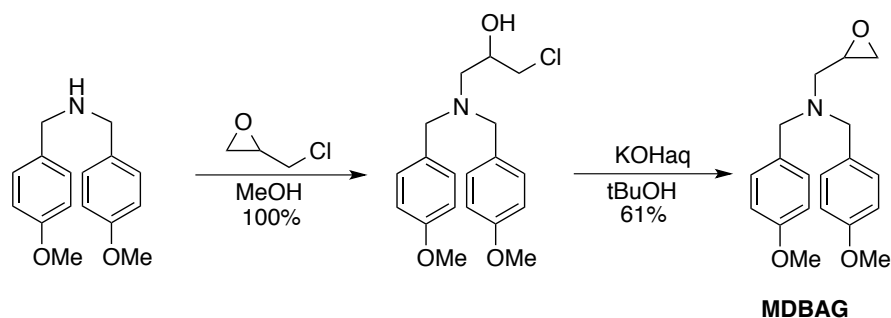
solvent was removed via rotary evaporation and the resultant material distilled under high vacuum (140 °C at 236 microns) to afford 296 g of product as a white crystalline solid.

2-step yield 80 % m.p. 38° C

Note: The yield is higher when the first step is carried out neat. During distillation no condenser is required, but slight heating of apparatus may be necessary because product is a solid at rt.

Rf = 0.71 in 5 % MeOH/CHCl₃

¹H NMR (500 MHz; CDCl₃): δ 7.27 (d, 8.6 4H), 6.89 (d, 8.6 4H), 3.83 (s, 6H), 3.76 (br, 1H).



1-(*N,N*-di-(4-methoxybenzyl)amino)-3-chloropropan-2-ol.

To a solution of 78.6 g (0.309 mol) of *N,N*-di(4-methoxybenzyl)amine in 500 mL anhydrous methanol was added 279 g (3.01 mol, 10 eq) of epichlorohydrin. The solution was stirred overnight at ambient temperature. The excess epichlorohydrin and methanol were removed via rotary evaporation to afford 108 g (100%) of pale yellow oil.

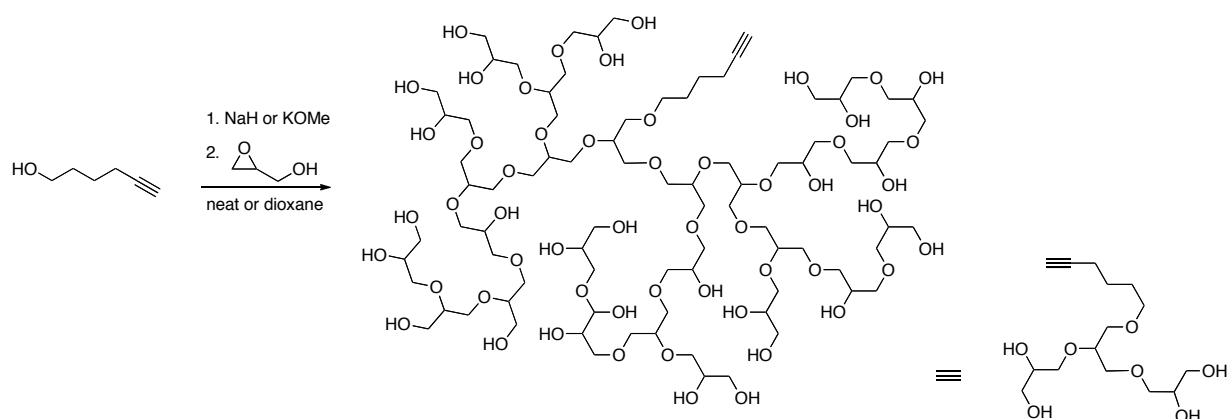
¹H NMR (500 MHz; CDCl₃): δ 7.20 (d, 8.7 4H), 6.87 (d, 8.7 4H), 3.80 (s, 6H), 3.69 (d, 13.4 2H), 3.45 (dd, 5.4, 2.4 2H), 3.44 (d, 13.4 2H), 3.33 (d, 2.0 1H), 2.60 (dd, 12.8, 4.8 1H), 2.55 (dd, 12.8, 8.7 1H).

***N,N*-di-4-methoxybenzyl-1-(oxiran-2-yl)methanamine (MDBAG).**

To a solution of 107.9 g (0.308 mol) of the above product in 750 mL in t-BuOH was added a solution of 29.4 g (0.525 mol) of KOH in 40 mL water. The reaction was heated to 60 °C and stirred 40 h under nitrogen. The reaction was cooled and filtered. To the filtrate was added 20 mL of diethyl ether, 20 mL of water and 20 mL of brine. The organic layer was separated and the solvent removed via rotary evaporation. The product was then distilled under high vac (162 °C at 83 microns) affording 59 g (61%) of a very viscous clear liquid which was stored over sieves.

¹H NMR (500 MHz; CDCl₃): δ 7.30 (d, 8.6 4H), 6.88 (d, 8.6 4H), 3.82 (s, 6H), 3.74 (d, 13.5 2H), 3.52 (d, 13.5 2H), 3.08 (m, 1H), 2.75 (dd, 13.8, 3.7 1H), 2.70 (t, 4.6 1H), 2.45-2.41 (m, 2H).

Synthesis of HPGs and Derivatives



Low Molecular Weight HPG¹³

To a flame-dried three neck RBF equipped with a mechanical stirrer, reflux condenser and syringe pump was added 0.50 mL (4.5 mmol) of 5-hexynol. To the system was added 21

mg (0.53 mmol) NaH (60% in mineral oil), and purged with nitrogen, cooled with liquid N₂ then put under high vacuum (liquid N₂ removed) until it returned to ambient temperature. This was repeated thrice. The reaction was heated to 80 °C and 47.5 mL (716 mmol, 158 eq) of glycidol was added via syringe pump at 1.5 mL/hr, Figure 5. After 35 h, the temperature was decreased to 50 °C and 60 mL of methanol added. Amberlite ion-exchange resin was allowed to stir in reaction for 1 h then removed via filtration. Fractions were isolated by fraction precipitation by diethylether followed by centrifugation.

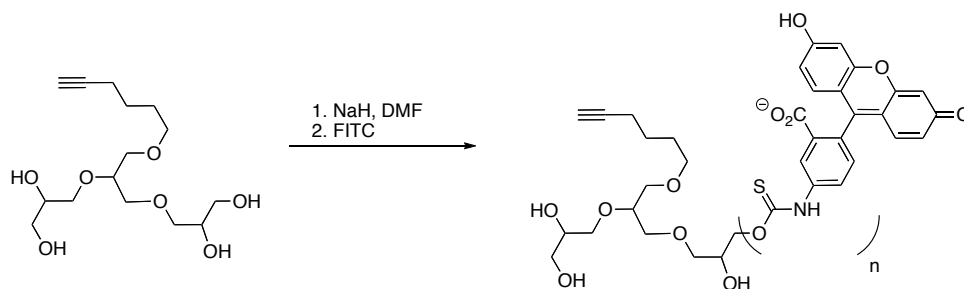
High Molecular Weight HPG (specifics for sample F)¹⁴

To a flame-dried three neck RBF equipped with a mechanical stirrer, reflux condenser and syringe pump was added 0.25 mL (2.3 mmol) of 5-hexynol. To the system was added 0.124 g (0.44 mmol, 0.19 eq) of potassium methoxide (25% by weight) and after thorough stirring, 20 mL anhydrous dioxane was added. The reaction was headed to 80 °C and 39 mL (588 mmol, 259 eq) of glycidol added at 1.5 mL per h. An hour after glycidol addition was complete, 60 mL of methanol and amberlite ion-exchange resin was



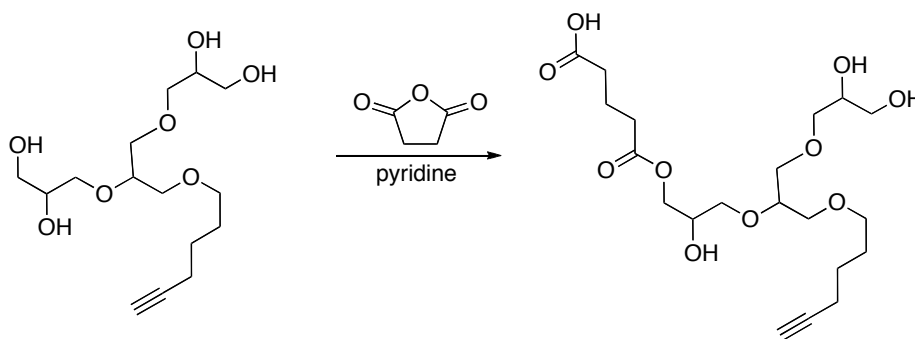
Figure 3.5: Typical set-up for HPG synthesis (top) and after all the glycidol has been added the HPG becomes very viscous (bottom).

added and the temperature decreased to 50° C. Resin was removed by filtration and the polymer precipitated by diethyl ether.



Conjugation of Fluorescein to HPG:

HPG polymer was dissolved in dry DMF and dried over sieves for 24 h. Sodium hydride was added to the polymer solution and stirred for 30 min. FITC was added and the reaction stirred 18 h at ambient temperature. Most of the DMF was removed by rotary evaporation. The remaining viscous liquid was dissolved in 20-30 mL of methanol and precipitated with 5-15 mL of diethyl ether. The solution was centrifuged to form to distinct layers, which were separated. The extremely viscous polymer was redissolved in 20-30 mL of methanol and reprecipitated with 5-15 mL of diethyl ether twice more. The polymer was dried down and dissolved in 20 % MeOH in pH 8.0 20 mM aqueous phosphate buffer. Free FITC was removed from FITC labeled polymer by prep gravity SEC using BioRad P2 resin in 20 % MeOH in pH 8.0 20 mM aqueous phosphate buffer. The resulting polymer was desalted by running through C8 with methanol.

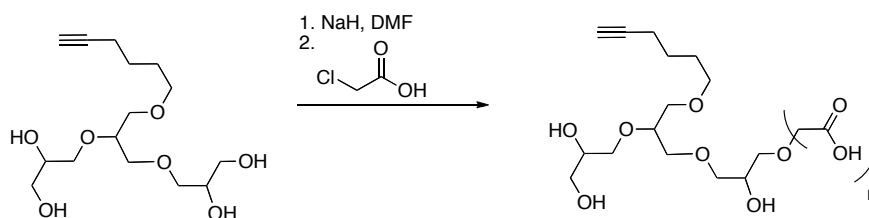


HPG-CO₂-C₃H₆-CO₂H

To a solution of 1.10 g (0.138 mmol) of HPG (MW:8000) in 12 mL dry pyridine was added 0.33 g (3.3 mmol, 24 eq.) of succinic anhydride. The reaction was warmed to 65 °C under Ar overnight. The pyridine was removed via rotary evaporation and the residue dissolved in 10 mL MeOH. The polymer was precipitated with diethylether and centrifuged (4000 rpm, 10 min, 4° C). The supernatant was removed and the polymer was redissolved and reprecipitated twice more.

¹H NMR analysis indicated ~ 11 acid groups/ polymer

HPG-CO₂H have been prepared with 34, 11, 5, and 3 acid groups/ polymer.



HPG-CH₂-CO₂H other method

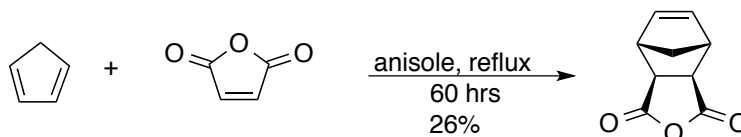
To a solution of 2.275 g (0.711 mmol) of HPG (M_n: 3200) in 50 mL of anhydrous DMF was added, over several minutes, 355 mg (8.89 mmol, 12 eq.) of NaH. After ten minutes, 1.21 g (12.8 mmol, 18 eq.) of chloroacetic acid was added and the reaction allowed to stir

overnight at ambient temperature. The solvent was removed via rotary evaporation and the residue dissolved in minimal methanol. The insoluble solid was removed via vacuum filtration and the polymer precipitated from the filtrate with diethylether. The solution was centrifuge and the supernatant decanted. The polymer was redissolved in methanol and reprecipitate twice more.

III.C. Synthesis of Fluorescent ONP and Precursors

This section details the synthesis of all compounds in Chapter II. Synthesis and Characterization of Norbornyl Based Fluorescent Organic Nanoparticles with Improved Photostability

Synthesis of Norbornyl Monomers



***Cis*-5-Norbornene-*exo*-2,3-dicarboxylic anhydride (carbic anhydride).**

A suspension of 247 g (2.52 mol) of malic anhydride in 1 L anisole was heated to 60° C. To the solution was added 215 mL (2.55 mol) of recently distilled cyclopentadiene and the reaction refluxed for 60 h. Most of the anisole (900 mL) was removed via vacuum distillation. The reaction solidified upon cooling and

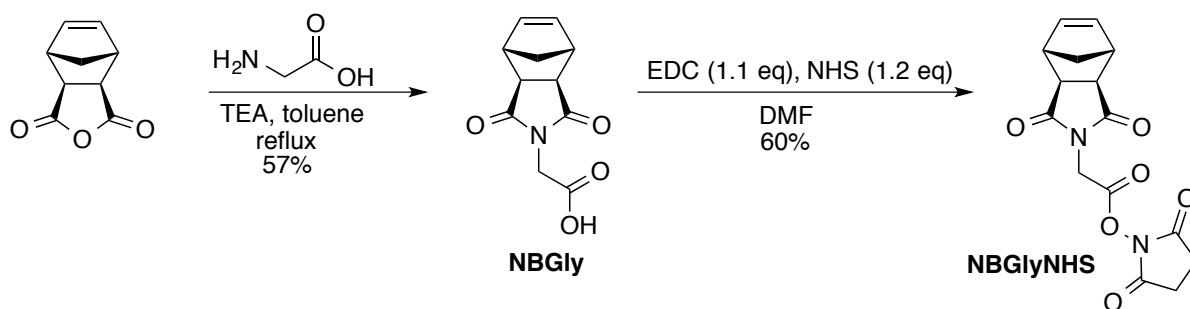


Figure 3.6: Recrystallization of *exo*-carbic anhydride from benzene

was recrystallized thrice with benzene. Supernatants were collected, benzene removed and stored to be used in the next synthesis. Off-white crystals (Figure 3.6) were isolated by vacuum filtration to afford 100.8 g (26%). Each fraction was confirmed 97+% exo product by ^1H NMR.

Rf: 0.67 in 20% EtOAc/PE stain with KMnO_4

^1H NMR (500 MHz; CDCl_3): δ 6.32 (t, 1.9 2H), 3.44 (td, 1.6, 0.4 2H), 3.00 (ddt, 1.5, 1.0, 0.5 2H), 1.66 (dt, 10.2, 1.4 1H), 1.43 (ddd, 10.2, 1.4, 0.7 1H). ^{13}C NMR (; CDCl_3): δ 171.7, 138.0, 48.8, 46.9, 44.2.



***N*-(glycine)-cis-5-norbornene-exo-dicarboximide (NBGly).¹⁵**

To a solution of 15.01 g (91.4 mmol) of carbic anhydride, in 90 mL of toluene was added 9.52 g (127 mmol, 1.4 eq.) of glycine and 1.5 mL (10.8 mmol, 0.11 eq.) of TEA. The mixture was refluxed overnight equipped with a Dean-Stark trap. The solvent was removed by rotary evaporation and the residue dissolved in 180 mL EtOAc and washed twice with 60 mL 0.2 N HCl. The organic layer was evaporated and the residue dissolved in 150 mL sat. NaHCO_3 and washed twice with 30 mL DCM. The aqueous layer was acidified with 12 mL concentrated HCl and the product was extracted with thrice with 150 mL CHCl_3 . The

organic layers were combined, dried with MgSO₄. The solvent was removed to afford 12.35 g (57 %) the desired product as a white solid. Yield: 46-78%

Rf: 0.14 in 10% MeOH/(DCM: CHCl₃) stain with KMnO₄

¹H NMR (500 MHz; CDCl₃): δ 10.36 (s, 1H), 6.31 (s, 2H), 4.28 (s, 2H), 3.32 (t, 1.6 2H), 2.78 (d, 1.2 2H), 1.62 (d, 10.0 1H), 1.51 (dt, 10.0, 1.5 1H).

¹³C NMR (126 MHz; DMSO): δ 176.9, 168.5, 137.8, 47.4, 44.7, 42.3, 39.3

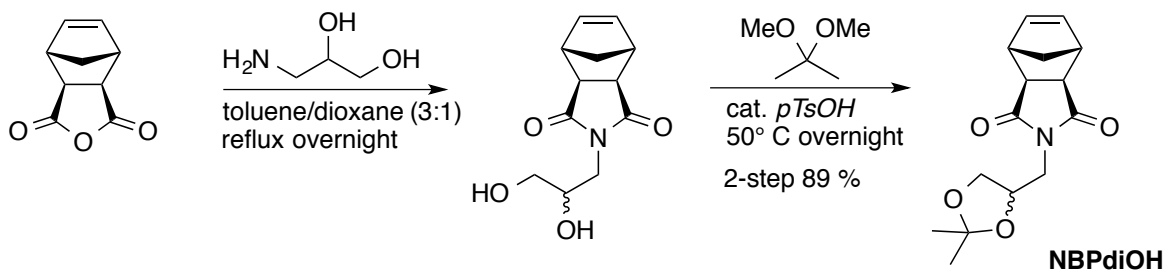
N-(glycine N-hydroxysuccinimide ester)-cis-5-norbornene-exo-dicarboximide
(NBGlyNHS).

To a flame-dried flask 3.99 g (18.1 mmol) of NBGly and 3.89 g (19.7 mmol) of EDC-HCl were added. The reagents were dissolved in 40 mL dry DMF and stirred at 35 °C for 10 min but remained cloudy. Upon addition of 2.59 g (22.5 mmol, 1.25 eq.) of NHS the solution turned translucent and was stirred at 40 °C overnight. The DMF was removed via rotary evaporation and the residue was dissolved in 140 mL of EtOAc and washed with 75 mL of sat. NaHCO₃. The aqueous layer was back extracted with 25 mL of EtOAc. The organic layers were combined and washed with 100 mL of brine and dried with MgSO₄. After removing the solvent, the residue was columned (with **dry** silica) in 70→ 90% EtOAc/PE, to afford 3.5 g (60%) of fine white powder. Note: yields decrease significantly with untreated/wet silica.

Rf: 0.52 in 80% EtOAc/PE stain with KMnO₄

MS ESI⁻ Calc'd: 221.07. Found: 220.0.

¹H NMR (500 MHz; CDCl₃): δ 6.30 (t, 1.8 2H), 4.56 (s, 2H), 3.32 (quintet, 1.7 2H), 2.83 (s, 4H), 2.78 (d, 1.2 2H), 1.55 (dt, 10.0, 1.4 1H), 1.51 (dq, 10.0, 1.5 1H).



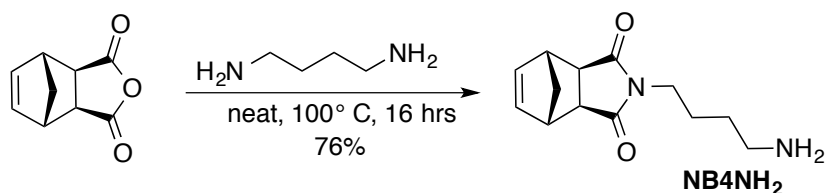
***N*-(2,3-dihydroxypropyl acetone)-*cis*-5-norbornene-*exo*-dicarboximide (NBPdiOH).**

A solution of 20.0 g (121.8 mmol) of carbic anhydride and 12.73 g (139.7 mmol) of 3-amino-1,2-propanediol in 420 mL of toluene and 150 mL of dioxane was refluxed overnight. Approximately 400 mL of solvent was removed and 4.6 g (24 mmol) of *p*-toluenesulfonic acid monohydrate and 150 mL (1.22 mol) of 2,2-dimethoxypropane were added and allowed to stir overnight. The solvent was removed and product purified by column chromatography in 20% EtOAc/PE to afford 29.9 g (89%) of fine white crystalline powder.

step 1 Rf: 0.45 in 10% MeOH/(DCM:CHCl₃) stain with KMnO₄

step 2 Rf: 0.33 in 20% EtOAc/PE stain with KMnO₄

¹H NMR (500 MHz; CDCl₃): δ 6.27 (t, 1.8 2H), 4.36 (ddt, 7.5, 6.2, 5.0 1H), 4.00 (dd, 8.7, 6.2 1H), 3.74 (dd, 13.4, 7.5 2H), 3.72 (d, 8.7, 5.0 2H), 3.45 (dd, 13.4, 4.9 1H), 3.27 (t, 1.6 2H), 2.69 (d, 1.2 2H), 1.49 (dt, 9.9, 1.5 1H), 1.40 (s, 3H), 1.33 (d, 9.9 1H). ¹³C NMR (126 MHz; DMSO): δ 177.58, 177.43, 137.61, 137.58, 108.7, 71.8, 66.7, 47.29, 47.12, 44.57, 44.55, 42.3, 41.0, 39.5, 26.7, 25.2



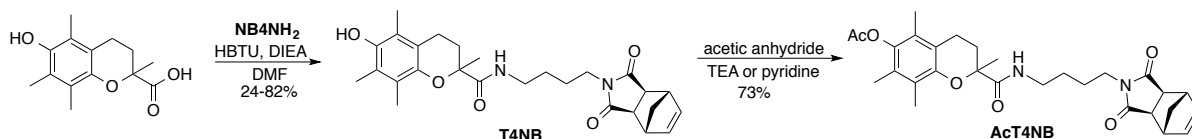
***N*-(4-aminobutyl)-cis-5-norbornene-exo-dicarboximide (NB4NH₂).**

A solution of 15.05 g (91.7 mmol) of carbic anhydride and 460 mL (4.58 mol) of 1,4-diaminobutane was stirred at 100 °C for 46 h. Most of the 1,4-diaminobutane (300 mL) was distilled off (b.p. 158° C). The resultant material was dry loaded and purified via flash chromatography in 5 → 9 % MeOH/1 % TEA/DCM to afford 16.2 g (76%) of pale yellow semi-solid. Note: Attempts were made to dissolve the product in organic solvent (EtOAc or chloroform) and wash out the diaminobutane that remained after distillation. This was unsuccessful because product went into both phases, even when the water was slightly basic. Lower yields (20-40%) were observed when reaction was done with solvent or shorter reaction times (24 h).

Rf: 0.15 in 10% MeOH/(DCM:CHCl₃) stain with KMnO₄

MS ESI⁺ Calc'd: 234.14. Found: 235.2.

¹H NMR (400 MHz; DMSO-*d*₆): δ 6.26 (s, 2H), 3.29 (t, 7.4 2H), 3.05 (s, 2H), 2.64 (s, 2H), 2.47 (t, 7.0 2H), 1.91 (s, 2H), 1.42 (dt, 15.0, 7.4 2H), 1.33 (d, 9.6 1H), 1.23 (dt, 15.0, 7.0 2H), 1.08 (d, 9.6 1H). ¹³C NMR (126 MHz; DMSO): δ 177.7, 137.6, 47.2, 44.5, 42.4, 41.0, 37.9, 30.3, 24.8



***N*-(4-(troloxylamido)butyl)-cis-5-norbornene-exo-dicarboximide (T4NB).**

A solution of 0.91 g (3.64 mmol) of Trolox, 888 mg (3.79 mmol, 1.04 eq) of NB₄NH₂, 1.76 g (4.64 mmol, 1.27) of HBTU and 2.0 mL (11.5 mmol) of DIEA in 10 mL dry DMF was allowed to stir overnight at ambient temperature. The solvent was removed and product purified by column chromatography in 1 → 5% MeOH/(DCM:CHCl₃) to afford 450 mg (24%) of light tan solid. The second time this reaction was done at 3 times the scale, the yield jumped to 82%.

Rf: 0.42 in 5% MeOH/(DCM:CHCl₃)

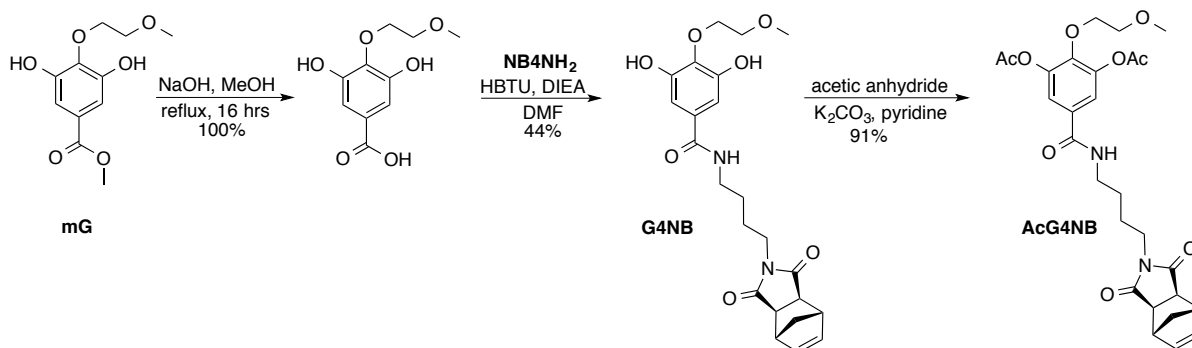
MS ESI- Calc'd: 466.25. Found: 465.2.

¹H NMR (500 MHz; CDCl₃): δ 6.42 (t, 5.9 1H), 6.26 (s, 2H), 4.86 (s, 1H), 3.34 (t, 6.5 2H), 3.28-3.24 (dd, 13.0, 6.0 1H), 3.24 (s, 2H), 3.15 (dd, 13.1, 6.0 1H), 2.64 (d, 0.5 2H), 2.59 (dt, 16.7, 5.9 1H), 2.51 (ddd, 16.7, 9.0, 6.9 1H), 2.33 (dt, 13.4, 6.0 1H), 2.16 (d, 5.4 6H), 2.07 (s, 3H), 1.83 (ddd, 13.4, 9.0, 6.0 1H), 1.48 (s, 3H), 1.47 (s, 1H), 1.37 (s, 4H), 1.14 (d, 9.8 1H). ¹³C NMR (126 MHz; CDCl₃): δ 178.0, 174.4, 145.9, 144.2, 137.8, 122.3, 121.6, 119.9, 117.9, 78.3, 47.8, 45.2, 42.8, 38.63, 38.52, 38.2, 29.7, 27.1, 25.0, 24.5, 20.6, 12.4, 12.0, 11.5

***N*-(4-(troloxyl(*O*-acetyl)amido)butyl)-cis-5-norbornene-exo-dicarboximide (AcT4NB).**

A solution of 3.84 g (8.23 mmol) of T4NB and 2.1 g, 15.2 mmol) of potassium carbonate in 40 mL acetic anhydride was stirred at 50 °C overnight. The reaction was allowed to cool and 50 mL methanol *slowly* added (exothermic: use caution to not boil the reaction). The solvent was removed via rotary evaporation and the residue dissolved in 30 mL chloroform. The organic layer was washed twice with 20 mL of brine, dried with MgSO₄

and the solvent removed to afford 3.06 g (73%) of light tan solid. Note: This procedure worked better than with TEA as the base or flash chromatography to purify.



(3,5-dihydroxy-4-(2-methoxyethoxy)benzoic acid).

To a solution of 1.08 g (4.45 mmol) of 3,5-dihydroxy-4-(2-methoxyethoxy)methyl benzoate, mG, in 9 mL methanol was added 2 mL of 10 M aqueous (20 mmol) NaOH. The solution was refluxed for 24 h. The pH was adjusted ~ 5 with 6 M HCl and the solvent was removed via rotary evaporation. The residue was titrated with water and vacuum filtered to afford 1.0 g (quant.) of white solid. Larger scales gave yields 75-99%.

Rf: 0.31 in 20% MeOH/(DCM:CHCl₃)

MS ESI- Calc'd: 228.06. Found: 227.0.

¹H NMR (500 MHz; DMSO-*d*₆): δ 8.98 (s, 1H), 6.91 (s, 2H), 4.01 (m, 2H), 3.59 (m, 2H), 3.31 (s, 3H).

N-(4-(3,5-dihydroxy 4-(2-methoxyethoxy) benzamido)butyl)-cis-5-norbornene-exo-dicarboximide (G4NB).

A solution of 666 mg (2.92 mmol) of 3,5-dihydroxy-4-(2-methoxyethoxy)benzoic acid, 718 mg (3.06 mmol, 1.05 eq) of NB₄NH₂, 1.16 g (3.06 mmol, 1.05 eq.) of HBTU and 2.0 mL (11.5 mmol, 3.9 eq.) of DIEA in 12 mL DMF was stirred at room temperature overnight. The solvent was removed via rotary evaporation and the residue purified by column chromatography in 5 → 10 % MeOH/(DCM:CHCl₃) to afford 575 mg (44%) of the desired product as an off-white solid. Upon repetition yields as high as 79% were achieved.

Rf: 0.49 in 10% MeOH/(DCM:CHCl₃) or 0.30 in 5% MeOH/(DCM:CHCl₃)

MS ESI- Calc'd: 444.19. Found: 443.1.

¹H NMR (500 MHz; DMSO-*d*₆): δ 9.04 (s, 2H), 8.17 (t, 5.6 1H), 6.79 (s, 2H), 6.30 (t, 1.7 2H), 4.04 (dd, 5.5, 4.4 2H), 3.60 (dd, 5.5, 4.4 2H), 3.36 (t, 6.8 2H), 3.31 (s, 3H), 3.16 (q, 6.1 2H), 3.09 (t, 1.5 2H), 2.68 (d, 1.0 2H), 1.50-1.39 (m, 5H), 1.36 (d, 9.7 1H), 1.12 (d, 9.7 1H). ¹³C NMR (126 MHz; DMSO): δ 177.6, 166.0, 150.2, 137.6, 136.5, 130.2, 106.6, 71.0, 70.8, 58.0, 47.2, 44.4, 42.3, 39.5, 38.6, 37.7, 26.6, 24.8.

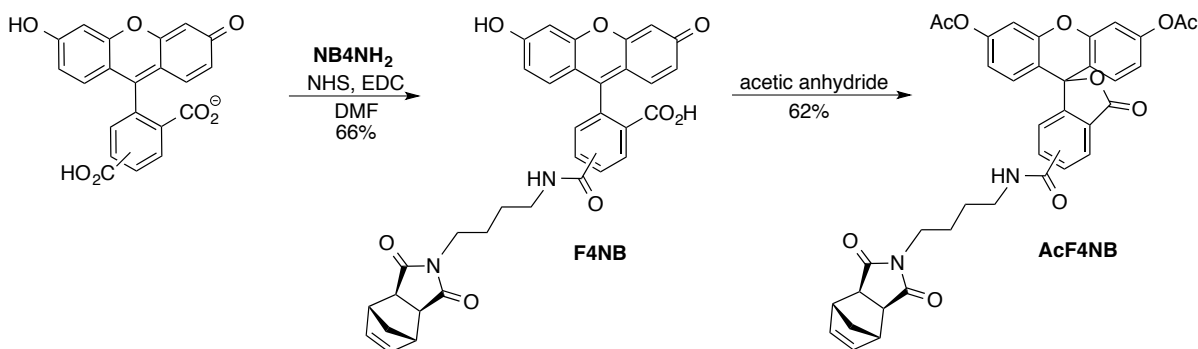
N-(4-(3,5-diacetoxy 4-(2-methoxyethoxy) benzamido)butyl)-cis-5-norbornene-exo-dicarboximide (AcG4NB).

To a solution of 315 mg (0.709 mmol) of G4NB in 25 mL acetic anhydride was added 200 mg (1.44 mmol) of potassium carbonate and 20 mL pyridine. The reaction was allowed to stir at room temperature overnight. The solvent was removed and the residue dissolved in 10 mL of EtOAc and washed twice with 10 mL water. The solvent was removed and the

product purified by column chromatography 5 → 10 % MeOH/(DCM:CHCl₃) to afford 342 mg (91%) of tan oil.

R_f: 0.55 in 5% MeOH/(DCM:CHCl₃)

¹H NMR (500 MHz; CDCl₃): δ 7.42 (s, 2H), 6.30 (t, 5.7 1H), 6.28 (t, 1.8 2H), 4.13-4.11 (m, 2H), 3.61-3.59 (m, 2H), 3.51 (t, 7.0 2H), 3.45 (q, 6.3 2H), 3.39 (s, 3H), 3.27 (t, 1.7 2H), 2.69 (d, 1.2 2H), 2.33 (s, 6H), 1.68-1.56 (m, 6H), 1.52 (dt, 9.9, 1.5 2H), 1.21 (d, 9.9 2H).



***N*-(4-(fluoresceinyl-5(6)-amido)butyl)-cis-5-norbornene-exo-dicarboximide (F4NB).**

A solution of 1.014 g (2.69 mmol) of 5(6)-carboxyfluorescein, 335 mg (2.91 mmol, 1.08 eq.) of NHS and 0.629 mg (3.24 mmol, 1.20 eq.) of EDC-HCl in 20 mL dry DMF was allowed to stir at room temperature for 50 min. To the reaction was added 677 mg (2.89 mmol, 1.07 eq.) of NB₄NH₂. The reaction was allowed to stir overnight at ambient temperature. The DMF was removed via rotary evaporation the residue was dissolved in ~ 30 mL of EtOAc. The organic layer was washed with 20 mL of water, 20 mL of 0.1 M HCl, 20 mL of brine and 20 mL of water. The solvent was removed and the residue purified via flash chromatography in 5 → 8 % MeOH/(DCM:CHCl₃). The orange product was isolated as a mixture of the 5 and 6 isomer, 1.082 g (66%).

5/6 R_f: 0.28 in 10% MeOH/(DCM:CHCl₃)

MS ESI: Calc'd EM: 592.18; (EM-2H)/2: 295.09) found: 295.1

isomer 5: ¹H NMR (500 MHz; DMSO-*d*₆): δ 10.17 (s, 2H), 8.84 (t, 5.7 1H), 8.46 (d, 1.5 1H), 8.24 (dd, 8.1, 1.5 1H), 7.38 (d, 8.1 1H), 6.70 (d, 2.6 2H), 6.59 (d, 8.7 2H), 6.56 (dd, 8.7, 2.6 2H), 6.29 (t, 1.9 2H), 3.40 (d, 6.5 4H), 3.09 (dt, 3.4, 1.7 2H), 2.69 (d, 0.7 2H), 1.53 (m, 4H), 1.35 (dt, 9.6, 1.5 1H), 1.13 (d, 9.6 1H). peak at 3.32 ppm occluded by water peak

isomer 6: ¹H NMR (500 MHz; DMSO-*d*₆): δ 10.17 (s, 1H), 8.69 (t, 5.6 1H), 8.16 (dd, 8.1, 1.2 1H), 8.08 (d, 8.1 1H), 7.66 (s, 1H), 6.69 (d, 2.6 2H), 6.59 (d, 8.6 2H), 6.55 (dd, 8.6, 2.6 2H), 6.27 (t, 1.7 2H), 3.20 (q, 5.9 2H), 3.03 (dt, 3.3, 1.7 2H), 2.63 (d, 1.1 2H), 1.42 (m, 4H), 1.28 (dt, 9.7, 1.4 1H), 1.06 (d, 9.7 1H). peak at 3.31 ppm occluded water peak

Mixture of isomers: ¹³C NMR (126 MHz; DMSO): δ 177.74, 177.68, 172.8, 168.24, 168.08, 164.56, 164.48, 159.6, 154.7, 152.7, 151.9, 140.8, 137.65, 137.62, 136.3, 134.7, 129.41, 129.29, 129.20, 128.2, 126.5, 124.9, 124.3, 123.2, 122.2, 112.77, 112.70, 109.19, 109.13, 102.3, 83.38, 83.34, 47.29, 47.24, 44.49, 44.46, 42.43, 42.34, 39.5, 38.97, 38.94, 37.75, 37.64, 26.55, 26.42, 24.95, 24.92.

***N*-(4-((3',6'-diacetoxy)fluoresceinyl-5(6)-amido)butyl)-cis-5-norbornene-exo-dicarboximide (AcF4NB).**

A solution of 410 mg (0.67 mmol) of F4NB in 6 mL acetic anhydride was allowed to stir at room temperature overnight. The solvent was removed via rotary evaporation and the residue dissolved in ~ 15 mL of EtOAc and washed twice with 10 mL of water. The EtOAc was removed and the residue purified by flash chromatography in 60 → 100 % EtOAc/PE. The 5 and 6 isomer could be separated but were combined to yield a pale yellow solid, 288

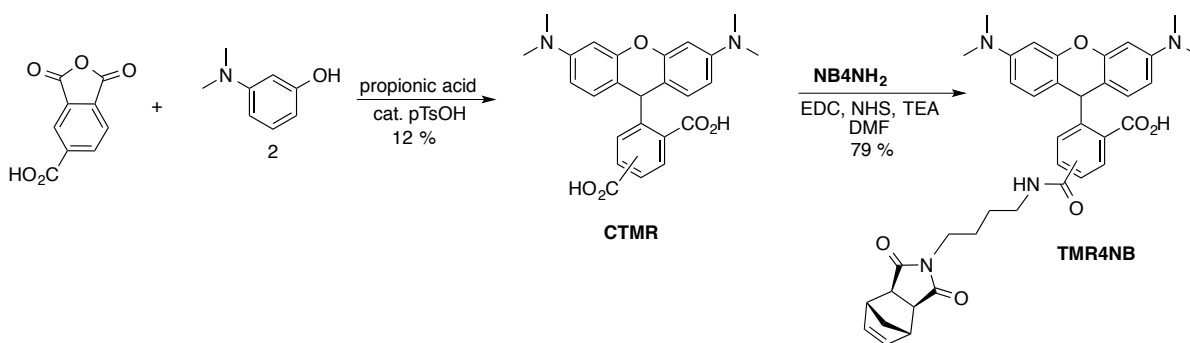
mg (62%). It was found later that addition of potassium carbonate increased the yield to 80%.

isomer 5: Rf: 0.43 in 80% EtOAc/PE

^1H NMR (500 MHz; $\text{DMSO-}d_6$): δ 8.85 (t, 5.8 1H), 8.51 (dd, 1.6, 0.7 1H), 8.26 (dd, 8.1, 1.6 1H), 7.53 (dd, 8.1, 0.7 1H), 7.30 (dd, 2.1, 0.6 2H), 6.95 (dd, 8.7, 2.1 2H), 6.93 (dd, 8.7, 0.6 2H), 6.30 (t, 1.7 2H), 3.39 (t, 6.5 2H), 3.32 (occ, 2H), 3.09 (quintet, 1.6 2H), 2.69 (d, 0.8 2H), 2.29 (s, 6H), 1.53 (m, 2H), 1.51 (m, 2H), 1.36 (dt, 9.7, 1.4 1H), 1.13 (d, 9.7 1H). Peak at 3.32 ppm occulted by trace water.

isomer 6: Rf: 0.35 in 80% EtOAc/PE

^1H NMR (500 MHz; $\text{DMSO-}d_6$): δ 8.69 (t, 5.7 1H), 8.21 (dd, 8.1, 1.4 1H), 8.16 (dd, 8.1, 0.7 1H), 7.79 (dd, 1.4, 0.7 1H), 7.31 (dt, 2.1, 0.6 2H), 6.97 (dd, 8.7, 2.1 2H), 6.95 (dd, 8.7, 0.6 2H), 6.28 (q, 1.7 2H), 3.32 (t, 6.6 2H), 3.20 (q, 6.1 2H), 3.04 (quintet, 1.8 2H), 2.64 (d, 1.3 2H), 2.29 (s, 6H), 1.44 (m, 2H), 1.42 (m, 2H), 1.30 (dt, 9.7, 1.5 1H), 1.07 (d, 9.7 1H). ^{13}C NMR (126 MHz; DMSO): δ 177.6, 168.8, 167.7, 164.3, 152.14, 152.12, 150.8, 141.2, 137.5, 129.9, 129.3, 127.6, 125.3, 122.2, 118.7, 115.7, 110.5, 81.2, 47.2, 44.4, 42.3, 39.5, 38.9, 37.6, 26.3, 24.8



5(6)-carboxy-N,N,N,N-tetramethylrhodamine (CTMR).

A suspension of 9.999 g (73.0 mmol) of dimethylaminophenol, 7.008g (36.5 mmol) of 1,2,4-benzenetricarboxyanhydride and 322 mg (1.6 mmol) of p-tolueneic sulfonic acid in 500 mL

propionic acid was refluxed for two days. The solvent was removed via rotary evaporation and azeotroped with water. Dark purple product was isolated via flash chromatography in 20 →60 % MeOH/DCM as a mixture as 5/6 isomer in an approx. 4:5 ratio, 1.88 g, 4.35 mmol (11.9 %). The reaction was also tried with butyric acid as the solvent and catalytic sulfuric acid but resulted in a 5% yield.

MS ESI⁺ Calc'd: 430.15 lactone form. Found: 431.0.

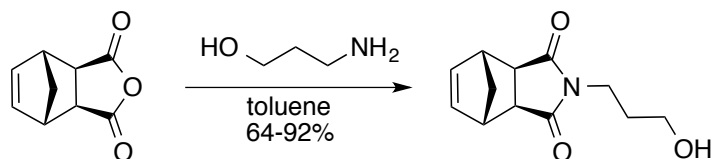
¹H NMR (500 MHz; CD₃OD): δ 8.79 (d, 1.5 1H), 8.27 (d, 1.2 1H), 8.25 (d, 1.6 1H), 8.17 (d, 8.2 1H), 7.86 (d, 1.6 1H), 7.38 (d, 7.9 1H), 7.25 (d, 9.5 2H), 7.23 (d, 9.5 2H), 7.032 (dd, 9.5, 1.0 2H), 7.027 (dd, 9.4, 0.8 2H), 6.93 (d, 2.6 2H), 6.92 (d, 2.6 2H), 3.28 (s, 24H).

N-(4-(N,N,N,N-tetramethylrhodaminyl-5(6)-amido)butyl)-cis-5-norbornene-exo-dicarboximide (TMR4NB).

A solution of 578 mg (1.38 mmol) of 5(6)-carboxytetramethylrhodamine, 168 mg (1.46 mmol, 1.05 eq.) of NHS and 315 mg (1.85 mmol, 1.3 eq.) of EDC-HCl in 15 mL dry DMF was allowed to stir at room temperature for 20 min. Then, 350 mg (1.49 mmol, 1.08 eq.) of NB₄NH₂ was added and the reaction was allowed to stir overnight. The DMF was removed via rotary evaporation and the residue was dissolved in ~ 20 mL of EtOAc. The organic layer was washed with 10 mL of water, 10 mL of 0.1 M HCl, and 10 mL of brine. The organic layer was dried with MgSO₄ and filtered. The solvent was removed and the residue purified via flash chromatography in 10 →25 % MeOH/DCM. The product (d. purple solid) was isolated as a mixture of the 5 and 6 isomer, 700 mg (79%). Note: isomers could be separated with *careful* chromatography.

MS ESI⁺ Calc'd: 646.28 lactone form. Found: 647.1.

isomer 5: ^1H NMR (500 MHz; CD_3OD): δ 8.66 (d, 1.5 1H), 8.16 (dd, 7.9, 1.5 1H), 7.45 (d, 7.9 1H), 7.18 (d, 9.5 2H), 7.04 (dd, 9.5, 2.4 2H), 6.96 (d, 2.4 2H), 6.33 (t, 1.7 2H), 3.55 (m, 2H), 3.48 (m, 2H), 3.30 (s, 12H), 3.19 (t, 1.7 2H), 2.73 (d, 1.1 2H), 1.68 (m, 4H), 1.50 (dt, 9.8, 1.4 1H), 1.26 (d, 9.8 1H). isomer 6: ^1H NMR (500 MHz; CD_3OD): δ 8.27 (d, 8.2 1H), 8.12 (dd, 8.2, 1.8 1H), 7.74 (d, 1.8 1H), 7.20 (d, 9.5 2H), 7.04 (dd, 9.5, 2.5 2H), 6.96 (d, 2.5 2H), 6.30 (t, 1.7 2H), 3.48 (m, 2H), 3.40 (m, 2H), 3.30 (s, 12H), 3.12 (t, 1.6 2H), 2.68 (d, 1.0 2H), 1.60 (m, 4H), 1.42 (dt, 9.8, 1.4 1H), 1.18 (d, 9.8 1H).

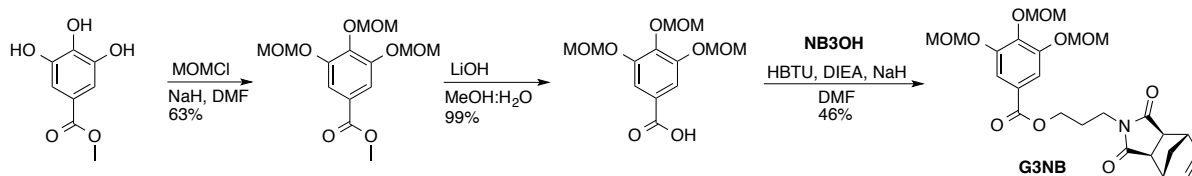


***N*-(3-hydroxypropyl)-cis-5-norbornene-exo-dicarboximide (NB3OH).**

A solution of 6.10 g (37.2) of carbic anhydride and 4.00 g (53.3 mmol, 1.4 eq.) of 3-aminopropanol in 50 mL toluene was refluxed overnight. The solvent was removed via rotary evaporation and the residue dissolved in 75 mL of EtOAc. The organic layer was washed twice with 25 mL of brine. The organic layer was dried with MgSO_4 , filtered and the solvent removed via rotary evaporation. The residue was purified by flash chromatography in 40 \rightarrow 60 % EtOAc/hexanes to afford 7.53 g (92%) as a light yellow to clear oil. On a 20 g scale the yield dropped to 64%. Note: The above procedure worked better than the neat trial.

MS ESI- Calc'd: 221.11. Found: 220.0.

^1H NMR (500 MHz; CDCl_3): δ 6.29 (s, 2H), 3.64 (t, 6.3 2H), 3.54 (t, 5.8 2H), 3.28 (s, 2H), 2.71 (s, 2H), 2.60 (s br, 1H), 1.77 (dd, 6.3, 5.8 2H), 1.54 (d, 9.9 1H), 1.23 (d, 9.9 1H). ^{13}C NMR (126 MHz; CDCl_3): δ 178.5, 137.7, 59.1, 47.8, 45.1, 42.7, 35.2, 30.6.



Methyl 3,4,5-tris(methoxymethoxy)benzoate.¹⁶

A solution of 21.28 g (116 mmol) of methyl gallate and 30.0 mL (397 mmol) of chloromethyl methyl ether in ~350 mL anhydrous DMF was cooled to 0 °C under N₂. To the reaction was added 16.68 g (417 mmol) of NaH (60% in mineral oil), in three aliquots over a 30 min period. The reaction was allowed to stir 15 h then quenched with 20 mL of water. The reaction was concentrated by rotary evaporation to ~ 100 mL and then dissolved in 500 mL of EtOAc. The organic layer was washed with 250 mL of sat. aq. NH₄Cl and twice with 250 mL brine. The organic layer was dried with MgSO₄, filtered and the solvent removed via rotary evaporation. The product was purified by flash chromatography in 10 →20 % EtOAc/hexanes. The product was isolated as a clear viscous liquid, 20.04 g (63%). The reaction at half this scale resulted in only 38% yield. Note: Attempts to tri-protect gallic acid resulted in a mixture of tetra, tri and di protected product.

MS ESI- Calc'd: 302.10. Found: 301.0.

¹H NMR (500 MHz; CDCl₃): δ 7.53 (s, 2H), 5.24 (s, 4H), 5.21 (s, 2H), 3.88 (s, 3H), 3.61 (s, 3H), 3.51 (s, 6H). ¹³C NMR (126 MHz; CDCl₃): δ 166.4, 150.8, 140.8, 126.0, 111.7, 98.6, 95.4, 57.3, 56.5, 52.3

3,4,5-tris(methoxymethoxy)benzoic acid.¹⁷

A solution of 19.95 g (61.7 mmol) of methyl 3,4,5-tris(methoxymethoxy)benzoate and 41.96 g (253 mmol, 4.1 eq) of LiOH · H₂O in 230 mL of methanol and 60 mL of water was heated to 80 °C for an hour. The reaction was neutralized with 100 mL of 2 M HCl and the solvent removed via rotary evaporation. The product was titrated with water, vacuum filtered and dried under high vacuum to afford 18.6 g (quant.) white solid. During one repetition of this reaction too much water was used to titrate and the yield dropped to 75%.

MS ESI- Calc'd: 302.1. Found: 301.0.

¹H NMR (500 MHz; DMSO-*d*₆): δ 7.36 (s, 2H), 5.15 (s, 4H), 5.03 (s, 2H), 3.89 (s, 1H), 3.46 (s, 3H), 3.36 (s, 6H). ¹³C NMR (126 MHz; DMSO): δ 169.4, 149.7, 137.9, 133.9, 111.1, 97.8, 94.8, 56.6, 55.9.

N-(4-(3,4,5-tris(methoxymethoxy)benzoate)propyl)-cis-5-norbornene-exo-dicarboximide (G3NB).

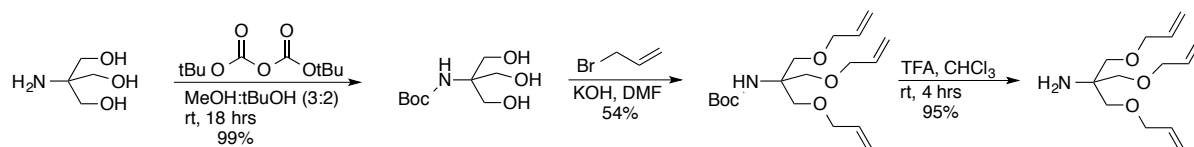
A solution of 3.90 g (17.6 mmol, 1.3 eq.) of NB3OH and 0.79 g (19.8 mmol, 1.47 eq.) of NaH in 60 mL anhydrous DMF was allowed to react for 10 min. The solution was then added to the reaction vessel with 4.09 g (13.5 mmol) of 3,4,5- tris(methoxymethoxy)benzoic acid, 5.63 g (13.9 mmol, 1.0 eq) of HBTU and 7.0 mL (40 mmol, 3 eq.) of DIEA in 100 mL anhydrous DMF. The reaction was allowed stirred overnight (with needle vent) at ambient temperature. The reaction was quenched with 2 mL water and the solvent was removed via rotary evaporation. The product was isolated by flash column chromatography in 40 →60 % EtOAc/hexanes to afford 3.2 g, 6.3 mmol (46 %) of viscous pale yellow oil. Note:

There's an impurity that comes off just before the product, it stains white with vanillin stain and the product stains purple. Using EDC as a coupling agent resulted in a 28 % yield.

Rf = 0.29 in 50 % EtOAc/PE

^1H NMR (500 MHz; CDCl_3): δ 7.54 (s, 2H), 6.28 (d, 1.5 2H), 5.25 (s, 4H), 5.21 (s, 2H), 4.29 (t, 6.4 2H), 3.64 (t, 7.2 2H), 3.61 (s, 3H), 3.51 (s, 6H), 3.27 (s, 2H), 2.68 (s, 2H), 2.07-2.01 (m, 4H), 1.52 (d, 9.9 1H), 1.23 (d, 10.0 1H).

Synthesis of Various Small Molecules for ONP



N-Boc Tris.¹⁸

A suspension of 12.39 g (102 mmol) of Tris in 94 mL MeOH and 94 mL *t*-BuOH was added to a solution of 29.0 g (0.133 mmol, 1.3 eq.) of di-*t*-butyldicarbonate in 150 mL *t*-BuOH and stirred at room temperature for 19 h. The solvent was removed via rotary evaporation and product precipitated with cold EtOAc and vacuum filtered to afford 21.6 g, 99% of fluffy white solid. Yield: 86-99%

Rf: 0.44 in 10% MeOH/(DCM: CHCl₃) stain with KMnO₄

^1H NMR (400 MHz; DMSO-*d*₆): δ 5.77 (s, 1H), 4.51 (t, 5.6 3H), 3.51 (d, 5.7 6H), 3.36 (d, 1.0 3H), 1.37 (s, 9H). ^{13}C NMR (126 MHz; DMSO): δ 155.2, 78.0, 60.6, 60.4, 28.4.

N-Boctriallyltris.¹⁸

To a solution of 20 g (90 mmol) of *N*-BocTris in ~225 mL dry DMF was added 43.6 mL (504 mmol, 5.6 eq.) of allyl bromide. At the rate of ~1 g per minute was added 29.6 g (528 mmol, 5.9 eq.), of finely ground KOH which slightly warmed the flask. The reaction was put on ice for 5 min and the remaining KOH was added. The reaction was removed from ice after 15 additional minutes. The reaction stirred overnight at ambient temperature. The undissolved KOH was filtered off and the solvent was removed via rotary evaporation. The product was isolated by column chromatography in 5% EtOAc/PE to afford 16.2 g (54%) of a white solid. Note: KOH needs to be ground into a fine powder! Failure to do so results in yields as low as 14% despite vigorous stirring.

R_f: 0.69 in 20% EtOAc/PE

¹H NMR (500 MHz; CDCl₃): δ 5.88 (ddt, 17.2, 10.6, 5.4 3H), 5.25 (dq, 17.2, 1.7 3H), 5.15 (dq, 10.4, 1.4 3H), 3.98 (dt, 5.5, 1.4 6H), 3.70 (s, 6H), 1.42 (s, 9H). ¹³C NMR (126 MHz; CDCl₃): δ 155.2, 135.2, 117.1, 79.3, 72.7, 69.5, 58.9, 28.8

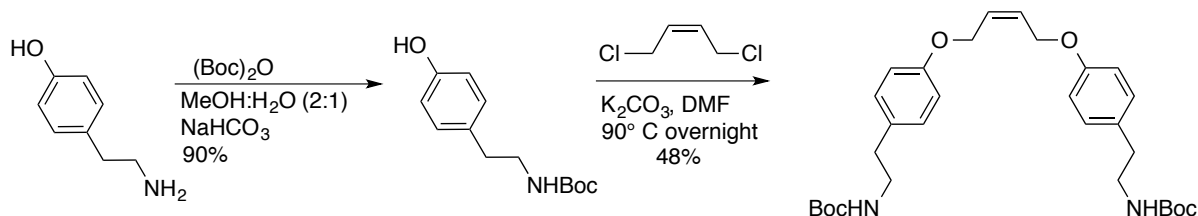
Triallyltris.¹⁸

To a solution of 8.15 g (23.9 mmol) of *N*-Boctriallyltris in 60 mL of DCM was added 28 mL of TFA. The reaction was stirred for 4 h at room temperature. The solvent was removed and the residue dissolved in 100 mL of EtOAc. The organic layer was washed with 50 mL of 5% Na₂CO₃ and 50 mL brine then dried with MgSO₄. The solvent was removed to afford 5.5 g, 95% the desired product as a pale yellow oil. Yield: 81-95%

R_f: 0.35 in 5% MeOH/(DCM:CHCl₃) stain with KMnO₄

MS ESI⁺ Calc'd: 241.17. Found: 242.3.

^1H NMR (500 MHz; CDCl_3): δ 5.86 (ddt, 17.2, 10.7, 5.4 3H), 5.69 (brs, 2H), 5.25 (dq, 17.3, 1.6 3H), 5.17 (dd, 10.4, 1.5 3H), 3.99 (dt, 5.6, 1.4 6H), 3.51 (s, 6H). ^{13}C NMR (126 MHz; CDCl_3): δ 134.4, 117.2, 72.4, 69.6, 58.1



***N*-Boc Tyramine.**¹⁹

To a solution of 5.03 g (36.7 mmol) of tyramine in 150 mL MeOH:H₂O (2:1) was added 9.2 g (110 mmol, 3 eq.) of NaHCO₃ and 12.1 g (55.4 mmol, 1.5 eq.) of di-*t*-butyldicarbonate. The reaction was stirred at room temperature for 22 h. The reaction volume was reduced to ~60 mL via rotary evaporation and then solubilized in 100 mL EtOAc. The organic layer was washed with 100 mL of 1 M HCl, 100 mL of brine and dried with MgSO₄. The solvent was removed via rotary evaporation and the residue was purified via column chromatography in 50% EtOAc/PE to afford 7.9 g (90 %) of sticky clear oil. Yield: 90-99%

Rf: 0.59 in 50% EtOAc/PE

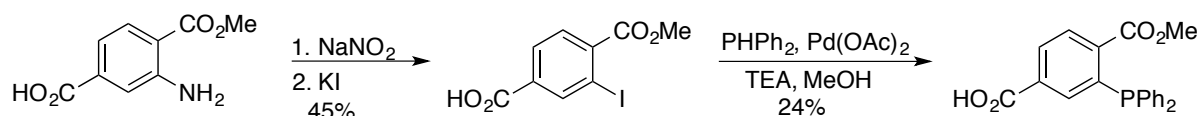
^1H NMR (400 MHz; CDCl_3): δ 7.00 (d, 8.4 2H), 6.78 (d, 8.4 2H), 4.66 (s, 1H), 3.33 (q, 6.4 2H), 2.69 (t, 7.0 2H), 1.44 (s, 9H). ^{13}C NMR (101 MHz; CDCl_3): δ 156.4, 154.9, 130.3, 129.9, 115.6, 79.7, 42.2, 35.4, 28.5

***Z*-1,4-bis(*O*-((*N*-Boc)tyraminyl))but-2-ene (CTA-TyrNHBoc).**²⁰

A solution of 2.18 g (9.19 mmol, 2.2 eq.) of *N*-Boc tyramine, 0.44 mL (4.2 mmol) of 1,4-dichlorobut-2-ene and 1.90 g (13.7 mmol, 3.3 eq.) of K₂CO₃ in 20 mL anhydrous DMF was

heated to 90 °C overnight. The DMF was removed via rotary evaporation and the residue dissolved in 50 mL of DCM. The organic layer was washed with 50 mL of water then 60 mL of brine and dried with MgSO₄. The product was purified by column chromatography in 2% MeOH/DCM to afford 1.06 g (48%) of white solid.

¹H NMR (500 MHz; CDCl₃): δ 7.10 (d, 8.4 2H), 6.85 (d, 8.4 2H), 5.93 (t, 3.4 1H), 4.65 (d, 4.0 2H), 4.54 (s, 1H), 3.34 (q, 6.4 2H), 2.73 (t, 6.8 2H), 1.43 (s, 9H).



***1-methyl-2-iodoterephthalate.*²¹**

A solution of 9.90 g (50.7 mmol) of 1-methyl-2-aminoterephthalate in 100 mL of concentrated HCl was cooled to 0 °C via ice bath. A solution of 3.6 g (52.2 mmol) of NaNO₂ in 20 mL water was added drop-wise over 30 min. The ice was removed and the reaction was allowed to stir an additional 30 min. The reaction was filtered through glass wool into a RBF with 83.6 g (520 mmol) of KI in ~125 mL of water. The reaction was stirred an hour then diluted with 1.5 L of DCM. The organic layer was separated and washed twice with 200 mL of saturated Na₂SO₃, twice with 400 mL of water and once with 400 mL of brine. The combined aqueous layers were back extracted 10 times with 200 mL of DCM, until the yellow stopped washing out. The combined organic layers were dried with MgSO₄ and the solvent was removed. The residue was dissolved in ~150 mL of methanol and ~250 mL of water was added slowly until the solution turned cloudy. The solution was cooled at 4 °C

for 4 h then filtered. The product contained ~ 5 % impurity and was reprecipitated to afford 7.04 g (45%) of a pale yellow powder.

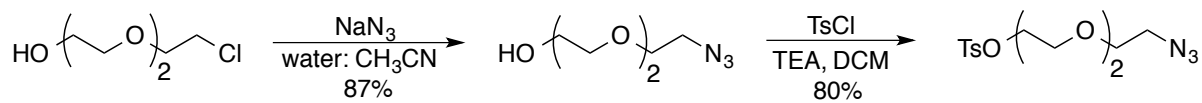
^1H NMR (500 MHz; CDCl_3): δ 8.69 (d, 1.6 1H), 8.12 (ddd, 8.1, 1.6, 0.5 1H), 7.84 (d, 8.1 1H), 3.97 (s, 3H). ^{13}C NMR (126 MHz; CDCl_3): δ 169.6, 166.7, 142.7, 140.3, 132.6, 130.7, 129.6, 93.5, 53.0

1-methyl-2-diphenylphosphinoterephthalate.²²

A mixture of 2.98 g (9.74 mmol) of 1-methyl-2-iodoterephthalate, 37 mg (1.65 mmol, 0.17 eq.) of palladium (II) acetate, and 3.0 mL (22 mmol, 2.2 eq.) of TEA was dissolved in 30 mL of dry oxygen-free methanol (purged with Ar for 2 h). The reaction momentarily moved to a glove box to add 1.7 mL (9.77 mmol, 1 eq.) of diphenylphosphine and then the reaction stirred at 70 °C for 36 h under Ar. The solvent was removed via rotary evaporation and the residue was dissolved in 1.5 L 1:1 DCM:H₂O. The layers were separated and the organic layer was washed with 100 mL of 1 M HCl, dried with MgSO₄, and gravity filtered. Then the solvent was removed via rotary evaporation. The residue was dissolved in a minimal amount of methanol and an equivalent of water was added. The solution was cooled to 4 °C for 2 h. ^{31}P NMR indicates approximate ratio of 6:1 or two species with peaks consistent with the desired product and the oxide form as an impurity. The desired product was isolated by flash column chromatography in 2 % MeOH/DCM to afford 850 mg, 24% of pale yellow solid.

MS ESI- Calc'd: 364.09. Found: 362.9.

^1H NMR (500 MHz; CDCl_3): δ 8.09 (dd, 8.1, 3.3 1H), 8.06 (dd, 8.1, 1.2 1H), 7.67 (d, 3.3 1H), 7.36 (m, 6H), 7.29 (td, 7.4, 1.9 4H), 3.76 (s, 3H). ^{31}P NMR 3.69 ppm



Triethylene glycol monoazide.²³

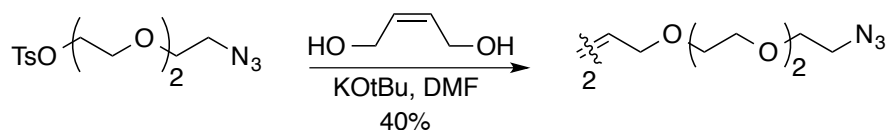
A solution of 17.65 g (105 mmol) of triethylene glycol monochloride, 15.08 g (232 mmol, 2.2 eq) of NaN₃ and 0.33 g (2.2 mmol) of NaI in 100 mL 3:1 water:acetonitrile was heated to 80 °C for 22 h. The product was extracted thrice with 50 mL chloroform. The organic layers were combined, dried with MgSO₄ and the solvent was removed via rotary evaporation to afford 15.99 g (87 %) of a clear liquid. Note: SM and product aren't clearly differentiable by ¹H NMR so monitor progress via ¹³C NMR.

¹H NMR (500 MHz; CDCl₃): δ 3.74-3.72 (m, 2H), 3.69-3.65 (m, 6H), 3.61-3.60 (m, 2H), 3.39 (t, 5.0 2H). ¹³C NMR (126 MHz; CDCl₃): δ 72.6, 70.8, 70.5, 70.2, 61.9, 50.7

2-(2-azidoethoxy)ethyl 4-methylbenzenesulfonate.²⁴

A solution of 7.72 g (44.1 mmol) of triethylene glycol monoazide, 9.83 g (51.6 mmol, 1.17 eq) of tosyl chloride and 9.9 mL (71 mmol, 1.6 eq.) of TEA in 50 mL DCM was stirred overnight at ambient temperature. To the reaction, 1.2 g (15.6 mmol) glycine and 20 mL of DCM were added and allowed to stir overnight. The reaction was washed thrice with 75 mL of brine. The aqueous washes were combined and back extracted with 75 mL of DCM. The organic layers were combined, dried with MgSO₄, filtered, and the solvent was removed via rotary evaporation. The product was isolated by flash column chromatography in 25 →50 % EtOAc/hexanes to afford 11.54 g, 80 % of a clear oil. Yield: (71-80%).

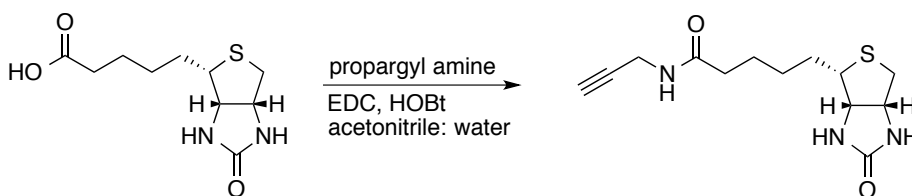
¹H NMR (500 MHz; CDCl₃): δ 7.80 (d, 8.1 2H), 7.34 (d, 8.1 2H), 4.16 (dd, 5.2, 4.4 2H), 3.71-3.69 (m, 2H), 3.64 (t, 5.1 2H), 3.60 (s, 4H), 3.36 (t, 5.0 2H), 2.45 (s, 3H).



(Z)-1,19-diazido-3,6,9,14,17-pentaoxonadec-11-ene (CTA-TEGN₃).

A solution of 11.54 g (35 mmol, 2.5 eq.) of tosylated triethylene glycol azide, 1.15 mL (14 mmol) of 1,4-cisbutenediol and 4.52 g (40.3 mmol, 2.9 eq.) of potassium t-butoxide in 100 mL DMF was stirred at 90 °C overnight. The solvent was removed via rotary evaporation. The product was isolated by flash column chromatography in 4 → 8 % MeOH/DCM to afford 2.28 g (40%) of a clear oil. Note: Attempts to form this product from triethylene glycol monoazide and 1,4-cis-dichlorobutene resulted in substitution on one side and elimination on the other.

¹H NMR (500 MHz; CDCl₃): δ 5.68 (m, 2H), 4.06 (m, 4H), 3.64-3.61 (m, 16H), 3.56 (d, 3.0 2H), 3.54 (d, 4.2 2H), 3.34 (t, 5.1 4H). ¹³C NMR (126 MHz; CDCl₃): δ 129.6, 70.90, 70.86, 70.2, 69.7, 67.1, 50.9

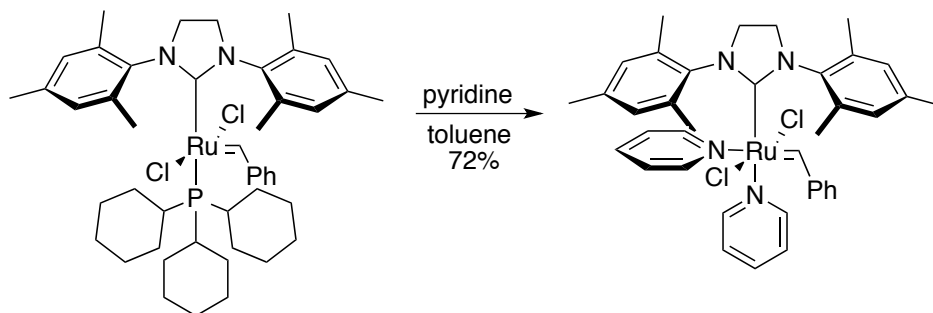


Propargyl biotin.

A solution of 500 mg (2.05 mmol) of biotin, 645 mg (3.36 mmol) of EDC-HCl, 400 mg (2.96 mmol) of HOBt and 340 μL (5.31 mmol) of propargyl amine in 10 mL of acetonitrile:water

(1:1) was stirred overnight at ambient temperature. The solvent was removed via rotary evaporation and purified via flash column chromatography in 5 → 12 % MeOH/DCM to afford 400 mg, 1.42 mmol (69 %) of white solid.

$^1\text{H NMR}$ (; DMSO- d_6): δ 8.22 (s, 1H), 6.42 (s, 1H), 6.35 (s, 1H), 4.30 (t, 6.8 1H), 4.13 (m, 1H), 3.83 (m, 2H), 3.10 (m, 1H), 3.08 (m, 1H), 2.82 (ddd, 12.3, 4.6, 2.1 1H), 2.57 (d, 12.3 1H), 2.08 (t, 6.8 2H), 1.60 (m, 1H), 1.42 (m, 3H), 1.30 (m, 2H).



ROMP catalyst: $\text{RuCl}_2(\text{pyridine})_2(\text{H}_2\text{IMes})(\text{CHPh})$.²⁵

To a solution of 242 mg (0.285 mmol) of Grubbs' II catalyst ($\text{RuCl}_2(\text{PCy}_3)(\text{H}_2\text{IMes})(\text{CHPh})$) in 0.5 mL of toluene in a scintillation vial was added 3 mL pyridine and swirled for 3 min. Additional pyridine (0.3 mL) was used to rinse the sides of the vial. Pentane (10 mL) was then layered on top and the vial stored in the freezer (-20°C) for 3 h. The catalyst was then vacuum filtered and washed with ~25 mL of pentane then dried on high vacuum to afford 150 mg (72%) of green powder. Note: Use as little solvent as possible because small increases in solvent lead to significantly lower yield.

$^1\text{H NMR}$ (500 MHz; CDCl_3): δ 8.63 (s, 2H), 7.82 (d, 2H), 7.63 (d, 7.5 3H), 7.48 (t, 7.3 2H), 7.32-7.29 (m, 2H), 7.08 (t, 7.8 5H), 6.98-6.96 (m, 2H), 6.75 (d, 0.3 2H), 4.20-4.19 (m, 2H),

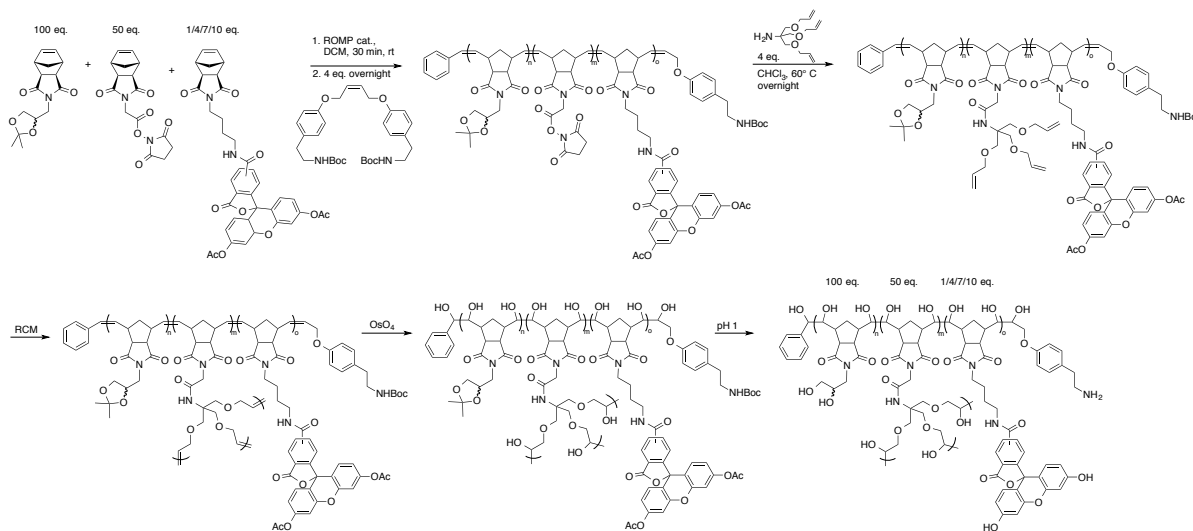
4.06-4.04 (m, 3H), 2.65 (s, 7H), 2.32 (d, 35.9 8H), 2.23 (s, 7H), 1.63 (s, 11H). note RuCHPh

H is downfield

Synthesis and Modification of ONPs

A table with the composition of all the ONP synthesized can be found in Chapter IV.

Appendices.



Ring Opening Metathesis Polymerizations of Norbornyl Monomers.

Monomers were massed into scintillation vials and dissolved in Ar-purged chloroform then topped with a septa to prevent evaporation. Solutions were stored in the freezer. ROMP catalyst was massed into a vial and dissolved in Ar-purged DCM. Solutions were less than 5 days old and stored in -80 °C freezer. Typical scale is a theoretical yield of 200 mg.

To a scintillation vial was added the required volume of each monomer, a stir bar and capped with a septa seal. The solution was Ar-purged and then ROMP catalyst was added to the stirring solution. After 30 minutes the chain transfer reagent was added and the reaction was allowed to stir overnight. The reaction was quenched with butylvinylether and allowed to stir 30 min. The

solution was rotary evaporated to dryness and dissolved in minimal DCM. The polymer was precipitated with di ethyl ether and centrifuged (5000 rpm, 10 min). The polymer was redissolved and precipitated twice more then dried under high vacuum.

Tris allyl Functionalization of ROMP polymers.

The polymer was dissolved in 10-20 mL chloroform:nitrobenzene (8:1) in a scintillation vial and one mass equivalent of tris allyl added. The vial was capped and heated at 50-60 °C (heating block) overnight. Most of the solvent was removed by rotary evaporation and the polymer redissolved in DCM. The polymer was precipitated with ether:hexane (2:1) and centrifuged. The polymer was sonicated with ether (2 x 12 mL) and methanol (2 x 12 mL) and centrifuged when necessary to decant the solvent. The polymer was then dried under high vacuum.

Ring Closing Metathesis of Allyl Containing Linear Polymers.

The polymer was dissolved in dry DCM (200 mL/ 50 mg) and heated to 35 °C (heating mantle) under N₂. Once the polymer is completely dissolved the Grubbs generation I was added (12 mg cat./ 50 mg polymer) as a solution in DCM. After 6 h and 24 h additional catalyst was added (6 mg cat./50 mg polymer) each time. After reacting 48 h, butyl vinyl ether was added (to quench the reaction (3 mL/ 50 mg polymer)) and stirred for 30 min. The DCM was removed via rotary evaporation and purified by column chromatography (eluted with DCM). The catalyst sticks to the silica and the polymer elutes (dark brown). The DCM was removed via rotary evaporation and the polymer was titrated and sonicated with ether yielding a brown powder.

Dihydroxylation of RCM Polymers.

The RCM product polymer (~120 mg) was dissolved in 20 mL acetone:water (7:3) in a scintillation vial. NMO (0.5 mL/ 60 mg polymer, 50% in water) was added as well as catalytic amounts of K_2OsO_4 . The vial was covered with a Kim wipe and heated to 40 °C (heating block) overnight. Additional water was added the next morning (fill vial). The reaction was allowed to continue until it appeared translucent green in color. The reaction was quenched with $NaHSO_3$ (750 mg) for two h then vacuum filtered.

Hydrolysis of Protecting Groups.

The filtrate from above was acidified to pH 1 with 2 M HCl and stirred overnight. The polymer was still not completely in solution so the reaction was basified to pH 14 with 4 M NaOH and stirred 2 h. The reaction was reduced to ~13 mL via rotary evaporation and dialyzed in cassettes with MWCO 10,000.

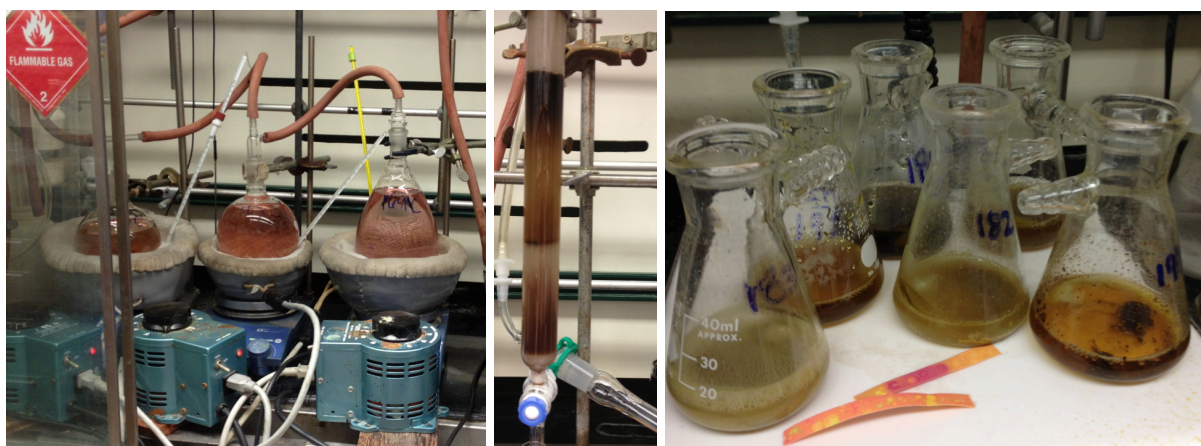


Figure 3.7: RCM reaction set-up (left), column of RCM product (center), hydrolysis of protecting groups (right).

Large Scale ONP Synthesis

Ring Opening Metathesis Polymerizations of Norbornyl Monomers.

Into a 500 mL RBF, 1.669 g (6.018 mmol, 100.4 eq) of NBPdiOH, 958 mg (3.010 mmol, 50.2 eq.) of NBGlyNHS and 165 mg (0.244 mmol, 4.07 eq.) of AcF4NB were massed and dissolved in 100 mL of chloroform. The solution and flask were then purged with Ar for 5 min. A solution of 43.6 mg (59.9 μ mol, 1 eq.) of ROMP catalyst in 4 mL deoxygenated DCM was added and the reaction stirred at room temperature for 20 minutes. To the reaction was added, 1.097 g (2.08 mmol, 35 eq.) of CTA-TyrNHBoc and the reaction stirred 4 h. To quench the catalyst, 15 mL (116 mmol) of butyl vinyl ether was added and the reaction stirred for 45 min. The solvent was removed by rotary evaporation and redissolved in 30 mL of DCM. The solution was transferred to two 50 mL tubes and polymer precipitated with 30 mL of diethylether then centrifuged (10 min at 4000 rpm). The brown supernatant was removed and the polymer was redissolved (contents of both tubes were combined, total volume of 28 mL) and precipitated with 22 mL of diethyl ether. The polymer was pulsed for 30 s in the centrifuge and the supernatant was poured off. The polymer was dried under high vacuum to afford 2.48 g (94 %) of an off-white solid.

Tris allyl Functionalization of ROMP polymers.

To a solution of 2.48 g (50.5 μ mol, 2.54 mmol activated ester) of ROMP polymer in 200 mL of chloroform:nitrobenzene (19:1) was added 2.9 g (12 mmol, 4.7 eq.) of triallyltris and the flask was sealed with a septa. The reaction was heated to 55 °C for 12 h. The solvent was removed via rotary evaporation and the residue transferred with DCM to a 50 mL tube (total vol. 22 mL). The polymer was precipitated with 25 mL diethylether:hexane (2:1) and

centrifuged (10 min at 4000 rpm). The supernatant was removed and the precipitate was redissolved with 10 mL of DCM and precipitated with 40 mL of diethyl ether. The polymer was pulse centrifuged and the supernatant removed. The polymer was dissolved in 20 mL of DCM, precipitated with 30 mL of methanol, sonicated for 5 min then centrifuged and the supernatant decanted. The polymer was then dried on high vacuum to afford 1.76 g (62 %) of an off-white solid.

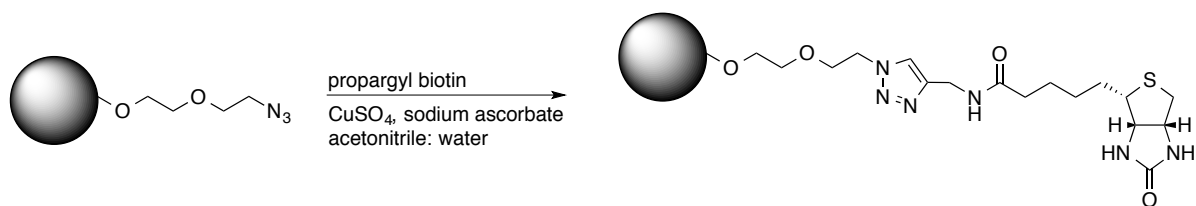
Ring Closing Metathesis of Allyl Containing Linear Polymers:

The above 1.76 g (35 μ mol) of polymer was dissolved in 5.0 L DCM in a 5 L 3-neck RBF. A solution of 445 mg (0.54 mmol) of Grubbs I catalyst in 5 mL DCM was added. The reaction, under nitrogen, was heated via heating mantle to maintain an internal temperature of 30 °C. After 20 h, 223 mg (0.27 mmol) additional Grubbs I catalyst was added. After total reaction time of 68 h the reaction was quenched with 25 mL (193 mmol) of butyl vinyl ether and stirred for 45 min. The solvent was removed via rotary evaporation. The polymer was columned and eluted with DCM to remove the bulk of the catalyst. The solvent was removed and the dark brown polymer carried forward.

Dihydroxylation and Hydrolysis:

To the RCM polymer product in a 300 mL RBF was added 200 mL acetone:water (7:3), 26 mg (70.6 μ mol) of K_2OsO_4 dihydrate and, 16 mL (77.2 mmol, 50 % wt. in water) of NMO. The reaction was allowed to stir with the bottom half of the flask heated in an oil bath at 50 °C covered by a Kimwipe. After 12 h most of the polymer has dissolved off the sides of the flask but it remained dark brown and little to none of the acetone had evaporated. The

temperature was increased to 65° C. After a total of 40 h the reaction was greenish and 8.0 g of sodium bisulfite (sold as mixture with sodium meta bisulfite) was added and stirred for an hour. Several large black clumps were present. The reaction was acidified to pH 1 with 5 mL of concentrated HCl. After stirring for 3 h the solution was basified to pH 12 with 4 M NaOH momentarily, then neutralized with 2 M HCl. The black clumps were dissolved with the addition of ~150 mL DI water. The reaction was vacuum filtered and most of the solvent was removed via rotary evaporation. When ~50 mL water (solid starts to form on the sides of the evaporation flask) remained the contents were transferred to dialysis tubing. The polymer was dialyzed (Spectra/Por dialysis membrane MWCO1000) against 4 L water for 14 h and solvent changed thrice. The volume was decreased via rotary evaporation then dried via lyophilization to afford a fluffy orange solid, 1.509 g, Figure 2.2. three step yield 88%



Conjugation of biotin to ONP:

ONP (with a terminal azide) (5-15 mg), 0.25 mL of 50 mM solution (12.5 μmol) of propargyl biotin, 10 μL of 2 M solution (20 μmol) of CuSO₄ and 20 μL of 1 M solution (20 μmol) of sodium ascorbate were stirred at room temperature for 60 h. The reaction was then dialyzed with MWCO 10,000 against water for ~ 48 h.

III.D. References

1. Kohmoto, S.; Mori, E.; Kishikawa, K. *J. Am. Chem. Soc.* **2007**, *129*, 13364. Room-temperature discotic nematic liquid crystals over a wide temperature range: alkali-metal-ion -induced phase transition from discotic nematic to columnar phases.
2. Müller, S.; Schlüter, A. D. *Chem. Eur. J.* **2005**, *11*, 5589. Synthesis of Water-Soluble, Multiple Functionalizable Dendrons for the Conversion of Large Dendrimers or Other Molecular Objects into Potential Drug Carriers.
3. Boger, D. L.; Borzilleri, R. M.; Nukui, S.; *J. Org. Chem.* **1996**, *61*, 3561. Synthesis of (R)-(4-methoxy-3, 5-dihydroxyphenyl) glycine derivatives: The central amino acid of vancomycin and related agents
4. Dodo, K.; Minato, T.; Noguchi-Yachide, T.; Suganuma, M.; Hasimoto, Y. *Bioorg. & Med. Chem.* **2008**, *16*, 7975. Antiproliferative and apoptosis-inducing activities of alkyl gallate and gallamide derivatives related to (-)-epigallocatechin gallate
5. Hyatt, J. A. *Synth. Commun.* **2008**, *38*, 8. Convenient Preparation of 2,7,8 - Trimethyl-6-hydroxychroman-2-carboxylic Acid (γ -Trolox)
6. Andrew Zill's Thesis
7. Koufaki, M.; Calogeropoulou, T.; Detsi, A.; Roditis, A.; Kourounakis, A. P.; Papazafiri, P.; Tsiakitzis, K.; Gaitanaki, C.; Beis, I.; Kourounakis, P. N. *J Med. Chem.* **2001**, *44*, 4300. Novel potent inhibitors of lipid peroxidation with protective effects against reperfusion arrhythmias
8. Ueno, Y.; Jiao, G.-S.; Burgess, K. *Synthesis*, **2004**, *47*, 3131. Preparation of 5- and 6-Carboxyfluorescein.

8. Ueno, Y.; Jiao, G.-S.; Burgess, K. *Synthesis*, **2004**, 2591. Preparation of 5-and 6-carboxyfluorescein.
9. Nam, N. H.; Ye, G.; Sun, G.; Parang, K. *J. Med. Chem.* **2004**, *47*, 3131. Conformationally constrained peptide analogues of pTyr-Glu-Glu-Ile as inhibitors of the Src SH2 domain binding
10. Salzberg, P. L. and Supniewski, J. V. *Organic Synthesis Coll.* Vol. *1*, p.119 (**1941**); Vol. *7*, p.8 (**1927**). β -Bromoethylphthalimide
11. Zakarinia, M.; Davary, H.; Hakimelahi, G. H. *Helvetica Chimica Acta.* **1990**, *73*, 912. The Syntheses of Purine and Pyrimidine Secoribo - nucleosides: Acyclo-uridine Derivative of Cyclophosphamide
12. a) Mangold, C.; Wurm, F.; Obermeier, B.; Frey, H. *Macromol.* **2010**, *43*, 2244. Functional Poly (ethylene glycol): PEG-Based Random Copolymers with 1, 2-Diol Side Chains and Terminal Amino Functionality. b) Bakalarz-Jeziorna, A.; Helinski, J.; Krawiecka B. *J. Chem. Soc., Perkin Trans. 1*, **2001**, 1086-1090. Synthesis of multifunctionalized phosphonic acid esters via opening of oxiranes and azetidinium salts with phosphoryl-substituted carbanions
13. Haag, R. *Chem. Eur. J.* **2001**, *7*, 327. Dendrimers and Hyperbranched Polymers as High - Loading Supports for Organic Synthesis
14. Kainthan, R. K.; Muliawan, E. B.; Hatzikiriakos, S. G.; Brooks, D. E. *Macromol.* **2006**, *39*, 7708. Synthesis, characterization, and viscoelastic properties of high molecular weight hyperbranched polyglycerols

15. Conrad, R. M.; Grubbs, R. H. *Angew. Chem. Int. Ed.* **2009**, *48*, 8328. Tunable, Temperature-Responsive Polynorbornenes with Side Chains Based on an Elastin Peptide Sequence
16. Node, M.; Kodama, S.; Hamashima, Y.; Katoh, T.; Nishide, K.; Kajimoto, T. *Chem. Pharm. Bull.* **2006**, *54*, 1662. Biomimetic synthesis of (+/-)-galanthamine and asymmetric synthesis of (-)-galanthamine using remote asymmetric induction.
17. Yamada, H.; Nagao, K.; Dokei, K.; Kasai, Y.; Michihata, N. *J. Am. Chem. Soc.* **2008**, *24*, 7566. Total synthesis of (-)-Corilagin
18. Segura, M.; Sansone, F.; Casnati, A.; Ungaro, R. *Synthesis* **2001**, 2105. Synthesis of lower rim polyhydroxylated calix[4]arenes.
19. Bernini, R.; Crisante, F.; Barontini, M.; Fabrizi, G. *Synthesis* **2009**, 3838. A New and Efficient Route for the Synthesis of Naturally Occurring Catecholamines
20. a) Matson, J. B.; Grubbs, R. H. *Macromol.* **2010**, *43*, 213. Monotelechelic poly (oxa) norbornenes by ring-opening metathesis polymerization using direct end-capping and cross-metathesis. b) Bai, Y.; Lu, H.; Ponnusamy, E.; Cheng, J. *Chem. Commun.* **2011**, 47, 10830. Synthesis of hybrid block copolymers via integrated ring-opening metathesis polymerization and polymerization of NCA
21. Saxon, E.; Bertozzi, C. R. *Science* **2000**, *287*, 2007. Cell Surface Engineering by a Modified Staudinger Reaction.
22. Canalle, L. A.; van Berkel, S. S.; de Haan, L. T.; van Hest, J. C. M. *Adv. Funct. Mater.* **2009**, *19*, 3463. Copper-Free Clickable Coatings

23. Lebeau, L.; Oudet, P.; Mioskowski, C. *Helvetica Chimica Acta*. **1991**, *74*, 1697. Synthesis of New Phospholipids Linked to Steroid-Hormone Derivatives Designed for Two - Dimensional Crystallization of Proteins
- 24 .Müller, M. K.; Brunsveld, L. *Angew. Chem. Int. Ed.* **2009**, *48*, 2921. A Supramolecular Polymer as a Self - Assembling Polyvalent Scaffold
25. Love, J. A.; Morgan, J. P.; Trnka, T. M.; Grubbs, R. H. *Angew. Chem. Int. Ed.* **2002**, *41*, 4035. A Practical and Highly Active Ruthenium-Based Catalyst that Effects the Cross Metathesis of Acrylonitrile

Appendices

Table of Contents

Appendix A. Data Work-up Methods

A.1. UV-vis and Fluorescence Spectroscopy Data Explanation of Data Work-up

A.2. Example Work-up of Photobleaching Data

Appendix B. Data Associated with Chapter I.

B.1. Relationship between MW determination techniques

B.2. SEC of select HPGs

B.3. Detailed Molecular Weight Values of HPG Series

B.4. SEC of HPG Purification: Dialysis verses Precipitation

Appendix C. Data Associated with Chapter II.

C.1. Index of ONP synthesized

C.2. SEC data of ONPs

C.3. UV, Fluorescence and Photobleaching Studies of ONPs

C.4. Determination of the pK_a of fluorescein on the ONPs

C.5. Effects of Metal Removal on the UV and Fluorescence of ONPs

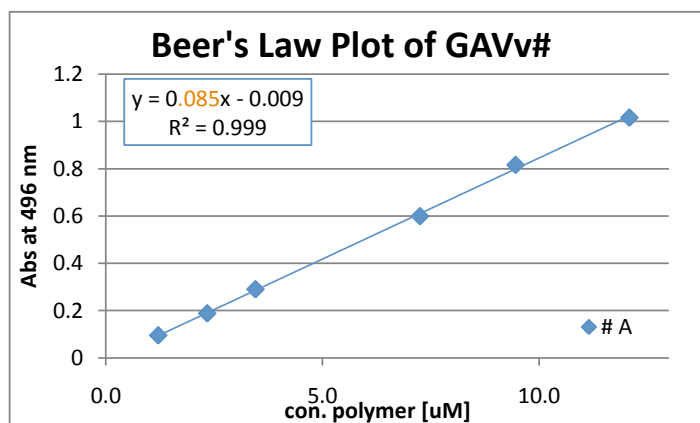
Appendix A. Data Work-up Methods

A.1. UV-vis and Fluorescence Spectroscopy Data Explanation of Data Work-up

The GAVv# corresponds to the page but also references on the data Table 1.4

Vial A

| | [A] $\mu\text{g/mL}$ | Abs @ λ_{max} | [A] μM | Abs @ 475 nm | \int_{480}^{600} fluorescence |
|-----|----------------------|------------------------------|-------------------|--------------|---------------------------------|
| A1 | 207 | 0.599 | 7.3 | 0.307 | 2.12E+08 |
| A2 | 270 | 0.816 | 9.5 | 0.418 | 2.89E+08 |
| A3 | 344 | 1.016 | 12.1 | 0.524 | |
| A3a | 34 | 0.095 | 1.2 | 0.047 | 3.81E+07 |
| A4 | 98 | 0.29 | 3.5 | 0.149 | 1.10E+08 |
| A5 | 67 | 0.188 | 2.3 | 0.095 | 7.35E+07 |



Plotting absorbance vs concentration and fitting the data provides the molar absorptivity

$$A = \epsilon lc$$

$$\epsilon = \text{Abs.}/\text{con.} \cdot l$$

$$= 0.085 (\text{Abs}/\mu\text{M})\text{cm}^{-1}$$

$$= 85,000(\text{Abs}/\text{M})\text{cm}^{-1}$$

the absorbance of fluorescein is $78,000 (\text{Abs}/\text{M})\text{cm}^{-1}$ under the conditions. Assuming the absorbance of fluorescein doesn't change appreciably upon conjugation the number of dye/polymer can be calculated

$$\epsilon_{\text{polymer}} / \epsilon_{\text{fluorescein}} = \text{dye/polymer}$$

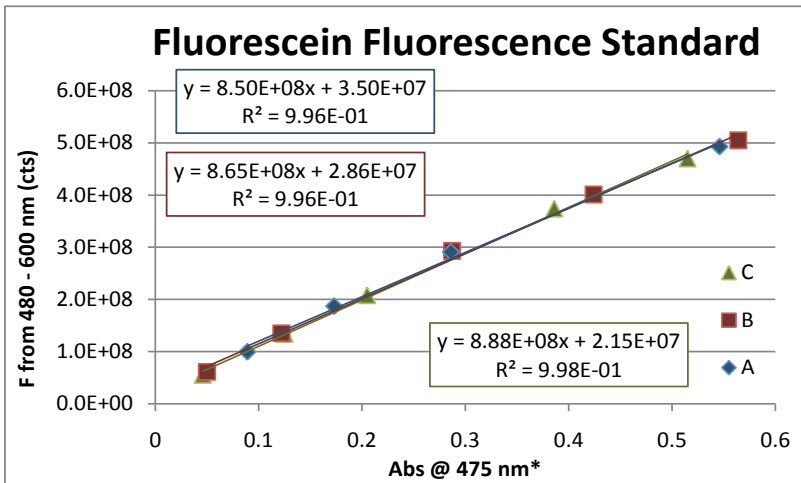
$$85,000/78,000 = 1.1 \text{ fluorescein}$$

all data is taken in triplicate and therefore the average is reported

| | $\epsilon_{\lambda_{\text{max}}}$ | fluorescence slope |
|--------|-----------------------------------|--------------------|
| vial A | 85,000 | 6.69E+08 |
| vial B | 91,900 | 6.69E+08 |
| vial C | 88,100 | 7.19E+08 |
| avg. | 88,300 | 6.86E+08 |

| | |
|-----------------------------------|----------|
| $\epsilon_{\lambda_{\text{max}}}$ | 88,300 |
| dye/poly | 1.1 |
| F slope | 6.86E+08 |
| F const. | 1.54E-09 |
| QY (Φ) | 1.06 |
| brightness | 9.33E+04 |
| rel. brightness | 1.3 |

To calculate quantum yield, Φ , it is necessary to determine the percentage of excited molecules that fluoresce (by definition). However, fluorescence is quantitated by comparison to a known fluorophore. This must be done each time the instrument is used in order to calibrate the "counts" detected. This corresponds to the F const. value in the table above.



The fluorescence integrated from 480 to 600 nm is plotted against absorbance at the excitation wavelength (475 nm)

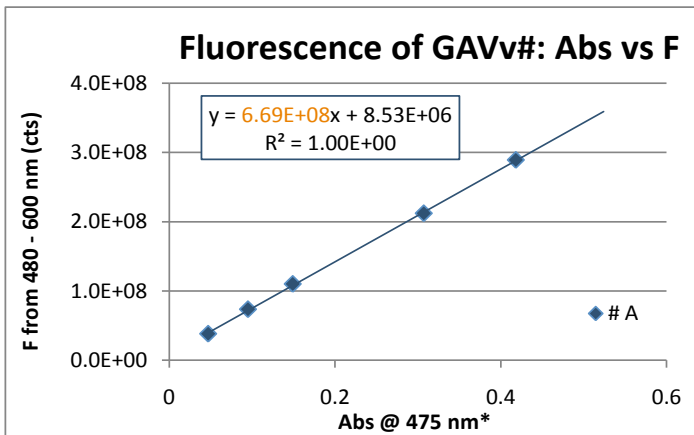
slope
 $8.50E+08$
 $8.65E+08$
 $8.88E+08$

 $8.68E+08$ avg.

Fluorescein is used as a standard and assumed to have a $\Phi = 0.9$

$$\Phi = \frac{\# \text{ of photons emitted}}{\# \text{ photons absorbed}} = 0.9 = \frac{(F \text{ counts})_i (F \text{ constant})}{\text{slope of above plot}}$$

$$0.9 = \frac{0.9}{8.68E+08} = 1.04E-9 = F \text{ const}$$



$QY (\Phi) = (F \text{ slope})(F \text{ const.})$
 brightness = $\epsilon\Phi$
 rel. brightness = $\frac{\text{sample brightness}}{\text{fluorescein brightness}}$

| | $\epsilon_{\lambda_{max}}$ | fluorescence slope |
|--------|----------------------------|--------------------|
| vial A | 85,000 | 6.69E+08 |
| vial B | 91,900 | 6.69E+08 |
| vial C | 88,100 | 7.19E+08 |
| avg. | 88,300 | 6.86E+08 |

$\epsilon_{\lambda_{max}}$ 88,300
 dye/poly 1.1
 F slope 6.86E+08
 F const. 1.04E-09
 QY (Φ) 0.71
 brightness 6.30E+04
 rel. brightness 0.9

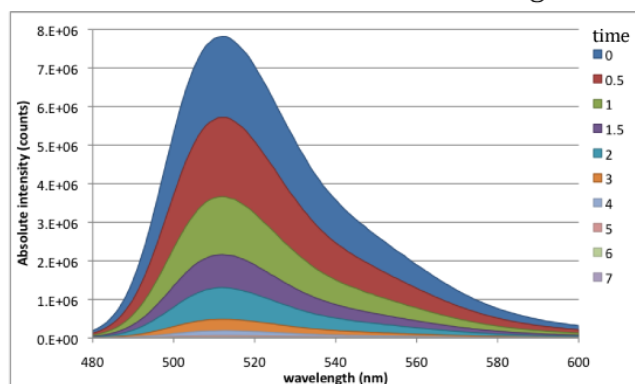
The data from HPG-fluorescein controls and ONP are compiled in Table 1.4 and IV.C.3 (pg 140), respectively.

A.2. Example Work-up Data for Photobleaching

This appendix is an explanation of how the photobleaching data was worked up.

Each sample (4 or 5 mL) was prepared at 1 μM in pH 8.0 sodium phosphate buffer. Samples were bleached for 6-12 hours and 200 μL aliquots were removed at time points. Once the trial was complete the fluorescence of the aliquots was studied. Example data shown below is of fluorescein, the standard.

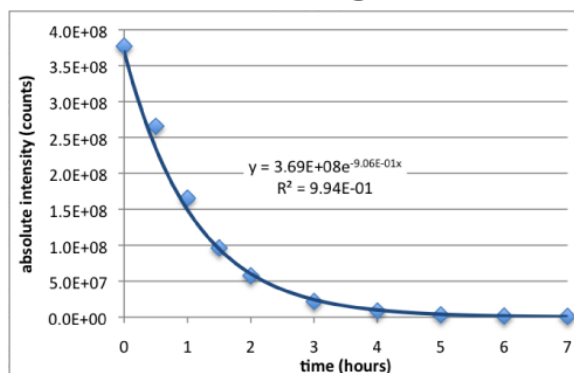
Overlay of the Fluorescence Spectra of the Aliquots of Fluorescein while Bleaching



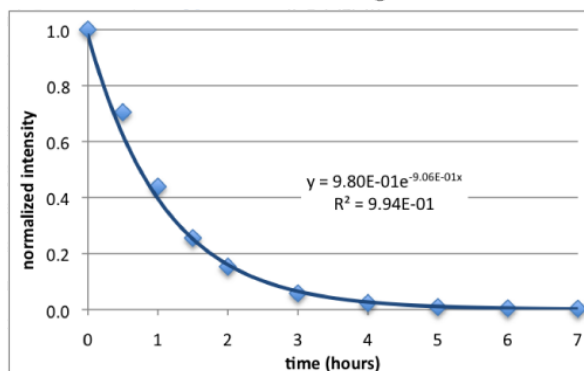
| time (hrs) | 0 | 0.5 | 1 | 1.5 | 2 | 3 | 4 | 5 | 6 | 7 |
|--------------|--------|--------|--------|--------|--------|--------|--------|--------|--------|--------|
| absolute F | 3.77E8 | 2.66E8 | 1.65E8 | 9.63E7 | 5.76E7 | 2.17E7 | 8.66E6 | 3.18E6 | 1.46E6 | 9.29E5 |
| normalized F | 1.00 | 0.70 | 0.44 | 0.26 | 0.15 | 0.06 | 0.02 | 0.01 | 0.004 | 0.002 |

The fluorescence data was exported as a table of counts at a given wavelength (to the nearest whole nanometer). These 121 values (from 480 to 600 nm) were summed for greater accuracy than if a single point value was taken. Each time point (aliquot) was then simplified to a single fluorescence value reported as "absolute fluorescence," as shown in the table and plot. To compare the stability of ONPs with different initial fluorescence it was helpful to plot the normalized bleaching plots together. The normalized plots were fit to an exponential curve. Setting y equal to 0.5 and solving for x allowed for the calculation of half-times. Half-times were the time calculated it takes the fluorescence to decrease to reach half the initial intensity.

Absolute Photobleaching of Fluorescein



Normalized Photobleaching of Fluorescein

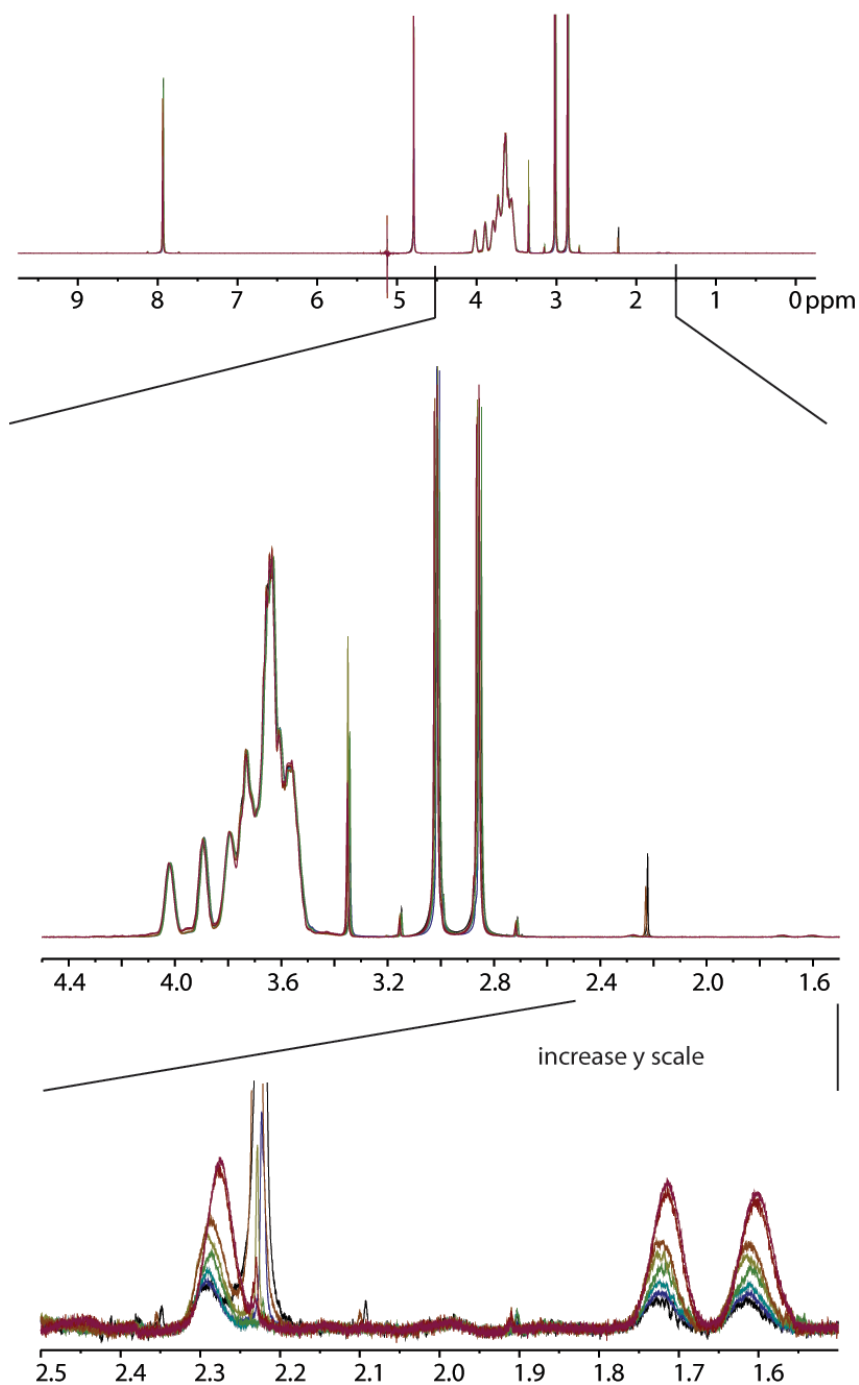


Appendix B. Data Associated with Chapter I.

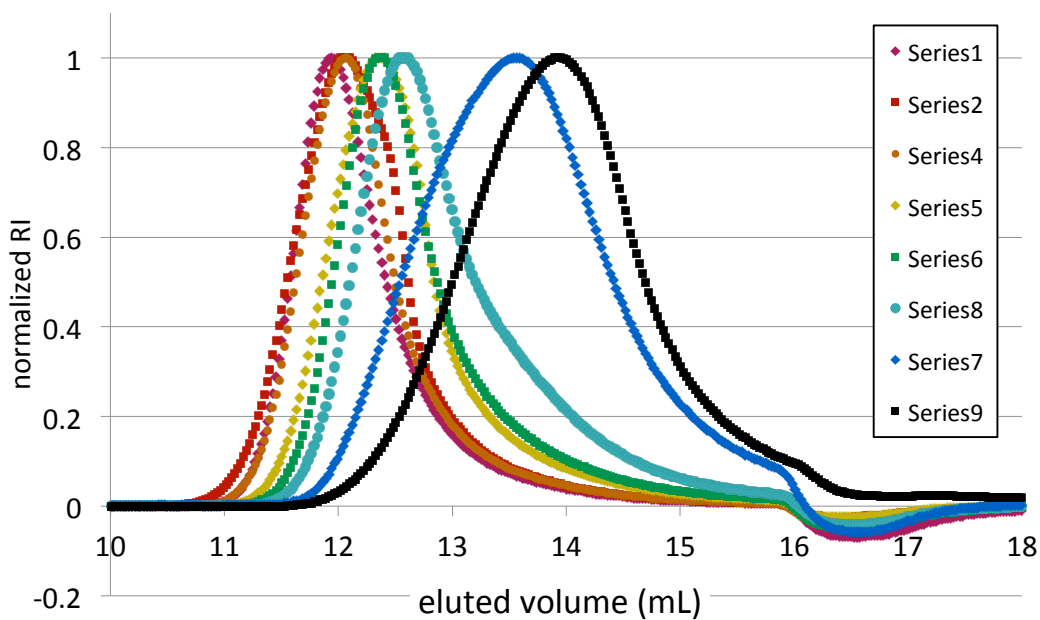
B.1. Relationship between MW determination techniques

The fractions of HPG was characterized by DMF SEC, water SEC and ^1H NMR. Each fraction was isolated and purified by multiple precipitations.

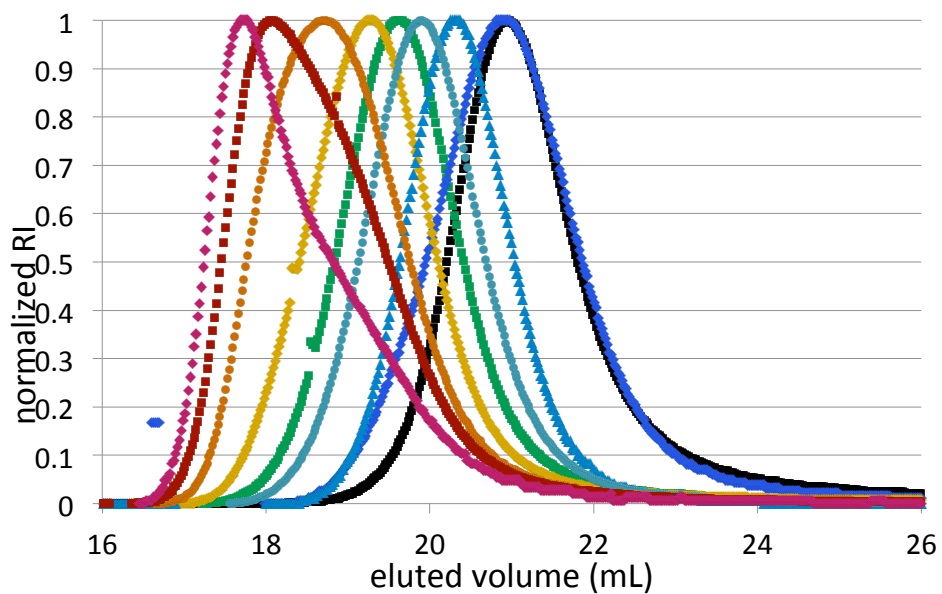
^1H NMR overlay of the fractions spiked with DMF



Refractive Index Chromatograph of Water SEC Traces of HPGs



Refractive Index Chromatograph of DMF SEC Traces of HPGs



Comparison of SEC estimate Mw & Mn of HPGs (kDa)

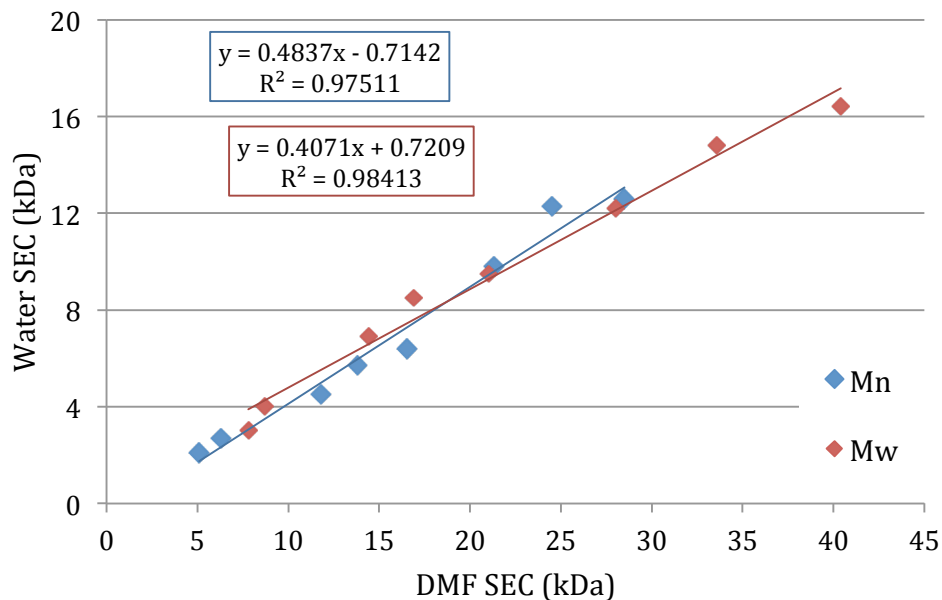


Table of MW values (kDa) determined by SEC and NMR

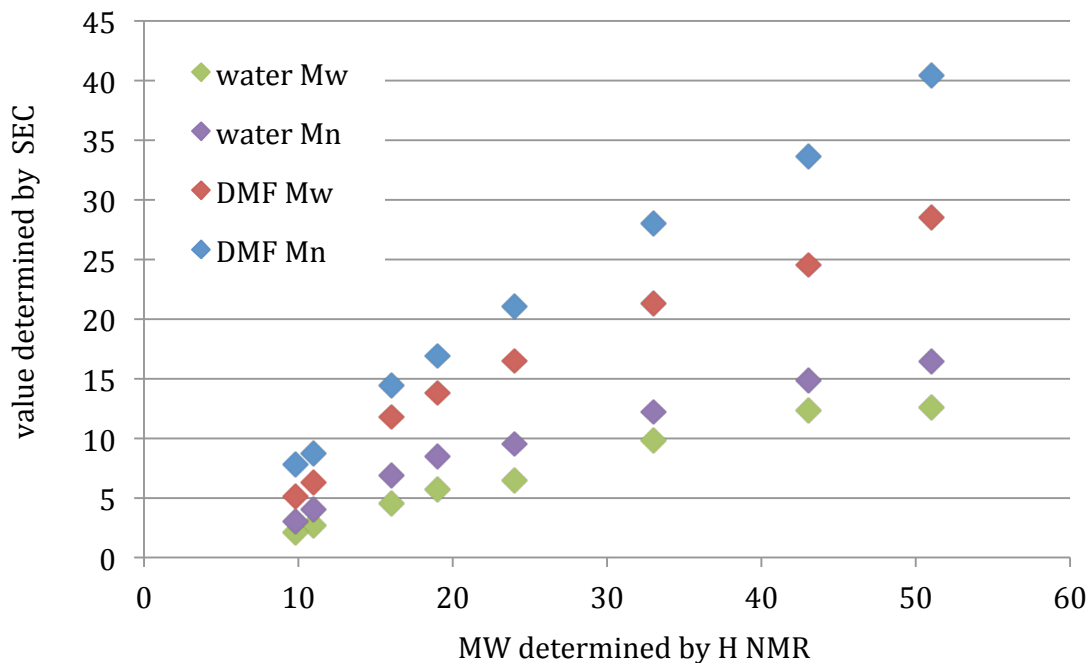
| frac | Mw | | Mn | | PDI | | NMR |
|------|-------|------|-------|------|-------|-----|-----|
| | water | DMF | water | DMF | water | DMF | |
| 1 | 12.6 | 28.5 | 16.4 | 40.4 | 1.3 | 1.4 | 51 |
| 2 | 12.3 | 24.5 | 14.8 | 33.6 | 1.3 | 1.4 | 43 |
| 3 | 9.8 | 21.3 | 12.2 | 28.0 | 1.4 | 1.3 | 33 |
| 4 | 6.4 | 16.5 | 9.5 | 21.0 | 1.5 | 1.3 | 24 |
| 5 | 5.7 | 13.8 | 8.5 | 16.9 | 1.5 | 1.2 | 19 |
| 6 | 4.5 | 11.8 | 6.9 | 14.4 | 1.5 | 1.2 | 16 |
| 8 | 2.7 | 6.3 | 4.0 | 8.7 | 1.5 | 1.4 | 11 |
| 9 | 2.1 | 5.1 | 3.0 | 7.8 | 1.4 | 1.5 | 10 |

water and DMF refer to the SEC solvent

water SEC is calibrated with PEG

DMF SEC was calibrated with PS

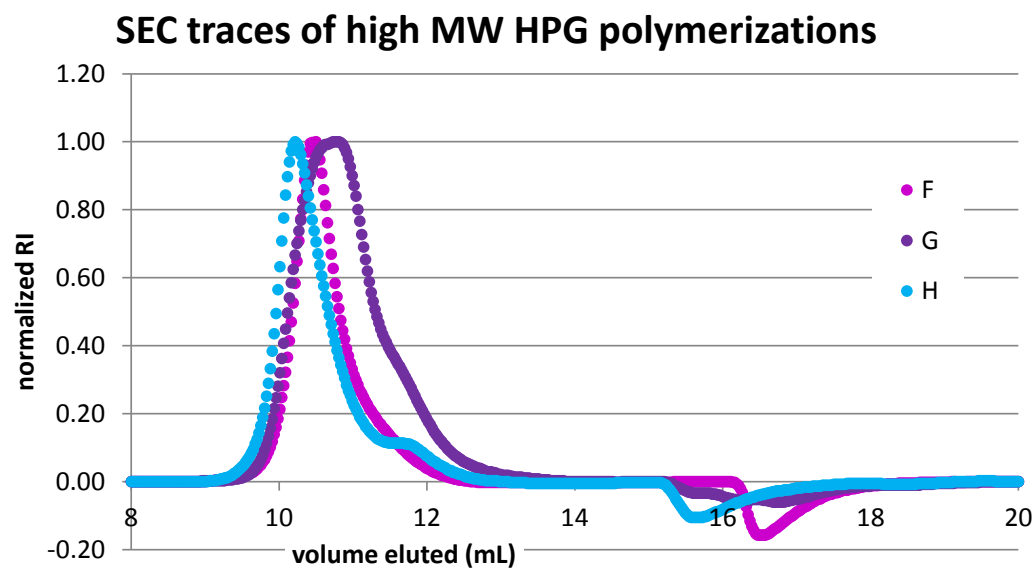
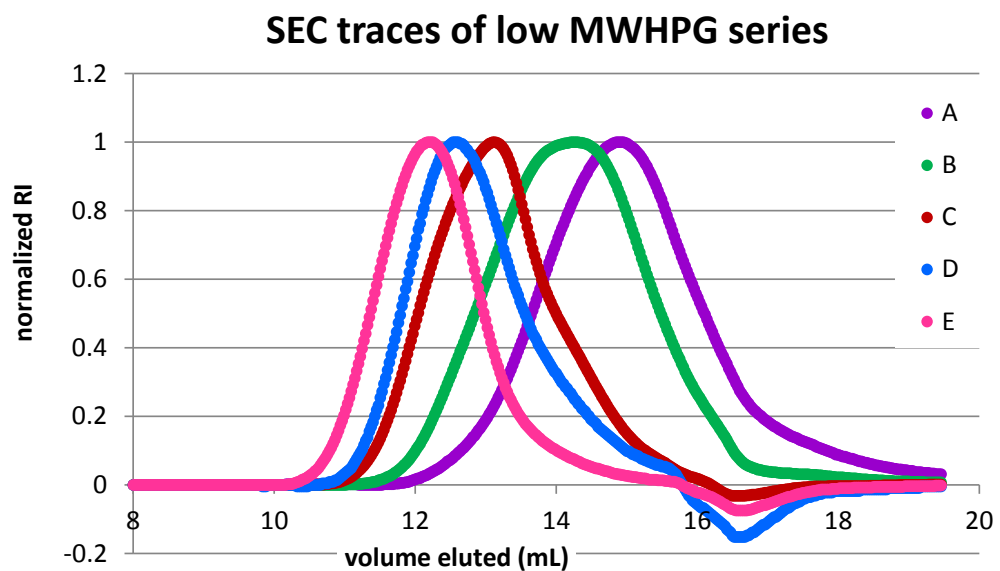
Comparison of water SEC and NMR est. MW of GAViv41 HPG (kDa)



The NMR values are based on the integration ratio between the glycidol protons and the hexynol methylene protons. NMR over estimates the MW because it assumes that all polymers originate with 5-hexynol. The values determined by SEC are in general a percentage of the NMR value. The relationship between the values determined by the two SEC systems is expected to be consistent. However, the relationship between the NMR MW and the SEC values is expected to change for each polymerization reaction (and possibly on the fraction) based on the percentage of polymer not initiated with 5-hexynol.

B.2. SEC of select HPGs

Water SEC traces, details can be found in Chapter III. Experimental

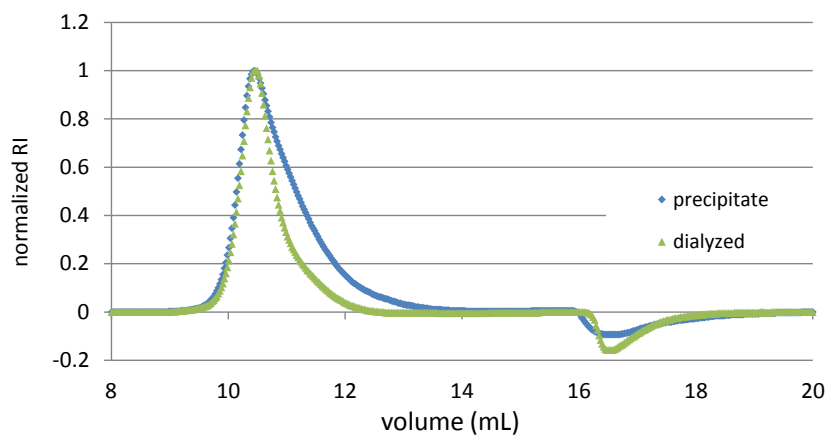


B.3. Detailed Molecular Weight Values of HPG Series

| "name" | water SEC | | | DMF SEC | | | MALS | | |
|------------|----------------|----------------|------|----------------|----------------|------|----------------|----------------|------|
| | M _n | M _w | PDI | M _n | M _w | PDI | M _n | M _w | PDI |
| A sample a | 1,256 | 1,798 | 1.43 | 1,415 | 1,797 | 1.27 | 6,279 | 6,875 | 1.09 |
| A sample b | 1,286 | 1,861 | 1.45 | 1,430 | 1,838 | 1.29 | 2,213 | 2,287 | 1.03 |
| A sample c | 1,155 | 1,605 | 1.39 | 1,514 | 1,899 | 1.25 | 1,799 | 1,945 | 1.08 |
| A | 1,232 | 1,755 | 1.4 | 1,453 | 1,845 | 1.3 | 3,430 | 3,702 | 1.1 |
| B sample a | 1,747 | 2,899 | 1.49 | 2,281 | 3,007 | 1.32 | 6,108 | 6,408 | 1.05 |
| B sample b | 1,448 | 2,368 | 1.64 | 2,318 | 3,104 | 1.34 | 4,018 | 4,684 | 1.17 |
| B sample c | 2,075 | 3,488 | 1.68 | 2,337 | 3,081 | 1.32 | 4,051 | 4,469 | 1.10 |
| B | 1,757 | 2,918 | 1.6 | 2,312 | 3,064 | 1.3 | 4,726 | 5,187 | 1.1 |
| C sample a | 3,651 | 6,214 | 1.70 | 4,329 | 5,337 | 1.23 | 10,320 | 10,540 | 1.02 |
| C sample b | 4,452 | 7,636 | 1.72 | 4,266 | 5,379 | 1.26 | 10,860 | 11,720 | 1.08 |
| C sample c | 3,456 | 5,628 | 1.63 | 4,291 | 5,334 | 1.24 | 13,590 | 13,990 | 1.03 |
| C | 3,853 | 6,493 | 1.7 | 4,295 | 5,350 | 1.2 | 11,590 | 12,083 | 1.0 |
| D sample a | 4,557 | 8,114 | 1.78 | 4,654 | 5,818 | 1.25 | 14,650 | 14,740 | 1.01 |
| D sample b | 4,469 | 7,860 | 1.76 | 4,455 | 5,759 | 1.29 | 12,880 | 12,940 | 1.00 |
| D sample c | 4,638 | 8,146 | 1.76 | 4,501 | 5,760 | 1.28 | 12,850 | 12,900 | 1.00 |
| D | 4,555 | 8,040 | 1.8 | 4,537 | 5,779 | 1.3 | 13,460 | 13,527 | 1.0 |
| E sample a | 7,785 | 13,059 | 1.68 | 8,000 | 10,000 | 1.25 | 46,950 | 51,750 | 1.10 |
| E sample b | 7,487 | 12,397 | 1.66 | 7,661 | 9,692 | 1.27 | 56,070 | 61,700 | 1.10 |
| E sample c | 6,756 | 11,427 | 1.67 | 7,648 | 9,509 | 1.24 | 35,250 | 39,370 | 1.12 |
| E | 7,343 | 12,294 | 1.7 | 7,770 | 9,734 | 1.3 | 46,090 | 50,940 | 1.1 |

Each were run in triplicate but samples a, b and c are not the same samples for the water and DMF SEC. DMF SEC samples and MALS samples are the same and were between 5 and 20 mg/mL.

B.4. SEC of HPG Purification: Dialysis versus Precipitation



A recently polymerized HPG was isolated by precipitation. The water SEC trace of this HPG is shown in blue. The HPG was then further purified by dialysis. The SEC trace is shown in green. These data indicate that dialysis was able to remove low molecular weight HPGs effectively reducing the polymers PDI.

Appendix C. Data Associated with Chapter II.

C.1. Index of ONP synthesized

| Name | ref. # | theo. MW (kDa) | NBPdiOH | NBGlyNHS | AcF4NB | AcT4NB | G3NB |
|------------------|--------|-------------------|---------|----------|--------|--------|------|
| ONP150-1F | 139 | 47.2 | 100 | 50 | 1 | | |
| ONP150-4F | 140 | 49.0 | 100 | 50 | 4 | | |
| ONP150-7F | 141 | 50.8 | 100 | 50 | 7 | | |
| ONP150-10F | 142 | 52.6 | 100 | 50 | 10 | | |
| ONP150-15F | 143 | 55.5 | 100 | 50 | 15 | | |
| ONP150-4F-40T | 165 | 67.1 | 100 | 50 | 4 | 40 | |
| ONP150-4F-4T-a | 166 | 50.8 | 100 | 50 | 4 | 4 | |
| ONP150-4F-10T-a | 167 | 53.5 | 100 | 50 | 4 | 10 | |
| ONP150-4F-20T-a | 168 | 58.1 | 100 | 50 | 4 | 20 | |
| ONP150-4F-60T | 169 | 76.2 | 100 | 50 | 4 | 60 | |
| ONP150-4F-4T-b | 180 | 50.8 | 100 | 50 | 4 | 4 | |
| ONP150-4F-10T-b | 181 | 53.5 | 100 | 50 | 4 | 10 | |
| ONP150-4F-10T-c | 182 | 53.5 | 100 | 50 | 4 | 10 | |
| ONP150-4F-20T-b | 183 | 58.1 | 100 | 50 | 4 | 20 | |
| ONP75-10F | 191 | 29.4 | 50 | 25 | 10 | | |
| ONP75-15F | 192 | 32.3 | 50 | 25 | 15 | | |
| ONP75-4F | 200 | 25.8 | 50 | 25 | 4 | | |
| ONP75-20F | 201 | 35.3 | 50 | 25 | 20 | | |
| ONP38-4F | 202 | 14.2 | 25 | 12.5 | 4 | | |
| ONP38-10F | 203 | 17.8 | 25 | 12.5 | 10 | | |
| ONP40-4F | 204 | 16.4 | 20 | 20 | 4 | | |
| ONP40-10F | 205 | 20.0 | 20 | 20 | 10 | | |
| ONP150-4F-LS | 223 | 49.0 | 100 | 50 | 4 | | |
| ONP150-4F-4G | 20 | 50.5 | 100 | 50 | 4 | | 4 |
| ONP150-4F-10G | 21 | 53.0 | 100 | 50 | 4 | | 10 |
| ONP150-4F-20G | 22 | 57.0 | 100 | 50 | 4 | | 20 |
| ONP150-10F-10G | 23 | 56.5 | 100 | 50 | 10 | | 10 |
| ONP150-10F-20G | 24 | 60.6 | 100 | 50 | 10 | | 20 |
| ONP150-10F-30G | 25 | 64.7 | 100 | 50 | 10 | | 30 |
| ONP75-3F-3G | 30 | 26.3 | 50 | 25 | 3 | | 3 |
| ONP75-3F-6G | 31 | 27.5 | 50 | 25 | 3 | | 6 |
| ONP75-3F-9G | 32 | 28.8 | 50 | 25 | 3 | | 9 |
| ONP75-6F-6G | 33 | 29.3 | 50 | 25 | 6 | | 6 |
| ONP75-6F-12G | 34 | 31.8 | 50 | 25 | 6 | | 12 |
| ONP75-6F-18G | 35 | 34.2 | 50 | 25 | 6 | | 18 |
| ONP150-10F-B | 52 | 52.6 | 100 | 50 | 10 | | |
| ONP150-10F-10G-B | 53 | 56.7 | 100 | 50 | 10 | | 10 |
| ONP150-10F-10T-B | 54 | 57.1 | 100 | 50 | 10 | 10 | |

ref #139-223 have CTA-TyrNHBoc, 20-35 have Ph as a terminal group and 52-55 have CTA-TEGN₃,

Nomenclature is ONP followed by the number of NBPdiOH and NBGlyNHS monomer units (to give a rough indication of size)- # of fluorescein monomers-# of AFA units, T = trolox, G = gallate. An additional letter, a,b,c indicates if the polymer was synthesized with the same composition multiple times. LS indicates this polymer was prepared on the large scale, 1-2 g. B indicates biotin was conjugated to these polymers.

C.2. SEC data of ONPs

| Name | Ref # | ROMP | | ROMP allyl | | RCM | |
|------------------|-------|-------|-------|------------|-------|-------|-------|
| | | Mn | Mw | Mn | Mw | Mn | Mw |
| ONP150-1F | 139 | 76.04 | 76.25 | 74.36 | 74.64 | 65.39 | 66.92 |
| ONP150-4F | 140 | 76.71 | 76.88 | 74.71 | 75.11 | 66.49 | 67.41 |
| ONP150-7F | 141 | 77.11 | 77.34 | 75.57 | 75.92 | 67.49 | 68.16 |
| ONP150-10F | 142 | 77.80 | 77.98 | 76.74 | 77.01 | 67.84 | 68.64 |
| ONP150-15F | 143 | 78.42 | 78.62 | 74.76 | 75.56 | 67.65 | 68.47 |
| ONP150-4F-40T | 165 | 79.30 | 79.50 | 76.90 | 77.40 | 74.20 | 74.80 |
| ONP150-4F-4T-a | 166 | 75.80 | 76.00 | 73.20 | 74.80 | 67.30 | 68.10 |
| ONP150-4F-10T-a | 167 | 72.40 | 73.10 | 75.70 | 76.00 | 67.80 | 68.80 |
| ONP150-4F-20T-a | 168 | 74.70 | 75.10 | 75.90 | 76.30 | 70.00 | 70.90 |
| ONP150-4F-60T | 169 | 78.10 | 78.60 | 76.70 | 71.20 | 75.00 | 75.50 |
| ONP150-4F-4T-b | 180 | 76.83 | 77.71 | 75.03 | 76.06 | 72.62 | 73.59 |
| ONP150-4F-10T-b | 181 | 75.26 | 75.89 | 72.57 | 73.60 | 73.73 | 74.50 |
| ONP150-4F-10T-c | 182 | 75.77 | 76.57 | 76.31 | 77.12 | 72.96 | 74.02 |
| ONP150-4F-20T-c | 183 | 74.36 | 75.22 | 74.28 | 75.06 | 71.85 | 72.72 |
| ONP75-10F | 191 | 69.14 | 70.98 | 64.75 | 67.25 | 63.72 | 64.67 |
| ONP75-15F | 192 | 68.95 | 69.47 | 67.51 | 68.30 | 59.63 | 60.43 |
| ONP75-4F | 200 | 64.69 | 65.25 | 57.66 | 58.59 | 54.94 | 55.67 |
| ONP75-20F | 201 | 69.92 | 70.30 | 68.55 | 68.97 | 63.86 | 64.76 |
| ONP38-4F | 202 | 48.22 | 48.79 | 44.87 | 45.64 | | |
| ONP38-10F | 203 | 54.17 | 54.72 | 48.19 | 49.55 | 46.63 | 47.98 |
| ONP40-4F | 204 | 48.92 | 49.94 | 41.79 | 43.53 | | |
| ONP40-10F | 205 | 55.58 | 56.30 | 48.30 | 50.12 | 46.57 | 48.29 |
| ONP150-4F-LS | 223 | 76.14 | 76.68 | 74.57 | 75.25 | 70.72 | 71.43 |
| ONP150-4F-4G | 20 | 70.60 | 72.02 | 78.59 | 78.85 | | |
| ONP150-4F-10G | 21 | 75.90 | 76.69 | | | | |
| ONP150-4F-20G | 22 | 75.42 | 76.15 | | | | |
| ONP150-10F-20G | 24 | 72.10 | 73.52 | | | 73.99 | 74.77 |
| ONP150-10F-30G | 25 | 75.18 | 76.31 | | | | |
| ONP75-3F-3G | 30 | 64.97 | 66.03 | 58.57 | 60.31 | 61.21 | 62.71 |
| ONP75-3F-6G | 31 | 59.14 | 60.51 | 66.34 | 67.02 | 60.68 | 62.40 |
| ONP75-3F-9G | 32 | 66.44 | 66.96 | 57.35 | 59.16 | 60.68 | 61.79 |
| ONP75-6F-12G | 34 | 66.45 | 66.85 | | | | |
| ONP75-6F-18G | 35 | 66.75 | 67.33 | 66.81 | 67.42 | | |
| ONP150-10F-B | 52 | 66.84 | 70.17 | 77.78 | 78.27 | | |
| ONP150-10F-10G-B | 53 | 74.35 | 75.59 | 75.93 | 77.01 | | |
| ONP150-10F-10T-B | 54 | 72.36 | 73.65 | 79.51 | 79.72 | 71.09 | 72.08 |

Blanks are due to software malfunctions or insufficient sample to run.

Reported as kDa. Data determined by comparison to polystyrene standard.

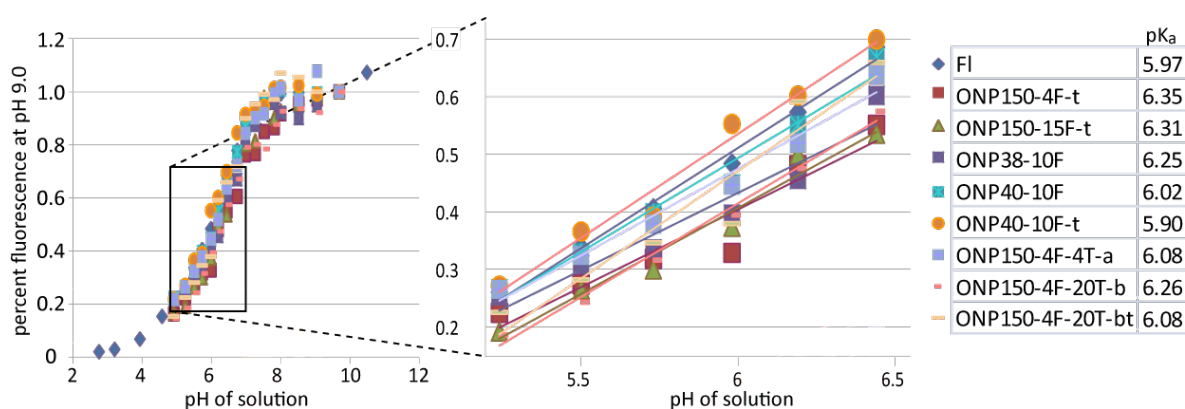
DMF SEC details can be found in Chapter III. Experimental

C.3. UV, Fluorescence and Photobleaching of ONPs

| name | ref # | theo. MW (kDa) | λ_{\max} (nm) | $\epsilon\lambda_{\max}$ (kAbs/Mcm) | QY (Φ) | brightness | half- time |
|------------------|--------|-------------------|--------------------------|--|---------------|------------|---------------|
| ONP150-1F | 139 | 47.2 | 501 | 38 | 0.31 | 12 | |
| ONP150-4F | 140 | 49.0 | 500 | 132 | 0.53 | 70 | 3.2 |
| ONP150-7F | 141 | 50.8 | 500 | 232 | 0.49 | 115 | 4.2 |
| ONP150-10F | 142 | 52.6 | 500 | 336 | 0.48 | 160 | 5.2 |
| ONP150-15F | 143 | 55.5 | 500 | 360 | 0.48 | 171 | 5.4 |
| ONP150-4F-40T | 165 | 67.1 | 496 | 221 | 0.56 | 124 | |
| ONP150-4F-4T-a | 166 | 50.8 | 497 | 135 | 0.65 | 88 | |
| ONP150-4F-10T-a | 167 | 53.5 | 496 | 126 | 0.6 | 75 | |
| ONP150-4F-20T-a | 168(1) | 58.1 | 501 | | | | |
| ONP150-4F-60T | 169 | 76.2 | 502 | 132 | 0.59 | 78 | |
| ONP150-4F-4T-b | 180 | 50.8 | 499 | 176 | 0.72 | 127 | |
| ONP150-4F-10T-b | 181 | 53.5 | 499 | 169 | 0.72 | 122 | |
| ONP150-4F-10T-c | 182 | 53.5 | 495 | 147 | 0.67 | 98 | |
| ONP150-4F-20T-c | 183 | 58.1 | 500 | 208 | 0.69 | 144 | |
| ONP75-10F | 191 | 29.4 | 496 | 296 | 0.31 | 92 | 5.7 |
| ONP75-15F | 192 | 32.3 | 505 | 473 | 0.58 | 277 | 9.7 |
| ONP75-4F | 200 | 25.8 | 494 | 90 | 0.49 | 44 | 1.9 |
| ONP75-20F | 201 | 35.3 | 496 | 697 | 0.17 | 116 | 6.9 |
| ONP38-4F | 202 | 14.2 | 499 | 138 | 0.47 | 65 | 3.9 |
| ONP38-10F | 203 | 17.8 | 497 | 266 | 0.33 | 89 | 4.7 |
| ONP40-4F | 204 | 16.4 | 496 | 133 | 0.37 | 49 | |
| ONP40-10F | 205 | 20.0 | 497 | 277 | 0.38 | 106 | |
| ONP150-4F-LS | 223 | 49 | 497 | 119 | 0.47 | 56 | |
| ONP150-4F-4G | 20 | 50.5 | 502 | 149 | 0.56 | 83 | 3.7 |
| ONP150-4F-10G | 21 | 53.0 | 501 | 88 | 0.43 | 38 | 1.8 |
| ONP150-4F-20G | 22 | 57.0 | 496 | 108 | 0.41 | 45 | 2.1 |
| ONP150-10F-20G | 24 | 60.6 | 498 | 279 | 0.51 | 142 | 4.3 |
| ONP150-10F-30G | 25 | 64.7 | 500 | 198 | 0.47 | 93 | 4.1 |
| ONP75-3F-3G | 30 | 26.3 | 504 | 44 | 0.46 | 20 | 4.8 |
| ONP75-3F-6G | 31 | 27.5 | 505 | 60 | 0.51 | 30 | 5.3 |
| ONP75-3F-9G | 32 | 28.8 | 506 | 46 | 0.38 | 18 | 5.7 |
| ONP75-6F-12G | 34 | 31.8 | 505 | 91 | 0.51 | 47 | 6.2 |
| ONP75-6F-18G | 35 | 34.2 | 506 | 68 | 0.43 | 30 | 5.4 |
| ONP150-10F-B | 52 | 52.6 | 505 | 126 | 0.39 | 49 | 6.6 |
| ONP150-10F-10G-B | 53 | 56.7 | 506 | 320 | 0.42 | 135 | 10.8 |
| ONP150-10F-10T-B | 54 | 57.1 | 507 | 372 | 0.48 | 177 | 8.9 |

C.4. Determination of the pK_a of fluorescein on the ONPs

The fluorescence of fluorescein is known to be pH dependent. It was thought pertinent to determine if the pK_a was altered when incorporated into the ONPs. A series of ONPs were studied. The ending -t in some of the ONPs names indicate that the sample was treated with Smopex-105 metal removing polymer prior to this study. The fluorescence of samples were collected at different pHs in sodium phosphate buffered solutions. The fluorescence was normalized to the fluorescence at pH 9 and plotted (shown below). The curves were fit to a linear equation in a small range between pH 5-7. Solving for the value of 0.5 (50 % of the maximum fluorescence) gave the pK_a . Using this technique the calculated pK_a of fluorescein was 5.97 but the known pK_a of fluorescein is 6.4. This error was derived from the incorrect assumption that protonated species has no fluorescence. What was significant was the fact that all but one of the ONPs tested had a higher pK_a than the free fluorescein. The fluorescein on the ONPs was expected to have lower pK_a s. This study has only been performed once and needs repeated before conclusions can be drawn. In the future, UV spectra should be collected and used to calculate the pK_a . If large enough samples are available it should give a more accurate value.



C.5 Effects of Metal Removal on the UV and Fluorescence of ONPs

Results of the treatment of ONP150-4F-LS with SiliMetS DMT metal removing polymer

| equivalents | initial | 0.47 | 1 | 2.1 | 3 |
|----------------------|---------|-------|-------|------|------|
| Os | 1751 | 8216 | 8824 | 7568 | 8647 |
| Ru | 4407 | 2026 | 1678 | 1361 | 1226 |
| total | 6158 | 10242 | 10502 | 8929 | 9873 |
| % material recovered | n/a | 84 | 63 | 69 | 45 |

Levels reported as ppm

In this case, the SiliMetS DMT did a poor job of removing the metals despite claims it's the best for removing ruthenium.

The data present below is the characterization of several ONPs before and after treatment with Smopex-105 to see if removing the metals altered the spectroscopic properties.

Characterization of ONPs prior to treatment

| ONP | λ_{\max} (nm) | $\epsilon_{\lambda_{\max}}$ (x1000) | abs/FI | QY (Φ) | rel. bright | Em. λ_{\max} (nm) | Os (ppm) | Ru (ppm) |
|------------------|-----------------------|-------------------------------------|--------|---------------|-------------|---------------------------|----------|----------|
| ONP150-7F | 500 | 231 | 33 | 0.49 | 1.63 | 525 | 7000 | 3600 |
| ONP75-10F | 496 | 296 | 29.6 | 0.31 | 1.31 | 521 | 280 | 7500 |
| ONP75-15F | 505 | 473 | 31.5 | 0.58 | 3.94 | 526 | 40400 | 9400 |
| ONP75-20F | 496 | 697 | 34.9 | 0.17 | 1.66 | 521 | 72800 | 11300 |
| ONP150-4F-20T-a | 501 | 137 | 34.3 | 0.69 | 1.36 | 524 | 14600 | 6800 |
| ONP150-4F-20T-a* | 496 | 167 | 41.8 | 0.58 | 1.38 | 521 | 6800 | 3400 |
| ONP150-4F-20T-b | 500 | 207 | 51.8 | 0.69 | 2.05 | 524 | 23000 | 9700 |

Characterization of ONPs after treatment with Smopex-105

| ONP | λ_{\max} (nm) | $\epsilon_{\lambda_{\max}}$ (x1000) | abs/FI | QY (Φ) | rel. bright | Em. λ_{\max} (nm) | Os (ppm) | Ru (ppm) |
|------------------|-----------------------|-------------------------------------|--------|---------------|-------------|---------------------------|----------|----------|
| ONP150-7F | 495 | 109 | 27.3 | 0.6 | 0.93 | 519 | 1510 | 1732 |
| ONP75-10F | 496 | 286 | 28.6 | 0.32 | 1.29 | 522 | 15 | 7 |
| ONP75-15F | 505 | 325 | 21.7 | 0.53 | 2.43 | 527 | 37 | 5532 |
| ONP75-20F | | | | | | | 922 | 2633 |
| ONP150-4F-20T-a | | | | | | | 208 | 3646 |
| ONP150-4F-20T-a* | 494 | 106 | 26.5 | 0.68 | 1.03 | 519 | 398 | 160 |
| ONP150-4F-20T-b | 498 | 136 | 34 | 0.58 | 1.12 | 523 | 37 | 3799 |

Change in Spectroscopic Properties

| ONP | λ_{\max} (nm) | $\epsilon_{\lambda_{\max}}$ (x1000) | abs/FI | QY (Φ) | rel. bright | Em. λ_{\max} (nm) |
|------------------|-----------------------|-------------------------------------|--------|---------------|-------------|---------------------------|
| ONP150-7F | -5 | -122 | | 0.11 | -0.7 | -6 |
| ONP75-10F | 0 | -10 | | 0.01 | -0.02 | 1 |
| ONP75-15F | 0 | -148 | | -0.05 | -1.51 | 1 |
| ONP72-20F | | | | | | |
| ONP150-4F-20T-a | | | | | | |
| ONP150-4F-20T-a* | -1 | -61 | | 0.1 | -0.35 | -2 |
| ONP150-4F-20T-b | -2 | -71 | | -0.11 | -0.93 | -1 |

The molar absorptivity of all the ONPs decreased, substantially in most cases. The effect on the quantum yield was inconsistent. In all cases the overall brightness of the ONP decreased when treated with the metal removing polymer.